UNIVERSIDAD COMPLUTENSE DE MADRID

FACULTAD DE CIENCIAS FÍSICAS

DEPARTAMENTO DE FÍSICA DE LA TIERRA, ASTRONOMÍA Y ASTROFÍSICA I

TESIS DOCTORAL

Ionosfera de Marte: calibración y análisis de datos, y modelado
Ionosphere of Mars : data calibration and analysis, and modelling

MEMORIA PARA OPTAR AL GRADO DE DOCTORA

PRESENTADA POR

Beatriz Sánchez-Cano Moreno de Redrojo

Directores

Miguel Herraiz Sarachega
Oliver Witasse
Gracia Rodríguez Caderot

Madrid, 2014

Beatriz Sánchez – Cano Moreno de Redrojo

Doctoral Thesis

Ionosfera de Marte: Calibración y análisis de datos, y modelado

Ionosphere of Mars: Data calibration and analysis, and modelling

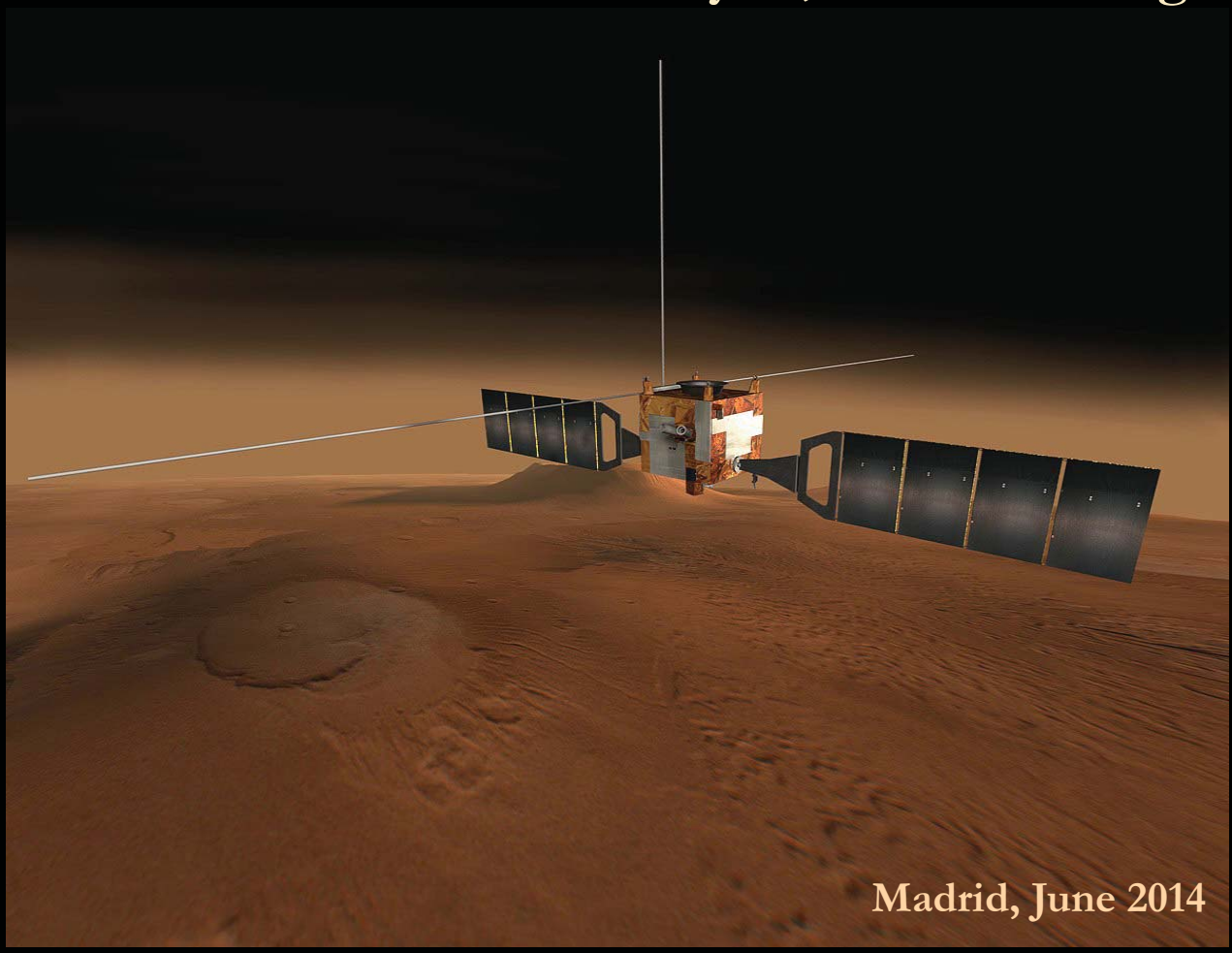

Madrid, June 2014

"Ionosfera de Marte: Calibración y análisis de datos, y modelado"

"Ionosphere of Mars: Data calibration and analysis, and modelling".

Memoria presentada para optar al Grado de Doctor con mención Europea en el Programa de Doctorado en Física de la Facultad de Ciencias Físicas de la Universidad Complutense de Madrid

Report submitted for the Degree of Doctor with European distinction to the Doctoral Programme in Physics of the Faculty of Physical Sciences at the Complutense University of Madrid

Beatriz Sánchez – Cano Moreno de Redrojo

Dirigida por /Directed by

Dr. Miguel Herraiz Sarachaga (Universidad Complutense de Madrid)
Dr. Olivier Witasse (European Space Agency)
Dr. Gracia Rodríguez Caderot (Universidad Complutense de Madrid)

Supervisada por /Supervised by

Prof. Sandro M. Radicella (Abdus Salam Intern. Center of Theoretical Physics)

Madrid, June 2014

Dpto. Física de la Tierra, Astronomía y Astrofísica I
Facultad de Ciencias Físicas, Universidad Complutense de Madrid.

This work has been funded first by Contract with the Projects AYA2009-14212-C05-05/ESP and AYA2008-06420-C04-03 and later, by a Pre-doctoral Research Fellowship from Universidad Complutense de Madrid, Madrid, Spain.

Besides, this study was carried out in the frame work and with the help of Projects: Participación científica en la misión a Marte MEIGA-METNET PRECURSOR, funded by the Spanish Ministry of Science and Innovation (AYA2011-29967-C05-02, AYA2009-14212-C05-05/ESP and AYA2008-06420-C04-03).

Two scientific stays at the center ESTEC of the European Space Agency (from September 1st to October, 12th, 2013 and from March 2nd to 22nd, 2014) were supported by ESTEC Faculty support funding.

ISBN: 978-84-616-9995-7

Per aspera ad astra

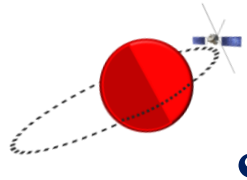

Scheme

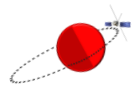

List of Figures

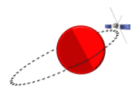

List of Tables

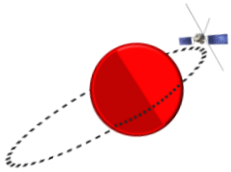

Preface

The mankind history is linked to the technological progress history. Curiosity, fascination and the basic instinct to explore the unknown are the engines that drive man to investigate other worlds looking for life beyond Earth.

In the case of Mars, all civilizations throughout history were attracted about its wandering movement in the sky, about its apparent size change observed from Earth and especially, about its pronounced red colour which once upon a time let Mars was known with the name of the god of war. The Mars' exploration has not been easy. The first mission to the reddish planet was the unsuccessful Soviet Marsnik-1 in 1960. Since then, a total of 48 missions have had the same goal: to further knowledge of our neighbour, to understand the evolution that has led to its current state and to search for live. Of this large amount of missions, only 22 were successful and currently 2 are in their journey. This quantity gives an idea of the complexity involved in such missions. However, the successes outweigh the failures and let the adventure continue with many other missions planned for the near future.

In this line the Meiga-MetNet Precursor project (AYA2011-29967-C05-02, AYA2009-14212-C05-05/ESP and AYA2008-06420-C04-03), which has largely supported this doctoral thesis, is framed. This project since its inception has been the driving force of this doctorate. Conceptually designed as a new type of atmospheric science mission to Mars (MetNet) by the consortium Finnish Meteorological Institute (FMI), Lavochkin Association (LA), Russian Space Research Institute (IKI) and Instituto Nacional de Técnica Aeroespacial (INTA), it has led to the creation of an authentic scientific environment devoted to martian studies within the Universidad Complutense de Madrid, where this work has been developed. Special mention deserves this University, who supported this doctoral project granting it with a pre-doctoral grant.

Since the early Mars flybys in the sixties of the last century, the knowledge of the Mars' ionosphere has evolved profoundly, becoming nowadays a subject of great interest in planetary sciences. There are still many open questions about it, such as: the importance of atmospheric escape for the evolution of the planet's climate; the Mars' ionosphere behaviour over a solar cycle; what causes the transient multiple layers in the ionosphere; what controls the transient nature of the ionopause; how solar forcing determines ionospheric properties… This thesis tries to solve one of these open questions: to analyse empirically the real behaviour of the martian ionosphere under different conditions (like solar incidence, solar flux, seasons…) taken advantage of the large amount of data from Mars Express mission of European Space Agency. It is important to remark that since up Mars Express arrival to Mars in December 2003, the

ionospheric knowledge was limited to few time-intervals of data because no continuous measurements of the ionosphere had been performed for such a long period. This spectacular improvement has been largely due to the MARSIS radar on board this mission. Since mid-2005, this instrument sounds the martian ionosphere in a similar way to the digisonde techniques used on Earth. MARSIS radar is allowing a great knowledge advance as never done before.

Since the conception of this PhD project, a fruitful cooperation with the European Space Research and Technology Centre (ESTEC) of the European Space Agency has been put in place. This collaboration has permitted to access, process and analyse the MARSIS ionospheric data set, still largely unexploited in Europe.

Based mainly on these data, the work done during this PhD has led to the development of the first empirical model of the dayside ionosphere of Mars (including the two main ionospheric layers), called NeMars (Sánchez – Cano et al., 2012, 2013). This model resembles the terrestrial ionosphere model NeQuick (Radicella and Letinger, 2001; Radicella, 2009) which was developed at the Abdus Salam International Center for Theoretical Physics (ICTP) in Trieste (Italy) in collaboration with the Univerisity of Graz (Austria) during the nineties of the last century. This model has been used by the European Space Agency in their Global Navigation Satellite System (GNSS), in particular by the GALILEO single frequency operations to compute ionospheric corrections.

Therefore, through the development of the NeMars model and the exhaustive analysis of some of its multiples applications, the aim of this doctoral thesis has been to contribute to the overall current knowledge of the ionosphere of Mars. In order to classify all the work done, this manuscript has been divided into five chapters. The first one is devoted to the general plasma physic theory used along this work, as well as to the main martian ionosphere characteristics and peculiarities. The second one is dedicated to MARSIS ionospheric dataset analysis and its comparison with other dataset like radio-occultation. The third chapter, which is the thickest part of this PhD, is committed to the development of the empirical model as well as its validation with other datasets. The fourth chapter analyses in detail a discrepancy in total electron content data, unsolved at the time of writing, giving a statistical analysis of comparisons among different datasets. And finally, the fifth chapter present a summary and a general discussion about all the topics presented in this dissertation. This work is complemented with 3 appendixes of information in the last part of this manuscript.

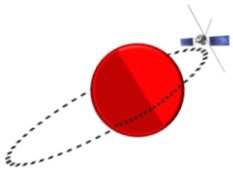

Summary (English version)

Introduction

The upper atmosphere of Mars, which includes the ionosphere, is the first region of the martian system in direct contact with the solar wind because Mars does not have a global magnetosphere. Therefore, the ionosphere is strongly conditioned by the solar activity variations. It plays an important role in the volatile escape processes that have dehydrated the planet over solar system history. In this way, it strongly affects the evolution of the climate and the habitability of Mars over geological time. A good knowledge of the Mars' upper atmosphere and ionosphere is important, as key elements of the entire system.

The knowledge gained about this atmospheric layer, as well as the global picture of Mars, has undergone an exponential evolution in the last 5-10 years thanks to the massive Mars' exploration carried out primarily by NASA and ESA space agencies. A better understanding of the ionosphere-plasma system has emerged mainly thanks to the almost 11 years of continuous measures of plasma properties by several instruments on board Mars Express: ASPERA, MaRS and MARSIS. Before, this knowledge was limited to a few time-intervals of data because no continuous measurements of the ionosphere had been performed for a long period. Consequently, for the first time in history, it is possible to analyse the martian ionosphere under a full solar cycle, something essential that can help the Mars' exploration. Hopefully, this comprehensive solar coverage will be enriched very soon with measurements taken simultaneously by the Mars Express and MAVEN (NASA mission Mars Atmosphere and Volatile EvolutioN) missions. Both spacecraft will make joint campaigns for a deeper analysis of the martian plasma characteristics, allowing exhaustive ionospheric studies by data comparison of each mission at the same time.

This doctoral work is under support of the Meiga-MetNet Precursor project, which has formed a big group of martian studies at Universidad Complutense de Madrid. Among these studies stand out those devoted to analyse the boundary layer, charge particles in the atmosphere, ionosphere, Phobos eclipse predictions, and cloud computing. In particular, the ionospheric group had a previous experience on the development of empirical modelling for the Earth ionosphere. For many years, the Group of Ionospheric Studies and Global Navigation Satellite System (GNSS) has had a very close relationship with Professor Radicella from the Abdus Salam International Centre for Theoretical Physics (ICTP) in Trieste (Italy). Prof. Radicella is one of the two designers of the NeQuick model (Radicella and Letinger, 2001; Radicella, 2009), which is

largely used for describing the Earth ionosphere in a very quick and accurate way. This doctoral thesis is framed in this context.

Objectives

With the objective to extrapolate the terrestrial ionospheric experience to Mars, a previous Master work was done about Mars Global Surveyor Radio Science experiment (Sánchez – Cano, 2010). The next step was to take advantage of the good coverage and accuracy of the Mars Express MARSIS radar instrument, which analysis has been the base of this work and which physics and retrieval procedure are similar to those uses by the Earth digisondes. This dataset had been largely unexploited in Europe, and allowed an original study about martian plasma.

The main purpose of this thesis has been to answer one of the key open questions: what is the behaviour of the martian ionosphere under different conditions (like solar incidence, solar activity, seasons, orbital distance to Sun…)?. In this context and considering that the link among all chapters of this doctoral thesis is the data analysis and interpretation of the MARSIS AIS data set, the work has been articulated into the following studies:

- ☼ To study the general plasma physics theory, as well as, Earth and Mars ionospheric plasma theory.
- ☼ To learn the data analysis by using the MARSIS AIS data analysis tool.
- ☼ To perform the data analysis and comparison between topside sounder profiles and radio-science profiles with similar characteristics.
- ☼ To analyse a large data set to build an empirical model, as well as, the role that some parameters have in the ionosphere formation.
- ☼ To study the Total Electron Content (TEC).

The collaboration with the European Space Research and Technology Centre (ESTEC) of the European Space Agency (ESA) and with the Abdus Salam International Center for Theoretical Physics (ICTP) led to the main definition of this work by using the MARSIS AIS dataset and the empirical model experience respectively.

Main results and conclusions

Data analysis

As already mentioned, the driver of this work has been the MARSIS AIS dataset analysis. Such data, called ionograms, are plots of the time delay of a frequency sweep. Although their access is free at the ESA Planetary Science Archive, there is no public software available for the data processing. A software, called MAISDAT tool, developed at ESTEC, has been used to analyse the data. In order to derive a vertical electron density profile, it is necessary to scale manually each individual ionogram, following a routine explained at Chapter 2. Since the amount of data is large, ionograms with the best visual characteristic (clear trace, presence of harmonics…) have been selected to ensure the best quality of information.

A comparison with electron density profiles derived from Mars Express radio-occultation data was done to analyse how close are both kinds of profiles, and therefore, to check that both the technique and the procedure used to derive the profile of electron density were correct. Radio-occultation technique is well known in the study of the Earth and planetary ionospheres and can be considered as a reliable reference, although its accuracy is one order of magnitude less than the topside sounder (see Paetzold et al., 2005 and Gurnett et al., 2008). After comparing different profiles acquired from both experiments under similar conditions, it was possible to remark that equivalent results were obtained, in particular in the region of maximum ionization. The differences at high altitudes could be due to differences in accuracy, clearly a point for future investigations.

This detailed analysis led to the publication of an article in the *open access* journal *Geoscientific Instrumentation, Methods and Data Systems (GI)*, devoted to geophysical instrumentation under the title "Retrieval of ionospheric profiles from the Mars Express MARSIS experiment data and comparison with radio-occultation data".

NeMars: empirical model

This data processing has been the backbone of this work, allowing the construction of an empirical model for the martian dayside ionosphere, called NeMars. It is remarkable that, although in every moment the model is called "empirical" for simplicity, in reality it should be called "semi-empirical" because it is not only based on the best-fitting data, it also follows general principles of ionospheric plasma physics. This model resembles the terrestrial ionosphere model NeQuick (Radicella and Letinger, 2001; Radicella, 2009) which was developed at the ICTP in Italy in collaboration with the Univerisity of Graz

(Austria) during the nineties of the last century. This model has been used by the European Space Agency in their Global Navigation Satellite System (GNSS), in particular by the GALILEO single frequency operations to compute ionospheric corrections.

NeMars model is mainly based on data from the low frequency radar MARSIS. Particularly, the behaviour of the main global ionospheric layer was based on AIS data (AIS electron density profiles only gives information of the ionospheric topside), and the secondary global layer was characterized with radio-occultation data from the NASA Mars Global Surveyor mission. The model predicts pretty well the main characteristics of both ionospheric regions (electron density and peak altitudes, scale heights, shape of the profiles and TEC of the entire ionosphere) in a simple and quick way from the following inputs: solar zenith angle, solar flux F10.7 as a proxy of the solar activity, and heliocentric distance.

The ionograms and radio-occultation profiles were carefully chosen one by one. It is important to remark that the measurements taken by the radio science experiment on board Mars Global Surveyor are restricted in solar zenith angle (70º-90º) and latitude (60º-85º North or South) due essentially to the observing geometry limitations between Mars and Earth orbits (Withers and Mendillo, 2005). Moreover, as the secondary peak in a radio-occultation profile is not always visible because is embedded in the main one, this layer has been examined in the most prominent case, when the secondary peak was clearly visible. The criterion was to know the peak behaviour in the visible cases and then, mathematically extrapolate to the rest (see Appendix I). Therefore, possible overestimation errors could be introduced although NeMars equations can describe the behaviour of this layer also when is embedded in the main one.

The whole model is based on the consideration that the martian ionosphere is in photochemical equilibrium and the two main layers can be represented by the α-Chapman theory. However, to give a more realistic description, other input parameters like solar activity or heliocentric distance have been included. Regarding the main layer, the electron density peak is calculated with high accuracy from the inputs solar zenith angle, solar flux index $F_{10.7}$ and heliocentric distance. However, the altitude of the main peak cannot be calculated from the same inputs as the large height variation of the AIS data and their slight variation with the solar activity hide the possible variation of the height peak with the $F_{10.7}$ index. Nevertheless, there is a significant dependence with the solar zenith angle and the statistics shows that with this unique dependence, the model adjusts reasonably well. Regarding the scale height, the MARSIS AIS data profile is better reproduced when a linearly variable scale

height with altitude and solar zenith angle is considered, being the median relative differences (%) between the real and the model profiles lower than 6% even at altitudes about 60 km over the maximum peak. This scale height hypothesis has been compared with previous works as Němec et al., (2011) where a constant scale height is used, showing that the approach of this Thesis works better even at high altitudes. In relation to the secondary layer, the shape of the electron density peak equations is similar to the main one with the foremost difference in that a constant scale height of 12 km has been considered.

In general, NeMars is a powerful tool to accurately and quickly describe the "normal and undisturbed" ionosphere of Mars at any location and time. However, given the selected data sample, the model does not address ionospheric disturbances. As a test, the model was compared with some electron profiles recorded during extreme conditions of magnetic field (from solar wind and from magnetic surface anomalies) and with profiles where a third layer at very low altitudes appears. In these cases, despite of the irregularities in the profiles, the modelled results were not far from reality. To deepen in this trend of research, the model will be improved in the next future to consider the magnetic field input from the solar wind and from the planet itself.

This work led to the publication of an article in the journal *Icarus* (cited twice at time of writing), under the title "An empirical model of the martian dayside ionosphere based on Mars Express MARSIS data". Recently, the most recent efforts of the scientific community are directed towards creating an International Reference Model for Mars ionosphere -called MIRI- taking advantage of the large available amount of Mars' ionosphere data and of the large scientific experience with the International Reference Model (IRI) for the Earth ionosphere (Mendillo et al., 2013b). This reference model is an international project sponsored by the Committee on Space Research (COSPAR) and the International Union of Radio Science (URSI). The work carried out in this thesis will most likely contribute to this model by providing processed MARSIS AIS data, outputs of the NeMars model, by sharing the experience in analysing different datasets and comparing them (MARSIS with radio-occultation, MARSIS AIS with MARSIS SubS…), and finally by sharing the critical analysis of the total electron content data sets.

Study of the Total Electron Content in the martian atmosphere: a critical assessment of multiple data sets

Once the model is run, several by-products can be obtained, in particular the total electron content (TEC). This parameter can be used to validate the model

by comparing the observational TEC values given by MARSIS with the estimates obtained with NeMars. Therefore, the NeMars TEC was compared with the TEC measurements deduced from MARSIS subsurface mode (Mouginot et al., 2008 –called also in this work "Grenoble" group- and Cartacci et al., 2013 –called also in this work "Rome" group-). The most intriguing result was that the TEC derived from MARSIS instrument, subsurface mode and ionosphere topside electron density integrated mode, are not consistent. Both modes practically give the same value, which is difficult to understand given the fact that the "subsurface" TEC corresponds to the entire ionosphere, while the "AIS" TEC corresponds only to the ionosphere above the main peak. Since the TEC values are currently difficult to reconcile, it was decided to carry out an objective and unbiased comparison between both techniques taking advantage of the large number of Mars Express orbits with ionospheric and subsurface data (including data from the MARSIS special campaign called "interleaved mode orbits") to characterise in detail the inconsistencies among the results obtained with the available datasets and to propose a way to reconcile them. This discrepancy within the MARSIS data set has been pointed out many times, but never clearly quantified up to now.

The comparisons were performed with 21 Mars Express orbits belonging to the period 14-04-2007 to 23-06-2011. The most remarkable results are that at night (χ>90º), when the ionosphere is weak and its effect on radio-wave practically negligible, both MARSIS SubS procedures ("Grenoble" and "Rome" retrievals) match satisfactorily. Close to the terminator (75º>χ>90º) the ionospheric effect on the dispersion of the electromagnetic signals starts to be appreciable and small differences in the datasets can be spotted. "Rome" matches quite well with the predictable values of NeMars model while "Grenoble" underestimates slightly. Furthermore, in the full dayside (60º>χ>75º), the difference between "Grenoble" and "Rome" datasets is high. In this case, the NeMars model has been used to test how large is the difference between these datasets, showing that the "Grenoble" values are clearly underestimated, while the "Rome" results are more consistent although with a slight overestimation -predicted in fact by Cartacci et al., 2013-.

The main conclusion is that "Grenoble" retrieval –the TEC archived in the ESA Planetary Science Archive-, although in principle physically and mathematically realistic, is almost equal to the TEC of the topside ionosphere; whilst the "Rome" retrieval is more similar to the ionosphere predicted by NeMars model despite the already mentioned overestimation of the result in the daytime. One remark is that "Grenoble" data have been positively compared with the model Mendillo et al., (2011) at Mendillo et al., (2013a). Arguably, at least these results

are not consistent with those obtained with the MARSIS radar sounder in the ionospheric mode.

Part of this work was published in the journal *Icarus*, under the title "An empirical model of the martian dayside ionosphere based on Mars Express MARSIS data" and under the title "Study of the Total Electron Content in the martian atmosphere: a critical assessment of the Mars Express MARSIS dataset", currently under review.

An important application of the empirical model develop in this doctoral thesis is to simulate the MARSIS experiment (in subsurface mode). These simulations could solve the current discrepancy in the TEC measurements commented above. Currently, the NeMars model outputs are being used to simulate the radio-wave propagation obtained with the MARSIS subsurface mode in the "Rome" retrieval by the MARSIS team to study the TEC retrieving techniques constrains and limits. To test the "Rome" algorithm for the correction of ionospheric distortion, NeMars model is being used to calculate the synthetic phase from all frequencies and bands of the signal. Once the entire process is run, simulated TEC can be retrieved. At this stage, the simulations seem to work properly giving similar results. In the near future, it is expected that MARSIS team can finish the simulations and the full validation of its technique. This way of using models to analyse data is something new and, in the frame of the on-going collaboration with the Mars Express MARSIS team, has been recently proven to be very fruitful.

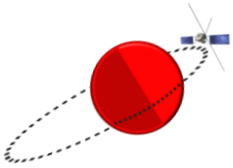

Resumen (versión Española)

Introducción

La alta atmósfera de Marte, que incluye la ionosfera, es la primera región del sistema marciano en contacto directo con el viento solar ya que Marte no posee una magnetosfera de carácter global. Por tanto, la ionosfera está fuertemente condicionada por la variación de la actividad solar. Esta actividad, juega un papel fundamental en los procesos de escape en la atmósfera, los cuales han deshidratado el planeta a lo largo de la historia del Sistema Solar, afectando intensamente a la evolución del clima y a la habitabilidad del planeta a lo largo del tiempo geológico. Un buen conocimiento de la alta atmósfera de Marte, así como de su ionosfera, constituye un elemento clave de dimensiones planetarias.

El conocimiento adquirido de esta capa atmosférica, así como de la imagen de Marte global, ha sufrido una evolución exponencial en los últimos 5-10 años gracias a la masiva exploración llevada a cabo principalmente por las agencias espaciales NASA y ESA. Un mejor conocimiento del sistema ionosfera-plasma ha emergido gracias a los casi 11 años de medidas continuas de distintas propiedades del plasma llevado a cabo por varios instrumentos a bordo de la sonda Mars Express, entre los que destacan: ASPERA, MaRS y MARSIS. Anteriormente, este conocimiento estuvo limitado a los pocos intervalos temporales de datos disponibles, ya que nunca una misión planetaria había podido realizar medidas continuas durante un largo periodo de tiempo en dicha ionosfera. Consiguientemente, por primera vez en la historia, es posible analizar la ionosfera de Marte bajo un ciclo solar completo, algo esencial que puede ayudar considerablemente a la exploración del planeta rojo. Con suerte, esta gran cobertura solar será enriquecida en unos meses con medidas simultáneas de las misiones Mars Express y MAVEN (NASA Mars Atmosphere and Volatile EvolutioN). Ambas misiones realizarán varias campañas conjuntas para un análisis más profundo de las características del plasma marciano, permitiendo estudios ionosféricos exhaustivos comparando datos tomados simultáneamente.

Todo el trabajo de esta tesis doctoral se ha enmarcado dentro del proyecto Meiga-MetNet Precursor, el cual ha formado un gran grupo de estudios marcianos en la Universidad Complutense de Madrid. Entre estos trabajos cabe destacar aquellos dedicados al análisis de la capa límite, de partículas cargadas en la atmósfera, de ionosfera, de predicciones de eclipses de la luna Fobos, y de "cloud computing". En concreto, el grupo ionosférico contaba con experiencia previa en el desarrollo de modelos empíricos para la ionosfera de la Tierra.

Durante muchos años, el Grupo de Estudios Ionosféricos y Técnicas de Posicionamiento Global por Satelite (GNSS) ha tenido una relación muy cercana con el Profesor Radicella del Abdus Salam International Centre for Theoretical Physics (ICTP) en Trieste (Italia). El Prof. Radicella es una de las dos personas que diseñaron el modelo ionosférico terrestre NeQuick (Radicella and Letinger, 2001; Radicella, 2009), el cual ha sido extensamente utilizado para describir la ionosfera de la Tierra de forma muy rápida y precisa. Esta tesis doctoral se enmarca también en este contexto.

Objetivos

Con el objetivo en mente de extrapolar la experiencia ionosférica terrestre a Marte, un trabajo previo de Master fue llevado a cabo sobre el experimento de Radio Ciencia a bordo de la sonda de la NASA Mars Global Surveyor (Sánchez – Cano, 2010). El siguiente paso, el cual ha originado esta tesis doctoral, fue el análisis exhaustivo del radar MARSIS a bordo de Mars Express, cuya física y forma de proceder es similar a la usada en las digisondas terrestres y hoy en día sigue proporcionando una excelente cobertura global del planeta con muy alta precisión en los datos. Estos datos han sido casi totalmente inexplorados en Europa, permitiendo así, un estudio original sobre el plasma marciano.

El principal objetivo de este trabajo doctoral ha sido dar respuesta a una de las preguntas sin respuesta clave: ¿cuál es el comportamiento de la ionosfera marciana bajo diferentes condiciones como incidencia solar, actividad solar, estaciones, distancia orbital al Sol…?. En este contexto y, considerando que el vínculo entre todos los capítulos de esta tesis doctoral ha sido el análisis e interpretación del conjunto de datos AIS de MARSIS, el trabajo se ha compuesto de los siguientes estudios:

- Estudio de la teoría general del plasma, así como su aplicación al plasma ionosférico de la Tierra y de Marte.
- Análisis de datos a partir de la herramienta de análisis de los datos MARSIS AIS.
- Comparación entre perfiles ionosféricos del sondeador MARSIS y de radio ciencia.
- Análisis de una gran base de datos para construir un modelo empírico, así como del papel que algunos parámetros tienen en la formación de la ionosfera.
- Estudio del Contenido Total de Electrones (TEC, por sus siglas en Inglés).

La colaboración llevada a cabo con el European Space Research and Technology Centre (ESTEC) de la Agencia Espacial Europea (ESA) y con el Abdus Salam International Center for Theoretical Physics (ICTP) ha ayudado a la definición principal de este trabajo utilizando la base de datos AIS de MARSIS y la experiencia de modelado empírico respectivamente.

Principales resultados y conclusiones

Análisis de datos

Como ha sido mencionado anteriormente, el conductor de este trabajo ha sido el análisis de la base de datos AIS MARSIS. Estos datos, llamados ionogramas, son representaciones del tiempo de retardo de un barrido de frecuencias. Aunque su acceso es libre en el Archivo de Ciencias Planetarias de la ESA, no existe ningún software disponible al público general para procesarlos. Sin embargo, el centro ESTEC de la ESA desarrolló un software llamado MAISDAT, que ha sido el utilizado en este trabajo. Con el fin de obtener el perfil vertical de densidad electrónica, fue necesario escalar manualmente cada ionograma de forma individual, siguiendo la rutina explicada en el Capítulo 2. Ya que la cantidad de datos disponibles es enorme, con el objetivo de asegurar la mejor calidad en la información, se seleccionaron los ionogramas con mejores características (traza limpia y clara, presencia de armónicos de plasma….). Diversas comparaciones fueron llevadas a cabo entre estos perfiles de densidad electrónica y los del experimento de radio-ocultación de la sonda Mars Express, con el objetivo de confirmar que la técnica utilizada para derivar los perfiles había sido la correcta. La técnica de radio-ocultación es bien conocida en la Tierra y en ionosferas planetarias y puede considerase como una referencia fiable, aunque su precisión en un orden de magnitud menor que la del sondeador (ver Paetzold et al., 2005 and Gurnett et al., 2008). Tras la comparación de estos diferentes tipos de perfiles con condiciones semejantes, fue posible observar la equivalencia en resultados de ambas técnicas, a pesar de una pequeña discrepancia a grandes alturas posiblemente debidas a las diferencias en precisión, lo cual constituye un claro punto para una posible futura investigación.

Este detallado análisis dio lugar a la publicación de un artículo en la revista *open access Geoscientific Instrumentation, Methods and Data Systems (GI)*, dedicada a la instrumentación científica bajo el título: “Retrieval of ionospheric profiles from the Mars Express MARSIS experiment data and comparison with radio-occultation data”.

NeMars: modelo empírico

El procesado de estos datos ha sido el hilo conductor de este trabajo, permitiendo la construcción de un modelo empírico para toda la zona diurna de la ionosfera llamado NeMars. Es notable que, aunque en todo momento el modelo es llamado "empírico" por simplicidad, en realidad debería ser llamado "semi-empírico" ya que no está solo basado en el mejor ajuste de los datos, sino que también respeta los principios generales de la teoría de plasma ionosférico. Este modelo se asemeja al modelo ionosférico terrestre NeQuick (Radicella and Letinger, 2001; Radicella, 2009), el cual fue desarrollado en el ICTP en Italia en colaboración estrecha con La Universidad de Graz (Austria) durante los años noventa del siglo pasado. Este modelo ha sido utilizado por la Agencia Espacial Europea en su Global Navigation Satellite System (GNSS), en particular en las operaciones de frecuencia individual de GALILEO para calcular correcciones ionosféricas.

El modelo NeMars está principalmente basado en datos del radar de bajas frecuencias MARSIS. Concretamente, el comportamiento de la capa principal ionosférica está basado en datos AIS (los perfiles de densidad electrónica de AIS sólo dan información acerca de la parte más alta de la ionosfera), y el comportamiento de la capa secundaria, está basado en datos de radio-ocultación de la misión de la NASA Mars Global Surveyor. El modelo predice bastante bien las principales características de ambas regiones ionosféricas (densidad electrónica y altura del pico, alturas de escala, forma de los perfiles y TEC de toda la ionosfera) de una forma muy simple y rápida a partir de los parámetros de entrada: ángulo cenital solar, flujo solar F10.7 como proxy de la actividad solar, y distancia heliocéntrica.

Los ionogramas, así como los perfiles de radio-ocultación, fueron cuidadosamente seleccionados uno por uno. Es importante notar que las medidas del experimento de radio ciencia de la misión Mars Global Surveyor están restringidas en ángulo cenital solar (70º-90º) y latitud (60º-85º Norte o Sur) debido esencialmente a limitaciones de la geometría de las órbitas de Marte y la Tierra (Withers and Mendillo, 2005). Por otra parte, como el pico secundario en un perfil de radio-ocultación no es siempre visible porque se encuentra incrustado en la capa principal, esta capa ha sido estudiada sólo en los casos más prominentes, cuando el pico secundario era visible. El criterio fue estudiar el comportamiento del pico en todos los casos visibles y después, matemáticamente extrapolar al resto de casos. Por tanto, alguna posible sobreestimación del error pudo ser introducida a pesar de que las ecuaciones del

modelo NeMars pueden describir el comportamiento de esta capa incluso cuando se encuentra incrustada en la principal.

El modelo en su totalidad está basado en la consideración de que la ionosfera de Marte se encuentra en equilibrio fotoquímico y que las dos capas principales pueden ser representadas por la teoría de capas α-Chapman. Sin embargo, para dar una descripción más realística, otros inputs como la actividad solar, el ángulo de incidencia solar o la propia órbita del planeta han sido incluidos. No obstante, la altura del pico principal no puede ser calculada a partir de los mismos parámetros debido a una gran variación en la altura en los datos AIS, al igual que la ligera variación producida por la actividad solar oculta la variación de la altura del pico con el índice $F_{10.7}$. Sin embargo, se aprecia una gran dependencia con el ángulo cenital solar y las estadísticas muestran cómo con esta única dependencia, el modelo representa razonablemente bien los datos. En cuanto a la altura de escala, el perfil obtenido a partir de los datos AIS de MARSIS es mejor reproducido cuando una altura de escala variable linealmente con la altura y con el ángulo cenital solar es considerada, siendo las diferencias relativas medias (%) entre los datos reales y los perfiles obtenidos con el modelo más pequeñas que el 6%, incluso a una altura por encima de 60 km desde el pico principal. Estos resultados han sido comparados con trabajos previos como el de Němec et al., (2011) donde se utiliza un altura de escala constante, mostrando que el enfoque de esta Tesis trabaja mucho mejor incluso a grandes alturas. En relación con la capa secundaria, la forma de las ecuaciones que describen el comportamiento de la densidad electrónica del pico es semejante a las de la capa principal con la salvedad de que la altura de escala puede considerarse constante en 12 km.

En términos generales, NeMars es una poderosa herramienta, precisa y rápida que describe el comportamiento de la ionosfera de Marte "en condiciones normales y no perturbadas" para cualquier posición y tiempo. Sin embargo, dada la naturaleza de los datos seleccionados, el modelo no debiera ajustar con condiciones perturbadoras. Como test para evaluar el grado de discrepancia, el modelo fue comparado con algunos de los perfiles de densidad electrónica registrados en las condiciones más extremas de campo magnético (procedente tanto del viento solar como de las anomalías magnéticas corticales del planeta) y con perfiles donde una tercera capa aparece a alturas muy bajas. En estos casos, a pesar de las irregularidades en los perfiles, los resultados modelados no se encontraban muy lejanos de la realidad. Para profundizar en estos detalles, el modelo será mejorado en el futuro próximo con la incorporación como parámetro de entrada del campo magnético procedente del viento solar, así como del propio planeta.

Este trabajo dio lugar a la publicación de un artículo en la revista *Icarus* (citado dos veces al tiempo de escritura de esta Tesis), bajo el título "An empirical model of the martian dayside ionosphere based on Mars Express MARSIS data". Recientemente, los esfuerzos de la comunidad científica han sido dirigidos a la creación de un Modelo Internacional de Referencia para la Ionosfera de Marte, llamado MIRI, tomando ventaja de la gran cantidad de datos disponibles de la ionosfera de Marte y de la gran experiencia acumulada para el caso de la Tierra como el Modelo Internacional de Referencia IRI (Mendillo et al., 2013b). Este modelo de referencia en un proyecto internacional que ha surgido bajo el amparo del Committee on Space Research (COSPAR) y de la International Union of Radio Science (URSI). El trabajo llevado a cabo en esta Tesis Doctoral con gran probabilidad formará parte de este modelo, proveyendo con datos MARSIS AIS procesados, parámetros de salida del modelo NeMars, así como compartiendo la experiencia obtenida en el análisis de diferentes bases de datos, comparación entre ellas (MARSIS con radio-ocultación, MARSIS AIS con MARSIS SubS…), y finalmente, compartiendo el análisis crítico obtenido en el análisis del contenido total de electrones.

Estudio del Contenido Total de Electrones en la atmósfera marciana: una evaluación crítica de múltiples bases de datos

Distintos subproductos del modelo pueden ser obtenidos. En particular, uno de ellos es el contenido total de electrones (TEC). Este parámetro puede ser usado para validar el modelo comparando los valores de TEC obtenidos con NeMars con el TEC de medidas deducidas del modo subsuperficie de MARSIS (Mouginot et al., 2008 –también llamado en este trabajo grupo de "Grenoble"- y Cartacci et al., 2013 –también llamado en este trabajo grupo de "Rome"-). El resultado más notable fue que el TEC derivado del instrumento MARSIS en ambos modos (ionosfera y subsuperficie), no eran consistentes. Ambos modos prácticamente alcanzaban el mismo valor, aunque es un hecho difícil de entender puesto que el TEC de subsuperficie corresponde con el de toda la ionosfera mientras que el del modo AIS se corresponde sólo con el TEC encontrado entre la nave y el máximo de ionización. Puesto que esta discrepancia era difícil de resolver, se decidió llevar a cabo una comparación objetiva entre ambas técnicas tomando ventaja del gran número de órbitas de Mars Express con datos en ambos modos de operación (incluyendo datos de la campaña especial de MARSIS llevada a cabo con este fin y nominada "interleaved mode") para caracterizar en detalle las inconsistencias entre los resultados obtenidos con las distintas bases de datos y proponer así una línea para reconciliarlos. Esta discrepancia en las bases de datos de MARSIS ha sido notificada muchas veces por la comunidad científica, pero nunca claramente cuantificada hasta ahora.

Las comparaciones fueron llevadas a cabo con 21 órbitas de Mars Express pertenecientes al periodo 14-04-2007 / 23-06-2011. El resultado más notable fue que en la zona nocturna (χ>90º), cuando la ionosfera es débil y su efecto en las ondas de radio prácticamente despreciable, ambas bases de datos de sub-superficie ("Grenoble" y "Roma") coinciden satisfactoriamente. Cerca del terminador del día (75º>χ>90º), el efecto de la ionosfera sobre la dispersión de las ondas electromagnéticas comienza a ser apreciable y pequeñas diferencias en las bases de datos se observan. La técnica de "Roma" ajusta bastante bien los valores predichos por el modelo NeMars, mientras que "Grenoble" bajo estima ligeramente. Más allá, en el pleno lado diurno (60º>χ>75º), la diferencia entre las bases de datos de "Grenoble" y "Roma" es muy alta. En ese caso, el modelo de NeMars ha sido utilizado para testear el tamaño de la diferencia entre ambas bases de datos, mostrando que los valores de "Grenoble" están claramente subestimando, mientras que los resultados de "Roma" son más consistentes aunque con una ligera sobreestimación –predicha de hecho por Cartacci et al., 2013-.

La principal conclusión es que el procesado de "Grenoble" –que corresponde con el TEC archivado en el Archivo de Ciencias Planetarias de la ESA- aunque en principio físicamente y matemáticamente realista, es casi igual que el TEC encontrado en la zona superior de la ionosfera; mientras que el procesado de "Roma" es más similar al de la ionosfera predicha por el modelo NeMars con la ya mencionada sobreestimación en la zona diurna. Es importante destacar que los datos de "Grenoble" han sido positivamente comparados con el modelo ionosférico Mendillo et al., (2011) en el trabajo Mendillo et al., (2013a). Al menos, estos resultados no son consistentes con aquellos obtenidos por el radar MARSIS en el modo ionosférico.

Parte de este trabajo ha sido publicado ya en la revista *Icarus*, bajo el título "An empirical model of the martian dayside ionosphere based on Mars Express MARSIS data" y se completará con otro trabajo con título "Study of the Total Electron Content in the martian atmosphere: a critical assessment of the Mars Express MARSIS dataset", actualmente en revisión.

Otra aplicación importante del modelo empírico desarrollado en esta tesis doctoral es la simulación del experimento MARSIS (en el modo subsuperficie). Estas simulaciones podrían resolver la actual discrepancia en las medidas de TEC comentadas anteriormente. Actualmente, los parámetros de salida del modelo están siendo utilizados para simular la propagación de las ondas de radio obtenidas con el modo subsuperficie de MARSIS en la técnica de "Roma" por el equipo MARSIS. De esta forma, se están estudiando las limitaciones de dicho procesado. Para probar el algoritmo de "Roma" para la corrección de la

dispersión ionosférica, el modelo NeMars está siendo utilizado para calcular la fase sintética de todas las frecuencias y bandas de la señal portadora. Una vez que el proceso se ha completado, el TEC sintético puede ser obtenido. A día de hoy, las simulaciones parecen dar los resultados esperados. En el futuro más cercano se espera que el equipo de MARSIS pueda finalizar las simulaciones y completar la validación de su técnica. Esta forma de trabajo usando modelos para el análisis de datos es algo nuevo y, en el marco de la colaboración actual con el equipo de MARSIS Mars Express, ha sido recientemente probada como muy fructífera.

"Ionosfera de Marte: Calibración y análisis de datos, y modelado"

"Ionosphere of Mars: Data calibration and analysis, and modelling".

Beatriz Sánchez – Cano Moreno de Redrojo

Tesis Doctoral / Doctoral Thesis

Madrid, June 2014

Dirigida por /Directed by

Dr. Miguel Herraiz Sarachaga (Universidad Complutense de Madrid)
Dr. Olivier Witasse (European Space Agency)
Dr. Gracia Rodríguez Caderot (Universidad Complutense de Madrid)

Supervisada por /Supervised by

Prof. Sandro M. Radicella (Abdus Salam Intern. Center of Theoretical Physics)

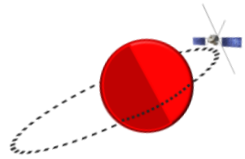

Chapter 1.

The ionosphere of Mars

☼ 2

1.1 Basics of aeronomy

The ionosphere is the conductive atmospheric layer formed by the ionization of the neutral atmosphere. This layer contains a significant number of free thermal electrons (with energy below 1 eV) and ions. All bodies in our solar system that have a surrounding neutral-gas envelope, due either to gravitational attraction (e.g. planets) or some other processes such as sublimation (e.g. comets), possess an ionosphere. The free electrons and ions are produced via ionization of the neutral particles both by extreme ultraviolet/X-rays radiation from the Sun and by collisions with energetic particles that penetrate the atmosphere (e.g. Schunk and Nagy, 2009).

The medium is a plasma that comprises positive ions and free electrons, and in general terms, it is neutral, since the Debye length of the ionosphere –a few tens of cm- is much smaller than the characteristic length of the martian ionosphere-. Typical scale heights are in the order of a few 10 or 100 km. The electron plasma frequencies are much larger than the neutral-electron collision frequencies. The plasma is characterized by a dynamic balance in which the net concentration of free electrons, the electron density, Ne, depends on the relative speed of the production and loss processes, which in their turn vary according to the type of ions existing in the plasma, their corresponding interactions with the neutral gas, and the solar flux (Chapman and Bartels, 1940). The degree of ionization depends on the intensity of the incoming radiation and on the -normally controlled- chemical follow-up reactions between ions, electrons and neutral particles which tend to restore electrical neutrality (Figure 1.1). Since the probability of such reactions increases in the downward direction as does the air density, an ionized *layer* is formed with at least one peak at an altitude which depends on this balance (Rawer, 1993).

Once the ionosphere is formed, the charge particles are affected by a myriad of processes, including chemical reactions, diffusion, wave disturbances, plasma instabilities, and transport due to electric and magnetic fields (e.g. Schunk and Nagy, 2009).

As a rule, the rate of electron density variation is governed by the continuity equation (1.1):

$$\frac{dn}{dt} = q - L - \nabla \cdot (n\boldsymbol{v}) \qquad 1.1$$

where q is the rate of ion-electron pairs production per unit of volume, L is the rate of electron loss due to recombination, and $\nabla \cdot (n\boldsymbol{v})$ is the electron loss due to the effects of transport, fundamentally vertical, with average drift velocity, v (Hargreaves, 1992). During the day the intensity of ionization radiation varies with the elevation of the Sun, and the electron density response. At night this classical source of ionization is removed and the electron density decays. However, ionization at night can occur due to the large day-to-night pressure gradients. The night-ward plasma flows from dayside across the terminators, being the main source of the nightside ionosphere. In addition, large streams of solar charged particles can collide with atoms and molecules in the atmosphere after being accelerated along magnetic field lines. These collisions result in countless little bursts of light, which make up the auroras.

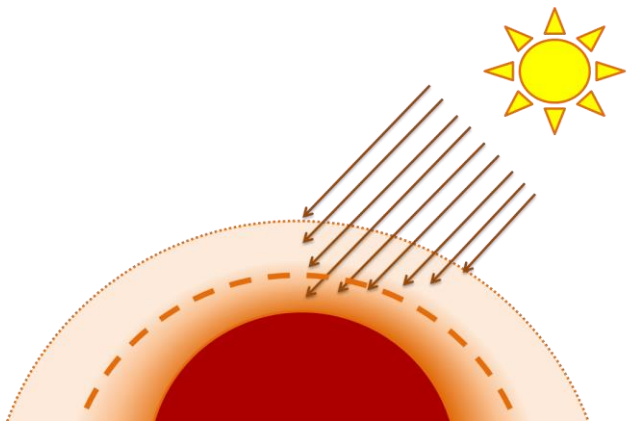

Figure 1.1: Scheme of the layer formation. From the topside atmosphere to the surface of the planet, the penetration of the incoming solar radiation decreases (brown arrows) while the concentration of the neutral atmosphere increases (orange degraded area: intense orange means more number of neutral particles). An ionospheric layer is formed with at least one peak (orange dashed line) at an altitude which depends on this dynamic balance between relative speed of the production and loss processes, type of ions existing in the plasma, solar radiation and interactions with the neutrals.

The first suggestion of the existence of the ionosphere on Earth can be traced to the 1800s, when Carl Gauss and Balfour Stewart hypothesized the existence of electric currents in the atmosphere to explain the observed variations of the magnetic field at the surface of the Earth. The existence of this layer was clearly established in 1901 when G. Marconi successfully transmitted radio signals across the Atlantic and the following year, A.E. Kennelly and O. Heaviside suggested that free electrical charges in the upper atmosphere could reflect radio waves. However until 1924, the Earth ionosphere was not measured. The firsts

were Breit-Tuve with their experiments of "pulse sounding" technique and Appleton and Barnett with their "frequency change" experiments (Schunk and Nagy, 2009). Thereafter in 1931, Sydney Chapman published the first hypothesis about its formation, which are still in force today and have been extrapolated to other planets. These assumptions are:

- The global atmosphere is in hydrostatic balance and in photochemical equilibrium.
- The incoming radiation is monochromatic and each photon produces a single electron.
- The atmospheric layers are horizontally stratified, electrically neutral, consist of a homogeneous gas formed by a single component, and remain in equilibrium.
- It is assumed that one ion species only is present, O_2^+ in the case of Mars.

Based on these assumptions, Chapman developed a formula that predicts the form of a simple ionospheric layer and how it varies during the day. This theoretical profile, called the *Chapman layer*, laid the foundation for later developments in ionospheric physics.

Henceforth the most useful plasma Chapman ionospheric equations are described. Nevertheless, more detailed information could be found at Chapman, (1931 a, b), Hargreaves, (1992), Cravens, (1997) or Schunk and Nagy, (2009).

The rate of ion-electron pairs production per unit of volume can be expressed as:

$$q = \eta \sigma n I \qquad 1.2$$

where I is the intensity of ionizing radiation at some level of the atmosphere and n is the concentration of atoms or molecules capable of being ionized by the radiation. For an atom or molecule to be ionized it must first absorb radiation, and the amount absorbed is expressed by the *absorption cross-section*,σ: if the flux of incident radiation is I (J/m^2 s) then the total energy absorbed per unit volume of the atmosphere per unit time is σnI. However, not all this energy will go into the ionization process, and the *ionization efficiency*, η, takes that into account, being the fraction of the absorbed radiation that goes into producing ionization.

The Chapman production function is usually written in a normalized form as:

$$q = q_{m0} \cdot exp(1 - z - sec\chi \cdot e^{-z}) \qquad 1.3$$

Here, z is the *reduced height* for the neutral gas, $z = (h - h_{m0})/H$, where H is the *neutral atmospheric scale height*. χ is the solar zenith angle, h_{m0} is the height of maximum production rate when the Sun is overhead (χ=0), and q_{m0} is the production rate at h_{m0}, also when the Sun is overhead.

By differentiating equation (1.3) it is readily proved that

$$z_m = ln(sec\chi) \qquad 1.4$$

where z_m is the reduced height of maximum production (the height at χ=0 being taken as zero). In other words, height of maximum production can be written as follow:

$$h_m = h_{m0} + H_m ln(sec\chi) \qquad 1.5$$

On the other hand, regarding the principle of chemical recombination, the rate of electron loss (L) depends on the way of the ion recombination. Equation (1.6) describes the most typical way of ionospheric recombination, under the assumptions of electrons recombine directly with positive ions and that no negative ions are present. If a neutral particle plus a photon are emitted (e.g. $M^+ + e^- \rightarrow M + h\nu$), the process is called *radiative recombination*. And if two neutrals particles are emitted in this process (e.g. $MN^+ + e^- \rightarrow M + N$), it is called *dissociative recombination*.

$$L = \alpha N^2 \qquad 1.6$$

where N is the *electron density* and α the *recombination coefficient*. At equilibrium, -that means from equation (1.1): $\frac{dn}{dt} = 0$, transport effects can be neglected $\nabla \cdot (n\boldsymbol{v}) \sim 0$, and therefore, L=q-, it is obtained:

$$q = \alpha N^2 \qquad 1.7$$

Taking the production rate q from the Chapman production function (equation 1.3), the Chapman function for the electron density in a layer can be written as:

$$N = N_{m0} \cdot exp\left[\frac{1}{2}(1 - z - sec\chi \cdot e^{-z})\right] \qquad 1.8$$

being the electron density at the peak of the layer:

$$N_m = N_{m0}\sqrt{cos\chi} \qquad 1.9$$

a layer with these properties is called an *α-Chapman layer*.

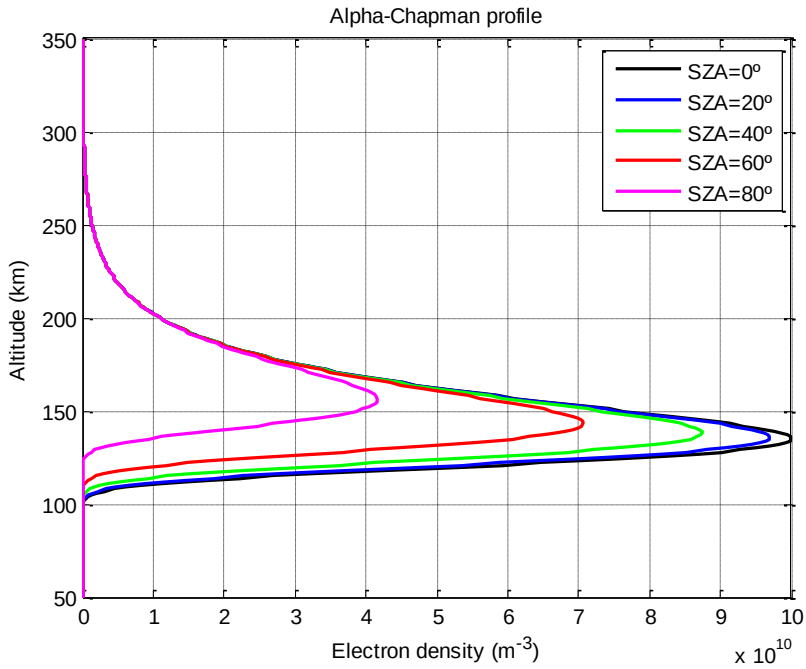

Figure 1.2: Theoretic α-Chapman layer profile (electron density variation with altitude) for different solar zenith angles.

In addition, the attachment to neutral particles to form negative ions can itself be regarded as another type of electron loss process (e.g. $M + e^- \rightarrow M^-$), called *recombination by attachment*. In this case, the loss rate is linear with N because the neutral species are assumed to be far the more numerous, in which case removing a few of them has no significant effect on the total remaining and the neutrals are effectively constant. Therefore, $L=\beta N$ where β is the *attachment coefficient*. At equilibrium,

$$q = \beta N \qquad 1.10$$

And taking q from the Chapman production function (equation 1.3) as before, Chapman function for the electron density in a layer can be expressed as:

$$N = N_{m0} \cdot exp(1 - z - sec\chi \cdot e^{-z}) \qquad 1.11$$

being the electron density at the peak of the layer:

$$N_m = N_{m0} cos\chi \qquad 1.12$$

such a layer is a *β-Chapman layer*.

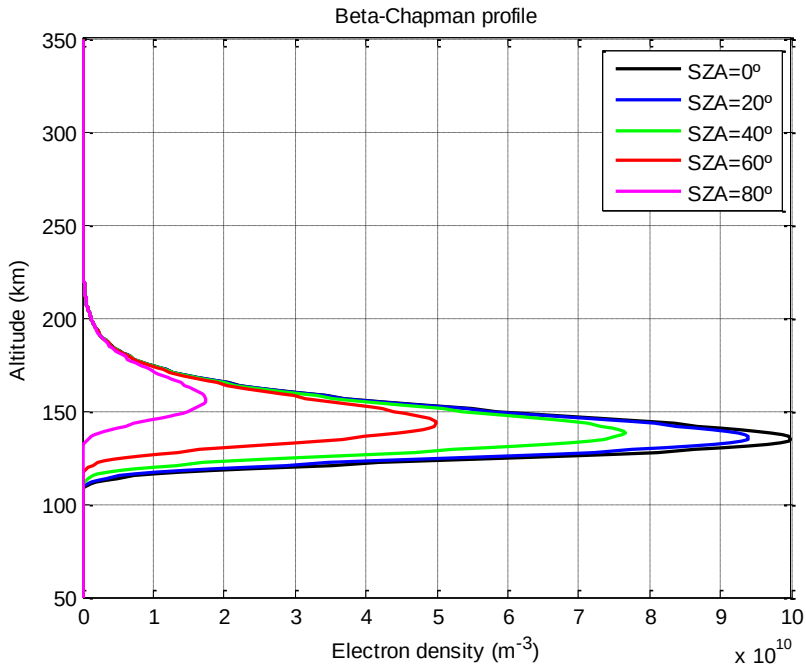

Figure 1.3: Theoretic β-Chapman layer profile (electron density variation with altitude) for different solar zenith angles.

It should be noted that these equations are not valid for very large values of solar zenith angles (corresponding to grazing incidence of the beam of radiation), because then the level surfaces traversed by the beam can no longer be treated as parallel planes, as they were when the distance along the beam between h and h - dh was taken as $\sec(\chi)\cdot dh$. The approximation is sufficiently accurate up to χ=85º (Chapman, 1931a) which along the equator on Earth corresponds to about 20 minutes after sunrise or before sunset. Therefore for χ>85º, Chapman grazing incidence function *Ch* (equation 1.13) must be included in equations (1.8) and (1.11) in the place of $\sec(\chi)$ (Chapman, 1931b).

$$Ch(d,\chi) = d \cdot sin\chi \int_0^{\chi} exp\left(d - d\frac{sin\chi}{sin\alpha}\right) cosec^2(\alpha) d\alpha \qquad 1.13$$

where d=R+h/H and R is the radius of the planet in meters.

1.2 Basics of Mars' ionosphere

The dayside ionosphere of Mars consists mainly of two layers (Figure 1.4). In general terms, the peak of the main layer is located between 125-140 km of altitude with a typical electron density range value of 0.5- $2x10^{11}$ electrons per m^{-3} (e.g. Whitten and Colin, 1974, Gurnett et al., 2005 or Peter et al., 2012) and is produced by the solar extreme-ultraviolet (EUV) photons between 10 nm and 90 nm (e.g. Witasse et al., 2008). With regard to the peak of the secondary layer since the flux of EUV photons is greatly attenuated here, it is formed mainly by the soft X-ray solar photons of 10 nm with a significant contribution to the ionization due to secondary electrons and photoelectrons, and it is located at around 110-115 km of altitude (e.g. Schunk and Nagy, 2009). This layer is considerably weaker than the main peak but it is not negligible since it contributes to about 10% of the Total Electron Content.

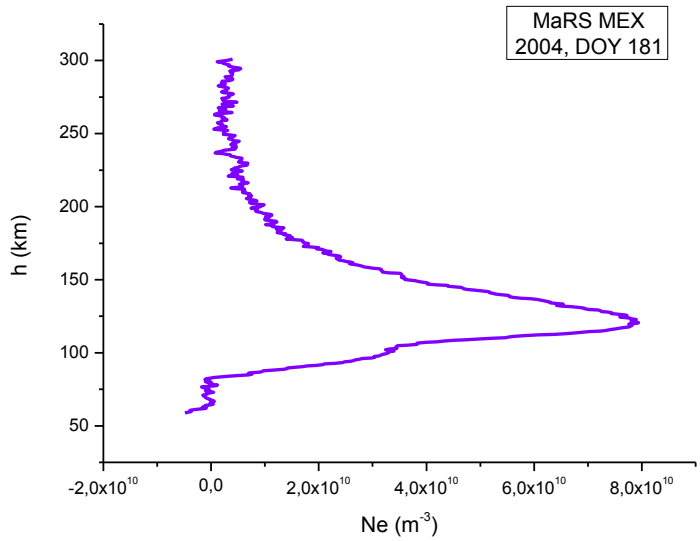

Figure 1.4: Typical dayside profile of the martian ionosphere. The main ionized layer is located at about 135 km of altitude and the second one at about 110 km. Credits: MaRS (radio science instrument on board Mars Express) radio-occultation profile (adapted from Sánchez – Cano et al., 2013).

Photochemical processes control the behaviour of the two main global ionospheric layers. In general terms, the martian ionosphere can be well represented to first order and over a limited altitude range by Chapman-type

layers (Gurnett et al., 2005, Pi et al., 2008, Withers, 2009, Mendillo et al 2011, Němec et al., 2011 or Sánchez – Cano et al., 2013). Specifically, if it is assumed to be in photochemical equilibrium, the dominant mechanism of ion loss is dissociative recombination which, as mentioned before, is based on ion recombination with free electrons to give neutral particles (e.g. Fox, 2009). If all these assumptions are included in equation 1.1, the final expression for the electron density, Ne, as a function of altitude and solar zenith angle is the so-called α-Chapman layer equation (equation 1.8) (Pi et al., 2008, Sánchez – Cano et al., 2010), which does not account for grazing incidence and therefore is valid only for not very large solar zenith angles.

Near the terminator, equation (1.13) must be included in (1.8). As just mentioned, this formulation is a very good first order approximation of the martian ionosphere. However, some variations which will be explained throughout this manuscript, are needed to introduce for a more detailed analysis.

Concerning the photochemical composition (Figure 1.5), the main ionospheric component is O_2^+. This ion can be created by the ionization of CO_2 -the main neutral atmospheric component- (Reactions 1 and 2), or by its reaction with O^+ (Reaction 3) (e.g. Schunk and Nagy, 2009). There is another major ionospheric component, O^+, which becomes comparable in concentration to that of O_2^+ above a certain altitude, typically 300 km (See Figure 1.5 and Reaction 4). N-bearing species, such as NO^+ and metal species derived from meteoroids, such as Mg+ and Fe+, may become a major species below 100 km (Molina-Cuberos et al., 2003; Withers, 2009).

$$CO_2 + h\nu \longrightarrow CO_2^+ + e \qquad \textbf{(Reaction 1)}$$

$$CO_2^+ + O \longrightarrow O_2^+ + CO \qquad \textbf{(Reaction 2)}$$

$$O^+ + CO_2 \longrightarrow O_2^+ + CO \qquad \textbf{(Reaction 3)}$$

$$CO_2^+ + O \longrightarrow O^+ + CO_2 \qquad \textbf{(Reaction 4)}$$

The ion temperature varies between 150 and 200 K at 120 km and reaches 2500 K at 300 km (Hanson et al., 1977). At this height, the value of the electron temperature is between 3500 - 4000 K (Hanson and Mantas, 1988).

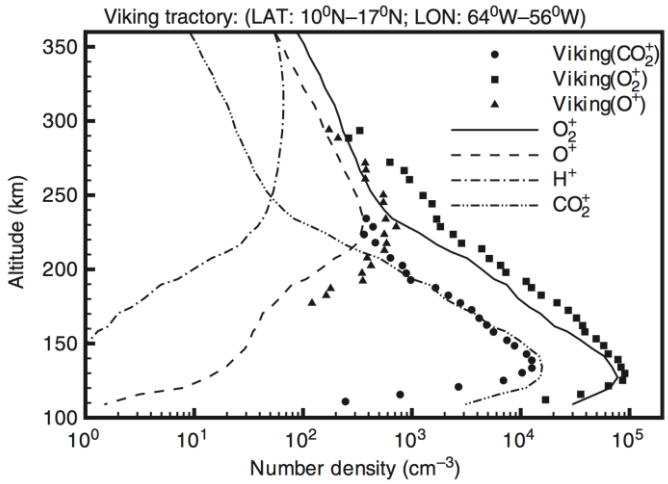

Figure 1.5: Ion density profiles measured by the *Viking 1* Radio Potential Analyzer (RPA) (Hanson et al., 1977) and calculated in a self-consistent manner by a three-dimensional MHD model (Ma et al., 2002).

Currently, our knowledge of the dayside martian ionosphere has been greatly enriched in the latest sixteen years by the discoveries of the American Mars Global Surveyor and the European Mars Express spacecraft. In particular, thanks to ten years of ionospheric data from Mars Express, the structure, variability and escape of the martian plasma are known in unprecedented detail, even if there are still some open questions. The main findings are described below.

1.2.1 Ionospheric structure

Although the Mars' ionosphere mainly is composed by two global layers, there are other structures (some sporadic, some continuous) which play important roles above and below the photochemical-controlled region (Figure 1.6).

One of the main Mars Express findings has been the discovery of the ionopause, which is the upper boundary of the martian-system in direct contact with the solar wind and whose presence was debated for many years. Duru et al., (2009) clearly show that the ionopause exists and the average altitude of the boundary, where the magnetic fields change from open to close, is almost constant and for solar zenith angles of 60º is located at approximately 500 km. On the other hand, a third layer that appears sporadically below the secondary

layer was discovered. This layer constitutes the lower boundary of the martian ionosphere and is produced by the ablation of meteoroids at altitudes between 65 and 110 km (e.g. Molina-Cuberos et al., 2003, Paetzold et al., 2005, Withers, 2009).

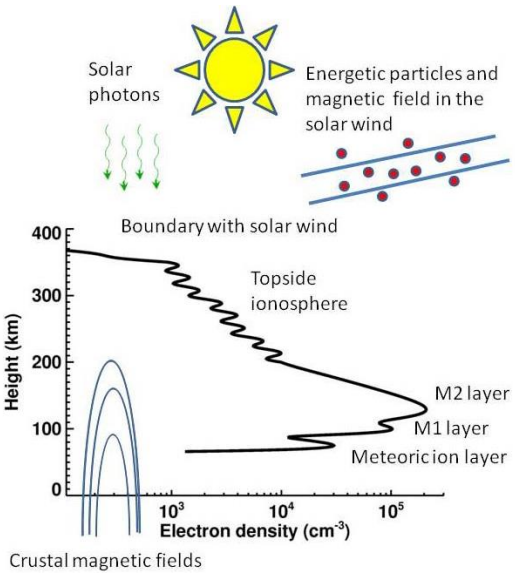

Figure 1.6: Schematic illustration of the full martian ionosphere system. In this figure M2 denotes main ionospheric peak and M1 secondary ionospheric peak (Withers et al., 2009 -white paper).

Some other important discoveries with temporary features have been made. One of them is the transitory secondary and tertiary layers (also known as bulges) above the main ionospheric peak at altitudes above about 200 km. These features, which are not often observed, are formed due to dynamical processes like the interaction with the solar wind in the upper levels of the ionosphere (Gurnett et al., 2008; Kopf et al., 2008). These layers are transitory and last about 60% of the time near the sub-solar point. Furthermore, a "third layer" has been observed in the 1% of observations at even higher altitudes (Kopf et al., 2008).

And finally, another important finding has been the detection of plasma bulges due to magnetic field, in particular, enhanced electron density over regions where the crustal magnetic field is strong and nearly vertical. This enhanced zone can reach 50 km above the surrounding ionosphere and it is believed that the increase in density can be caused by the heating of the electron gas which leads to a decrease of the recombination coefficient and an increase of the electron density (Duru et al., 2006, Nielsen et al., 2007 and Gurnett et al., 2008).

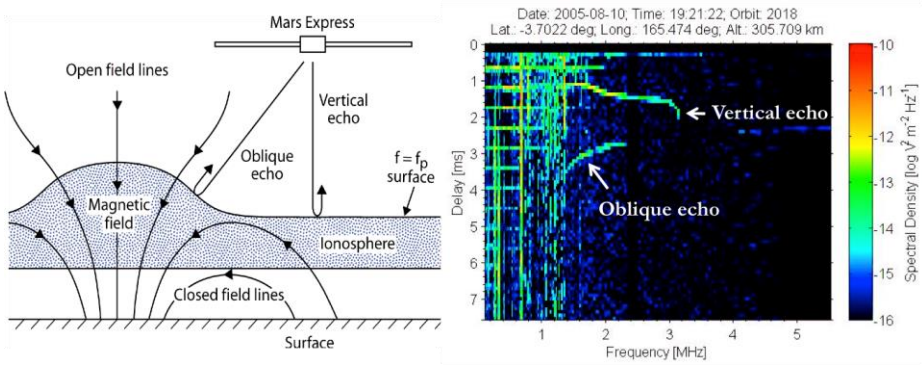

Figure 1.7: Left panel: enhanced areas of the ionosphere, which are thought to be responsible for oblique ionospheric echoes. As the spacecraft approaches the bulge in the ionosphere the sounder detects two different echoes, one due to the vertical reflexion from the horizontally stratified ionosphere, and the other one due to the oblique reflection from the bulge. The bulges are usually located in regions where the magnetic field is nearly vertical (Gurnett et al., 2005). Right panel: Typical ionogram with two echoes (vertical and oblique).

Sometimes, these bulges can be detected by the Mars Express MARSIS instrument. Specifically, the reflexion of some frequencies in this enhanced areas can be recorded as oblique echoes in the MARSIS *ionograms* -which are the basic unit of information of this instrument allowing retrieving electron density profiles (Andrews et al., 2014, submitted). The retrieving method will be explained in detail in Chapter 2. In these areas the sounder detects two different echoes (Figure 1.7), one due to the vertical reflexion from the ionosphere and the other one due to the oblique reflection from the bulge (Gurnett et al., 2005).

1.2.2 Ionospheric variability

Since the Sun is the main source of ionization of the ionosphere, any variation of the solar radiation produces large dynamics in the amount of electron density either in time and space. Some general examples are the *solar cycle variation*, the *diurnal variation* –which is due to the rotation of the planet-, or the *induced currents* in the ionosphere because of the *crustal magnetic field.*

These variations during the dayside can be observed easily in the shape of electron density profiles, as shown by Withers et al., (2012a). Using radio-occultation data form Mars Express MaRS instrument, it has been observed that the topside of the profile in only 10% of the cases clearly decrease with a single

scale height, around 25% of them has two different scale heights and about 10% have three regions with distinct scale heights. In addition, other factors such as the presence of an induced magnetic field can produce dramatic changes in the height of the top of the ionosphere. Figure 1.8 shows two different kinds of electron density profiles due to this effect. Left panel is a clear profile where the topside has been extremely compressed because of an intense solar activity, as for example a coronal mass ejection. The reason is that the magnetic field originating from the solar wind is compressed, its magnitude increases, and as a consequence it is able to penetrate to lower altitudes. Since the plasma follows the field lines, the result is a compression of the ionosphere. It is possible to observe an unusually low extent and clear ionopause (Fig 1.8, left panel). On the other side, right panel shows a profile, which has the greatest range of electron density in altitude reported for Mars: 600 km. This profile was situated over a strong magnetic field anomaly from the martian surface: 220 nT at 150 km (Arkani-Hamed, 2004). Therefore, the vertical thickness of the ionosphere changes by a factor of six between Figure 1.8-Left panel (100 km thick) and Figure 1.8-Right panel (600 km thick) (Withers et al., 2012a). In area controlled by the crustal anomalies, it is believed that the plasma can follow some vertical field lines, and therefore the ionosphere can expand by diffusion, vertically to very high altitudes. This shape-profile variability will be studied with more detailed in chapter 3.

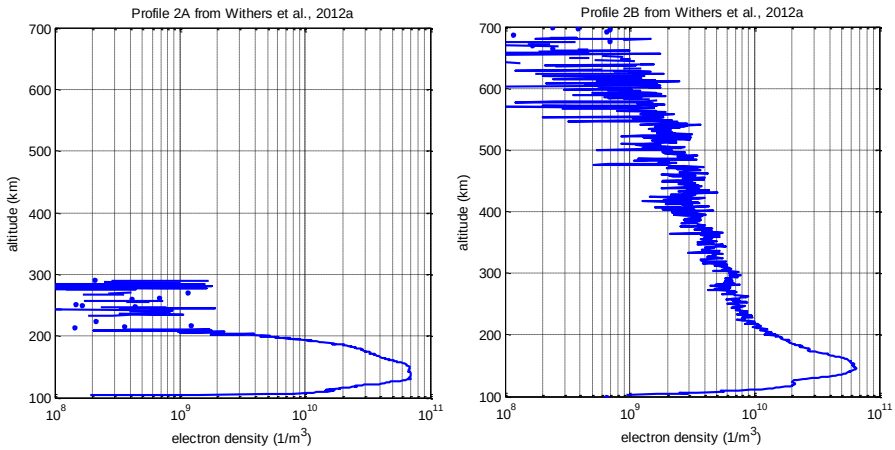

Figure 1.8: Two electron density profiles from Withers et al., (2012a) illustrating variations in the vertical extent of the ionosphere due to presence of solar magnetic field (2A) and crustal magnetic field (2B). Left panel: MaRS (Mars Express) profile at latitude 42ºN, longitude 24ºE, χ=69º, orbit 1949, date 2005-07-22, local time 11 hours. Right panel: MaRS (Mars Express) profile at latitude 82ºS, longitude 180ºE, χ=82º, orbit 9613, date 2011-07-14, local time 21 hours.

On the other hand, the nightside ionosphere is an important feature of the atmosphere and space environment of Mars. It participates in the global-scale plasma circulation and system of electromagnetic fields and currents, and is a conduit through which the energy and momentum of particles in the space environment are transferred into the neutral atmosphere and a reservoir from which volatile species are removed from Mars (Withers et al., 2012b). The understanding of the nightside ionosphere remains substantially incomplete, with very little published data compared to the dayside. It is important to note that the nightside ionosphere does not start at solar zenith angle of 90º because at ionospheric altitudes (e.g. 100 km to 200 km) there exists sunlit for solar zenith angles up to about 105º–110º (Lillis et al., 2009).

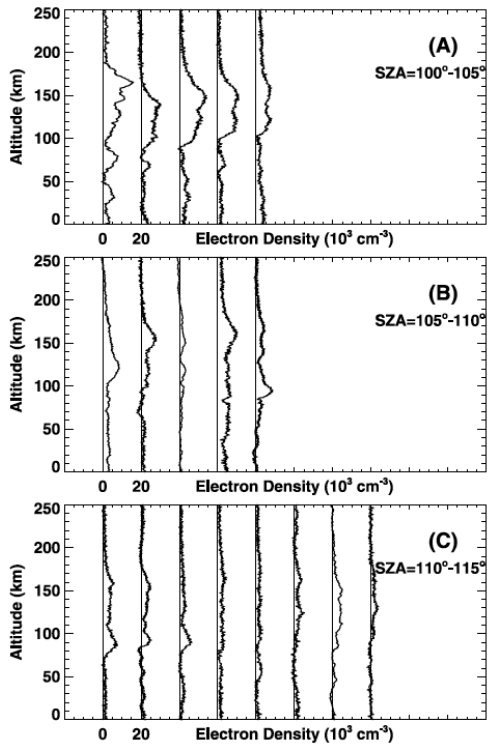

Figure 1.9: Mars Express MaRS nightside electron density profiles (Part I). Each profile in is offset from its neighbour by $2x10^4$ cm^{-3}. Vertical lines indicate zero electron density for each profile. Note that an altitude of 120 km is illuminated by sunlight for $\chi \leq 105^o$ (adapted from Withers et al., 2012b). In them, it is observed how the electron density decreases when solar zenith angle increases and the ionospheric shape varies.

The latest information about nightside part comes from Withers et al., (2012b). Using MaRS (Mars Express) data, they processed 37 vertical profiles of ionospheric electron density (see Figure 1.9 and 1.10). All observations and

models indicate that the nightside ionosphere of Mars varies irregularly with location and changes in nightside electron density over 260 km of horizontal distance must be accepted as highly likely. Peak electron densities decrease with increasing solar zenith angle up to 115º, consistent with transport of dayside plasma as an important plasma source. At higher solar zenith angles, neither peak density nor peak altitude depends on solar zenith angle, suggesting that the transport of dayside plasma is no longer an important plasma source. Electron precipitation is likely to be the dominant source here under normal circumstances, leading to peak altitudes of 130-170 km. The energy spectrum and pitch angle distribution of these precipitating electrons depend on the magnetic environment. During solar energetic particle events, low-altitude plasma densities are enhanced and peak altitudes can be 90 km, much lower than usual (Withers et al., 2012b). Moreover, for solar zenith angles higher than about 100º, Gurnett et al., (2008) reported "irregular patches" of ionosphere, with higher peak densities occurring in areas of strong crustal magnetic fields. Also for these values of solar zenith angle, Safaeinili et al., (2007) reported higher peak densities specifically where the crustal magnetic fields were closer to vertical than horizontal.

This irregularity and its correlation with crustal fields is consistent with some combination of electron impact ionization, transport from the dayside and dynamic magnetic field topology. All these phenomena control the nightside ionosphere (Lillis et al., 2009). At locations with strong crustal magnetic fields no such dependence on the solar zenith angle is observed, indicating that these magnetic fields are able to retard plasma transport processes. In such areas, the inclination of magnetic field becomes a key parameter: the occurrence rate of the nightside ionosphere is more than four times larger at locations where the magnetic field is nearly radial than at the locations where the magnetic field is nearly horizontal (Němec et al., 2010). Overall, the near-terminator nightside ionosphere is highly variable and is not well understood, while the deep nightside ionosphere (solar zenith angles between 125º–180º) remains completely unexplored (Withers, 2009; Lillis et al., 2009).

Despite these discoveries made in the last 10 years, there still remain some open questions, as the importance of atmospheric escape for the evolution of the planet's climate; what is the behaviour of the Mars' ionosphere over a solar cycle; what causes the transient multiple layers in the ionosphere; what controls the transient nature of the ionopause; how solar forcing determines ionospheric properties… Since the ionosphere of Mars forms an important part of the Mars system and plays a key role in the volatile escape processes that have dehydrated Mars over solar system history, a good knowledge of the ionospheric variability behaviour for any kind of condition is something essential.

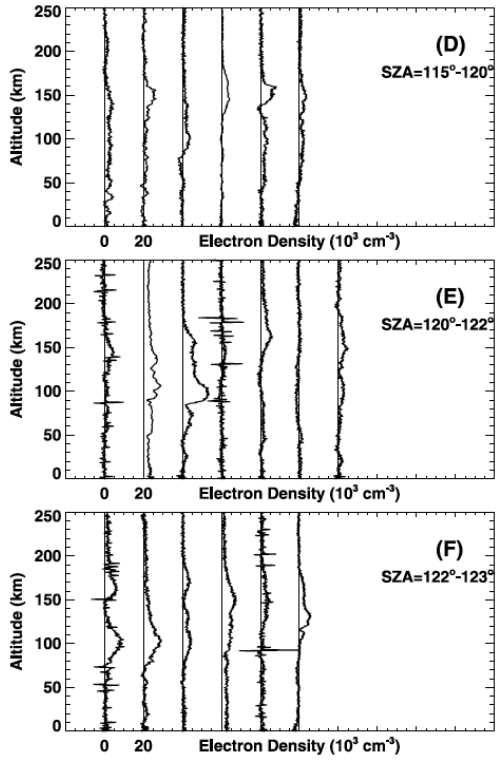

Figure 1.10: Mars Express MaRS nightside electron density profiles (Part II). Each profile in is offset from its neighbour by $2x10^4$ cm^{-3}. Vertical lines indicate zero electron density for each profile. Note that an altitude of 120 km is illuminated by sunlight for $\chi \leq 105°$ (adapted from Withers et al., 2012b). In them, it is observed how the electron density decreases when solar zenith angle increases and the ionospheric shape varies.

1.2.3 Ionospheric escape

If an ion is accelerated to an energy exceeding the planet's escape energy, it escapes the planet. This process is called the ion escape process mechanism, which has been measured and quantified in particular by the ASPERA-3 experiment aboard Mars Express (e.g. Lundin et al., 2009, Barabash et al., 2007). The planetary ions are accelerated by electric fields generated in the induced magnetosphere. The composition of this outflow reflects the depth of solar forcing in the martian ionosphere. The loss rates are of the order of a few grams per second. If propagated backward over a period of 3.5 billion years, the total removal is of 0.2 to 4 mbar of carbon dioxide and a few centimetres of water, which is very low, and cannot explain the total loss of the atmosphere over time.

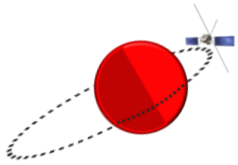

Chapter 2.

Data analysis

2.1 Data type

The current information about the martian ionosphere is known thanks to several different types of experiments: Retarding Potential Analyzer on board the two Vikings landers; Electron Reflectometer (ER) on board Mars Global Surveyor (MGS); ASPERA Energetic Neutral Atoms Analyzer on board Mars Express (MEX); radio-occultation on various orbiters; MARSIS ionospheric topside sounder and MARSIS measurement of Total Electron Content (TEC) aboard the Mars Express spacecraft; SHARAD measurement of Total Electron Content (TEC) aboard the Mars Reconnaissance Orbiter (MRO).

Information on the composition of the ionosphere essentially comes from the data acquired by the Retarding Potential Analyzer (RPA) during the descent of the Viking landers in 1976. Up to now -before MAVEN arrival to Mars expected for September 2014-, these instruments have provided the only two vertical in situ profiles on the composition of the martian dayside ionosphere (Hanson et al., 1977; Chen et al., 1978). They measured vertical profiles of O_2^+, CO_2^+ and O^+ between 100 km and 300 km. As mentioned in the previous chapter, the ion composition data are strong evidence for the presence and importance of atomic oxygen in the neutral atmosphere. Although CO_2 is the dominant neutral, O_2^+ is the dominant ion.

Information on the suprathermal (energetic) population of the ionosphere essentially comes from two sensors: the electron reflectometer (ER) aboard Mars Global Surveyor (Acuña et al., 1998) and the ion and electron spectrometers part of the ASPERA experiment on Mars Express (Barabash et al., 2004). The ER is a symmetrical quadspherical electrostatic analyzer with a field of view of 360° by 14°. The sensor can measure electron energy from 1 eV to 10 keV with a resolution $\Delta E/E$ of 0,25. The MEX spectrometers cover the range 10 eV to 20 keV with a resolution of 0,08. These instruments perform in-situ measurements; therefore the plasma characteristics are acquired at relatively high altitudes (above 250 km for MEX, and at 400 km for MGS).

Concerning the physical ionospheric properties, most of the information on the electron density has been gathered by the numerous radio-occultation experiments performed by the Mars, Mariner, Viking, Mars Global Surveyor and Mars Express satellites. This method, which will be explained in more detail in section 3 of this chapter, is the simplest and the most common ionospheric remote sensing technique that has been used outside the Earth. It is based on the fact that radio waves transmitted from a satellite, as it flies behind a solar

system body, pass through an atmosphere and ionosphere undergo refractive bending, which introduces a Doppler shift in addition to its free space value. This difference, commonly called Doppler residual, is proportional to the refractive index of the media through which the wave travels (Schunk and Nagy, 2009). These measurements allow retrieving of the vertical thermal electron density profile.

Furthermore, since mid-2005 another instrument called MARSIS (Mars Advanced Radar for Subsurface and Ionosphere Sounding) (Picardi et al., 2004) on board the European Mars Express mission (Chicarro et al., 2004), is operating and delivers a new dataset with a much better global coverage. In particular, in the so-called AIS mode (Active Ionospheric Sounding mode), MARSIS works as an ionospheric sounder and records ionograms (a data set of the received power as a function of the time delay and frequency) to analyze the electron density of the Mars topside ionosphere. This radio-sounding technique used by Mars Express sounder and digisondes on Earth share the same physical principles. From these data, it has been possible to gain knowledge on the martian ionosphere as never achieved before. Similarly, this instrument operates in another mode, called the subsurface-sounding mode, from which one can derive the total electron content of the ionosphere (Safaeinili et al., 2007, Mouginot et al., 2008, Lillis et al., 2010, Cartacci et al., 2013). SHARAD radar on board MRO shares exactly the same principles (Campbell et al., 2011 and 2013). Thanks to both operational modes of MARSIS instrument, the amount of available ionospheric data is the largest in history. As these data are in situ ionospheric measurements, with high accuracy and with an almost complete spatial (almost the whole planet) and temporal (nearly a full solar cycle) coverage, Mars Express MARSIS data have been selected as the most appropriate data for the study and modelling the ionosphere of Mars in this doctoral thesis. Both modes will be explained in detail throughout this manuscript.

2.2 Acquisition and processing of the MARSIS AIS data

The Mars Advanced Radar for Subsurface and Ionospheric Sounding (MARSIS) is a low-frequency radar instrument on board Mars Express mission. This instrument consists of a 40-meter tip-to-tip electric dipole antenna, a transmitter, a receiver and a digital data processing system (Picardi et al., 2004). Although its primary objective is to sound the most upper subsurface of Mars, it can also use to analyse the martian ionosphere in the Active Ionospheric Sounding (AIS) mode.

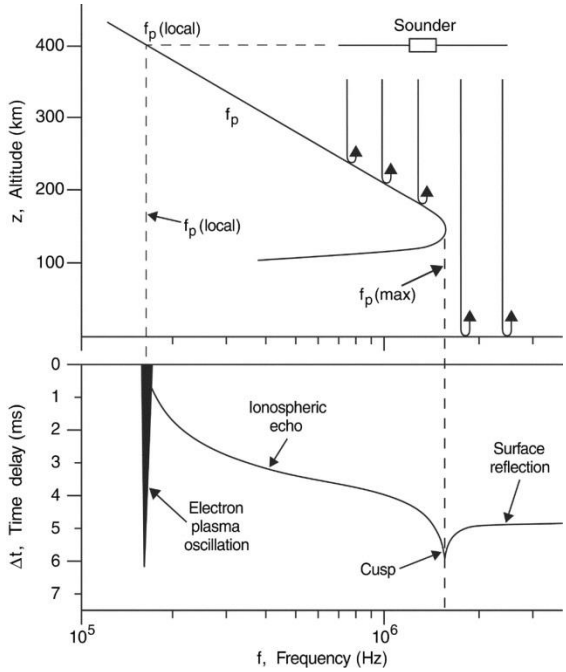

Figure 2.1: The top panel shows a representative profile of the electron plasma frequency (fp) in the martian ionosphere as a function of altitude z, and the bottom panel shows the corresponding ionogram, which is a plot of the delay time Δt for a sounder pulse at a frequency f to reflect and return to the spacecraft (From Gurnett et al., 2005).

In this mode the sounder of the spacecraft sends through the topside of the ionospheric plasma a vertical radio wave of the frequency f_w. The waves are propagated through layers of increasing electron density while its frequency is greater that the plasma frequency of the surrounding plasma. When it reaches the layer with $f_w=f_p$ (f_p is the *plasma frequency*) the wave is reflected and goes back to the sounder which measures the delay time between the signal emission and its echo reception (Figure 2.1). This cycle is repeated step by step for a range of wave frequencies covering the whole spectrum between the local plasma frequency at the altitude of the spacecraft and the maximum plasma frequency of the topside (Bauer, 2008). In particular, in this mode, the instrument transmits a 91.4 μs short monochromatic radio pulse and then listens for the echoes during 7.3 ms recording 80 samples of the electric field spectral density at a sampling rate of 91.4 μs.

MARSIS can emit radio frequency signals (RF) in a frequency range between 0.1 and 5.5 MHz at a maximum radiated power of 15 W. The maximum plasma frequency peak in the ionosphere of Mars is located at an average altitude

around 150 km. To record one complete ionogram this procedure is repeated for a set of 160 different frequencies taking 1.26 s in total. An ionogram is recorded every 7.54 s. The acquisition of MARSIS data is strongly controlled by the spacecraft orbit. Mars Express goes over a highly eccentric orbit with a periapsis altitude of about 275 km, an apoapsis altitude of about 11,000 km and a period of 6.75 h (Chicarro et al., 2004). Because of signal-to-noise limitations, ionospheric sounding data are only collected when the spacecraft is near periapsis.

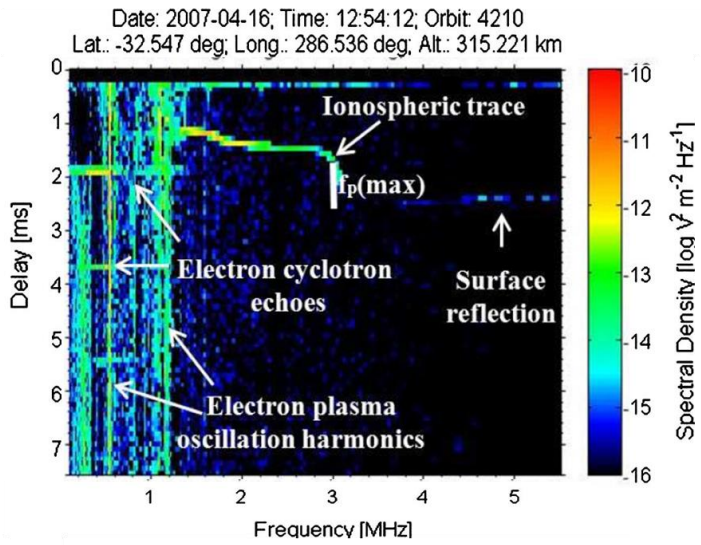

Figure 2.2: Example of an ionogram obtained from MARSIS instrument using MAISDAT tool. Main characteristics are labelled.

A typical MARSIS ionospheric sounding pass starts at an altitude of about 1200 km, continues through periapsis at about 275 km, and ends at an altitude of about 1200 km. The total duration of an ionospheric sounding pass usually is about 40 min (Gurnett et al., 2005) and around 280 ionograms can be recorded during this time. However, as the instrument has other modes of operation (the main one is the subsurface mode which objective is to map the martian subsurface to study the distribution of different buried materials, as water, in the upper layer of the martian crust (Picardi et al., 2005)), it is very common to find AIS for 10 minutes, then subsurface mode around the pericenter, and then AIS again.

An AIS ionogram (Figure 2.1 bottom part, Figure 2.2) is a two-dimensional plot of time delay and frequency. It represents the echo delay time for a series of signals with varying frequency. The frequency varies along the x-axis in the

image and the signal delay along the inverted y-axis. The echo is visualized by a colour coded spectral density of the E-field component of the returning electromagnetic wave. Starting at zero, the response delay increases with frequency. This part of the response trace is called *ionospheric echo* and corresponds to frequencies reflected in the ionosphere. When the frequency approaches the maximum plasma frequency $f_p(max)$ the delay increases dramatically due to the decreasing slope of the function $f_p(z)$. At the frequency just above $f_p(max)$, a cusp indicates when the signal frequency is high enough to pierce the ionospheric layer. This feature comes because as the frequency increases together with the electron density the pulse velocity decreases almost to zero at the critical frequency of the layer. If frequency keeps increasing, the waves reach the surface of the planet and experiment the reflection on the surface (Bauer, 2008). In the ionograms recorded close to the periapsis, almost always appear vertical lines at different frequencies called *plasma oscillation harmonics*. They come from the electro static plasma oscillations, which are detected by MARSIS receiver due to specific technical characteristics. These harmonics can actually be used to derive the local plasma frequency by measuring the spacing between the vertical lines (Duru et al., 2008). Other important features that appear sometimes in the AIS ionograms are the horizontal lines located in the left side of the ionograms and equally spaced in delay time. They are known as *electron cyclotron echoes* and their time spacing can be correlated with the cyclotron frequency of the local crustal magnetic field crossed by Mars Express (Gurnett et al., 2008).

The MARSIS AIS Dataset is available in the ESA's Planetary Science Archive (PSA). This type of data is written in binary files, where everyone contains all received records from the AIS operation phase of one orbit, i.e, they contain every ionogram. The data files are named FRM_AIS_RDR_XXXX.DAT where XXXX is the orbit number. All the geometrical information concerning the sounding events (coordinates of the spacecraft above Mars, altitude, solar angle conditions…) is contained in one single file, GEO_MARS.TAB, for all data files. There is also a C-program to read the binary file format. The currently available data (at time to write) corresponds to the period: June 2005 - July 2011, in particular between the orbits 1844-9569 (although not in every orbit AIS data have been recorded).

In order to process these data, the European Space Agency has developed a MATLAB software, called MAISDAT (Bauer, 2008). The methodology used to analyse the ionograms follows exactly the same procedures explained in Gurnett et al., (2005) and Morgan et al., (2008). With this software it is possible, among other many options, to perform the inversion of the ionospheric trace in order to obtain the electron density profiles, which are the most important

information that can be retrieved from the AIS data. To perform this operation, also known as *ionogram reduction*, MAISDAT uses a method based on an inversion of the integral equation (2.1):

$$\Delta t(f_w) = \frac{2}{c} \int_{z_{refl}}^{z_{sc}} \frac{dz}{\sqrt{1 - \left(f_p(z)/f_w\right)^2}} \qquad 2.1$$

whose formal solution is the Abel's equation (2.2):

$$\tilde{z}(f_p) = \frac{c}{\pi} \int_{\alpha_0}^{\pi/2} \Delta t(f_p \, sin\alpha) d\alpha \qquad 2.2$$

Δt is the delay time, f_w is the used frequency, f_p is the plasma frequency, c is the light speed, z_{sc} is the spacecraft altitude, z_{refl} is the altitude of the ionospheric reflexion, $sin\alpha = \frac{f_w}{f_p}$ with $f_w \leq f_p$ and $\sin \alpha_0 = \frac{f_p(z_{sc})}{f_p}$ (Gurnett et al., 2008).

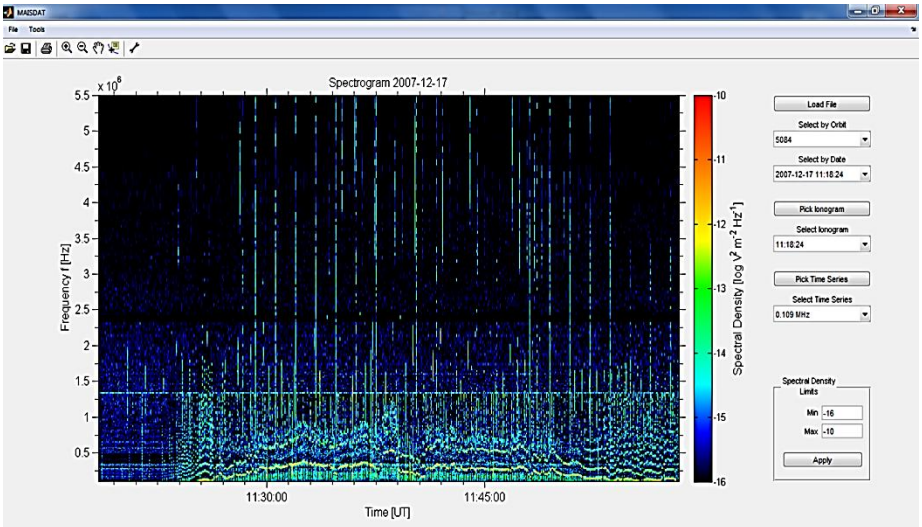

Figure 2.3: Example of a spectrogram obtained from MARSIS instrument using MAISDAT tool.

When MAISDAT is initiated, the main window that appears is a spectrogram -a sounding frequency versus time plot- (Figure 2.3) that is composed by stacking all the ionograms contained in the data file along their delay axis. The spectral density of the sounding echo for delay time and frequency values is displayed colour coded in the units: $V^2m^{-2}Hz^{-1}$. This window offers several options:

selecting a data file, opening an ionogram display, opening a time series display or setting the range of spectral density values to be mapped to the colour scale. To analyse the ionospheric trace, it is necessary to start selecting an orbit and an ionogram. Then, a new window with the ionogram tool display described above is shown (Figure 2.4).

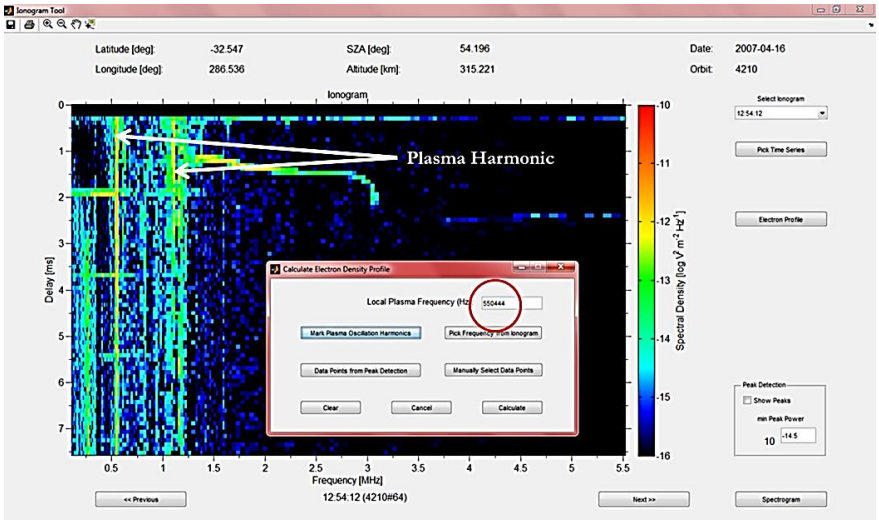

Figure 2.4: Harmonics of the local plasma frequency selection with MAISDAT tool. Red circle shows the value of the local plasma frequency in Hz for this particular ionogram.

To begin the inversion, it is necessary to know the plasma density in the vicinity of the spacecraft because the corrected range for each data point depends on the plasma density profile of the sounding wave path (Figure 2.4). This information can be obtained from the harmonics of the local plasma frequency as it is explained in Gurnett et al. (2008). These harmonics (vertical lines) are easily measured from their average frequency separation by digitizing the plot. Then, to determine the ionospheric trace (Figure 2.5) it is possible to follow either an automatic or a manual procedure. In the first case, it is usually complicated to select the correct trace due to several strong interferences at frequencies below 1 MHz. In the second case, this difficulty can be overcome by the user´s visual inspection.

In this thesis it is proposed to select a clear ionogram with a well-defined vertical signature of the trace in the highest frequencies, and to click on the bottom of this part of the trace because the corresponding frequency is the $f_p(max)$ which is directly proportional to the maximum ionization in the

ionosphere. To select and digitize the rest of the trace until the lowest frequency, where it is no longer distinguishable from noise, it is proposed to click on the top of the trace because it is the first record of the refection signal.

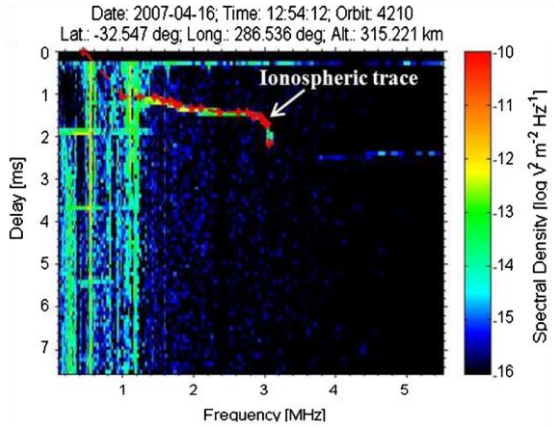

Figure 2.5: Trace identification for the ionogram reduction. In red it shows the identification of the trace as it is described in this document.

Then, the digitized information is analysed by MAISDAT, who gives the corrected and uncorrected electron density profiles of the ionogram (Figure 2.6).

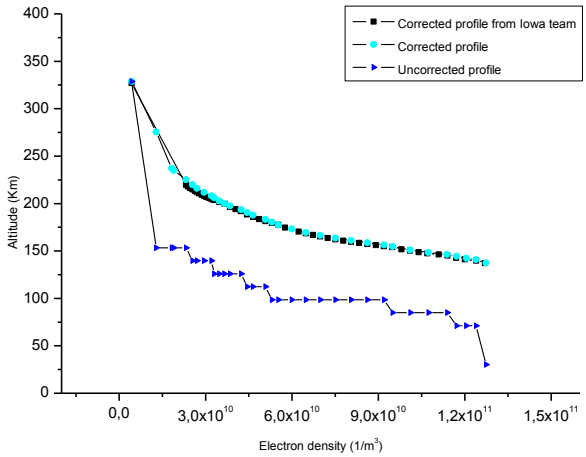

Figure 2.6: Example of topside ionospheric profiles obtained from the ionogram 178 in the orbit 2405 of Mars Express. There are two different kinds of profiles: the corrected profile where the true height, corrected by the oscillation harmonic in the frequency is used and the uncorrected one where the virtual height is considered. Another corrected profile, obtained at Iowa University by the MARSIS team, is also displayed. The agreement with the ionogram corrected is very remarkable, and confirms that the same method is applied to obtain the electron density.

The corrected profiles use the true height in the ionosphere corrected by the oscillation harmonic in the frequency, and the uncorrected profiles use the virtual height. It is important to note that these profiles only explore the top of the ionosphere, i.e. the plasma that exists from the place where Mars Express spacecraft is located to the region of maximum electron density. The electron density measure accuracy is about ±2% and the uncertainty of the altitude apparent range is about ±6.8 km. (Morgan et al., 2008 and 2013b).

The top of Figure 2.6 shows a typical profile from MARSIS radar with the corrected and uncorrected profiles obtained from the 178 ionogram of the orbit 2405. For comparisons, this figure also includes another corrected profile from the same ionogram obtained by the Iowa University team. The results match pretty well.

2.3 Mars Express data comparison

Mars Express spacecraft carries on board another instrument that is able to take measurements of the martian ionosphere, the Mars Radio Science (MaRS) instrument.

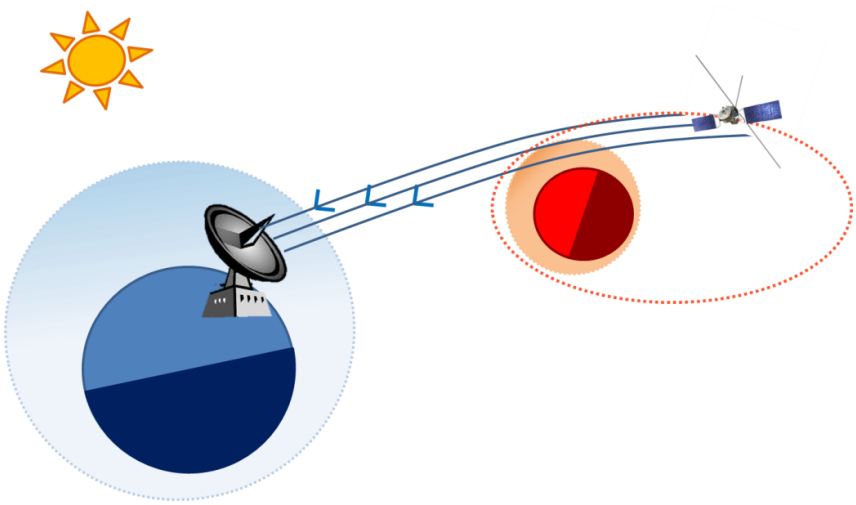

Figure 2.7: Scheme of typical Mars Express radio-occultation experiment. Earth is represented in blue, Mars in red, Mars Express orbit in red dashed line, Mars atmosphere-ionosphere in degraded orange and Earth atmosphere-ionosphere in degraded blue. Blue arrows symbolize the path of the radio signals from Mars Express to the Earth ground stations.

This experiment uses the Radio-Occultation technique to sound the ionosphere and to derive vertical electron density profiles. This procedure is completely different to the sounder method. In general terms, MARSIS sounder sends a sweep of vertical downward radio-signals and takes direct measures of the delay time of those frequencies. In its turn, MaRS sends a radio-signal at two frequencies (described below) through the atmosphere along the spacecraft-Earth line just at the moment when the spacecraft is occulted to the Earth antennas by Mars (Figure 2.7). From the change in the propagation path and the Doppler effect on the signals it is possible to retrieve the electron density profiles.

Radio-occultation measurements are remote sensing techniques used for measuring physical properties of a planetary ionosphere. Just in the moment when the spacecraft is occulted by Mars as seen from the Earth, the antenna emits radio signals in the X and S frequency bands (8.4 GHz and 2.3 GHz, respectively) which pass through the Mars's atmosphere and ionosphere (Figure 2.7). On Earth these radio signals are recorded. After correcting them by the Earth's ionosphere effect, measure the bending angle because of the martian atmosphere/ionosphere and use the standard scheme for processing radio-occultation data (Paetzold et al., 2005), the profile of electron density in the martian ionosphere path crossed by the signal can be retrieved.

Due to these differences in the technique, the profiles from MaRS are different from those given by MARSIS. While MaRS allows obtaining the profile of the ionosphere in the altitude range 80-1000 km, MARSIS only allows obtaining profiles from the topside to the maximum ionization peak. In addition, as MaRS requires an occultation, which occurs only during limited periods, and only once per orbit in the case of Mars Express, MARSIS provides a better planet coverage and horizontal spatial resolution, and can work with a larger solar zenith angle range.

Radio-science is a well-known technique, which has been used widely in the study of the Earth and other planets ionospheres. Therefore, in this thesis it considers these data as a reference to compare and validate the electron density profiles obtained from MARSIS soundings. To this end, different profiles from both kinds of experiments under similar conditions in term of solar zenith angle, solar longitude, martian latitude and solar activity ($F_{10.7}$ index) have been selected. Most of the time, these data show similar results especially in the region of maximum ionization where the value of the altitude and the electron density of the maximum peak are practically the same.

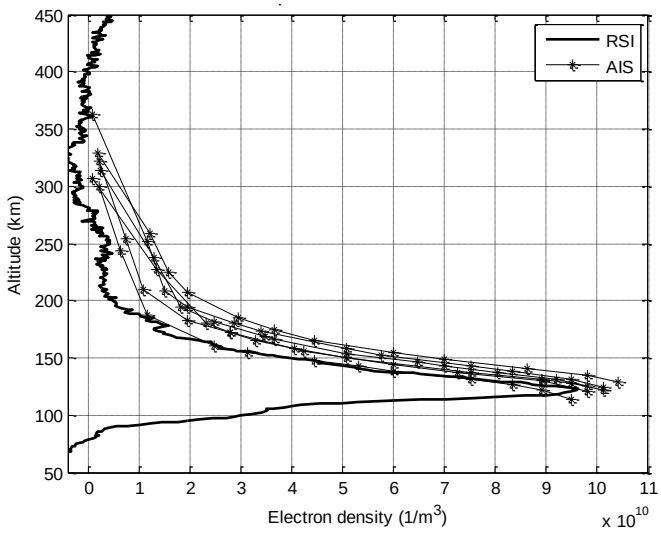

Figure 2.8: First comparison between a profile obtained from Mars Express Radio Science (Year: 2004, DOY: 180, Latitude: 10.2471º, χ=74.6059º, Ls=53.21º, $F_{10.7}$= 85) (bold line) and some topside profiles obtained from MARSIS instrument with similar conditions of location, solar zenith angle, solar activity and solar longitude (Orbit: 3065, ionograms: 20-40, χ=61-65º, Latitude= 11º-1º, Ls=59.65º, $F_{10.7}$= 80) (light lines).

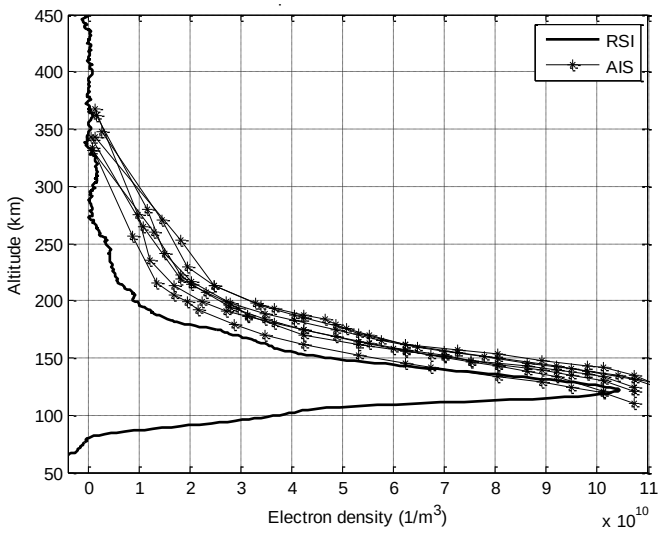

Figure 2.9: Second comparison between a profile obtained from Mars Express Radio Science (Year: 2006, DOY: 084, Latitude: 16.6432º, χ=54.3843º, Ls=30.15º, $F_{10.7}$= 76) (bold line) and some topside profiles obtained from MARSIS instrument with similar conditions of location, solar zenith angle, solar activity and solar longitude (Orbit: 5240, ionograms: 155-186, χ=50º-51º, Latitude=26º-11º, Ls=25.14º, $F_{10.7}$= 73) (light lines).

The biggest differences appear close to the topside of the ionosphere (about 180 km) where the presence of other physical processes like vertical transport due to diffusion or penetration of an induced magnetic field can play a significant role.

A typical example of this very good agreement is shown in Figure 2.8 where the MARSIS profile matches with the radio-occultation profile in the altitude range 130-190 km. The remaining of the MARSIS profiles is similar in electron density but with a small shift in altitude (by about 10%). Close to the maximum peak of ionization the results are practically the same in both cases with a deviation of about 11% in altitude and of about 5% in electron density. With respect to the electron density, the greatest differences reach almost the 50 % of the radio-occultation profile at 160 km. As for the altitudes, they can amount to the 40 % of the radio-occultation profile and appear close to the topside. Figure 2.9 is another example of this kind of comparison where the results are practically the same.

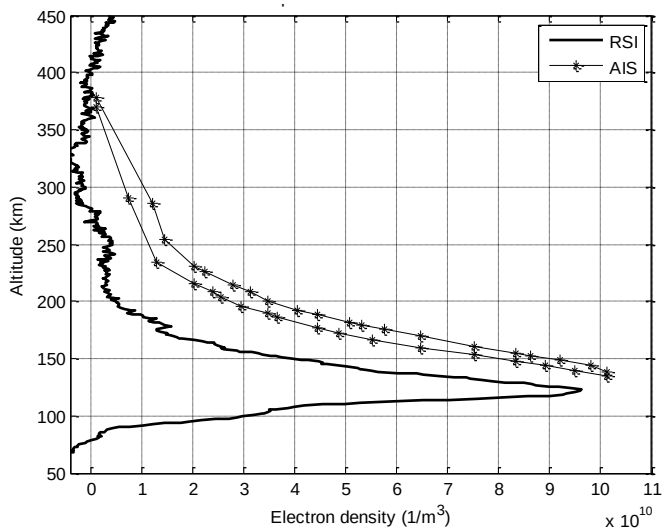

Figure 2.10: Third comparison between a profile obtained from Mars Express Radio Science (The same profile that in Figure 2.8, Year: 2004, DOY: 180, Latitude: 10.2471º, χ=74.6059º, Ls=53.21º, $F_{10.7}$= 85) (bold line) and two topside profiles obtained from MARSIS instrument with similar conditions of location, solar activity and solar longitude but different conditions for solar zenith angle (Orbit: 3065, ionograms: 2-4, χ=57-58º, Latitude=19.9º-18.9º, Ls=59.65º, $F_{10.7}$= 80) (light lines).

However, when the difference in some of the considered parameters increases, the degree of similitude in the comparison decreases. Figures 2.8 and 2.10 show the same radio-occultation profile, which is compared with MARSIS profiles from the same orbit. The only differences between these last profiles are the values of solar zenith angle and latitude, which have increased in the second

case. It is possible to observe that in Figure 2.10 both kinds of profiles do not match as well as in Figure 2.8 where the conditions of every parameter are more similar. This result indicates that if similar conditions of solar zenith angle, season, latitude and solar activity are not considered, large differences in the adjustments can appear.

It is important to note that MaRS data were selected not close to the terminator, to avoid problems of the spherical symmetry assumed in the radio-science data retrieval technique. Nevertheless, this good agreement between the profiles obtained from two different instruments give confidence in this data analysis methodology.

2.4 Discussion and summary

In order to describe the ionospheric soundings obtained by MARSIS instrument working in the Active Ionospheric Sounding (AIS) mode, this manuscript presents the main characteristics of this equipment, the shape and location of the AIS dataset and the structure and particularities of the AIS ionograms. In the same way, the methodology adopted to produce the inversion of these ionograms is described by introducing the MAISDAT tool. This MATLAB utility uses the Abel equation as base for processing and is able, among other many options, to obtain the electron density distribution.

To start with the inversion routine in MAISDAT following the Bauer (2008) procedure, the first step is to calculate the plasma frequency at the spacecraft altitude using the harmonic lines (vertical lines in the left part of the ionogram). So, it is important to choose ionograms not only with a good ionospheric trace (especially in the highest frequencies) but with good harmonics too. The next step is to select and digitize the ionospheric trace in a manual way starting with the highest frequencies. In the vertical part of the trace it is advisable to select the bottom zone and in the rest of the trace the upper part of the pixel because this part corresponds to the first record of the reflection signal. The manual fitting goes on until the lowest frequency, where the trace is no longer distinguishable from noise. Finally, MAISDAT processes the digitized data to calculate the electron profile of the ionogram.

A comparison between AIS electron density profiles and MaRS radio-science electron density profiles from the Mars Express radio-occultation experiment has been accomplished to validate the ionospheric profiles obtained. As the radio-occultation technique is well known in the study of the Earth and

planetary ionospheres, can be considered as a reliable reference. In this thesis, different profiles from both kinds of experiments with similar conditions of solar zenith angle, solar longitude, martian latitude and solar activity, have been compared. In a large number of cases, the comparison shows similar results, especially in the maximum region of ionization where the value of the altitude and the electron density of the maximum peak are practically the same for both kinds of data. These comparisons give confidence that the MAISDAT processing is correct.

The martian ionosphere formation is influenced by many factors. The most typical are the absence of a global magnetic field, the solar radiation or the solar activity. For this reason, one of the most important goals of this doctoral thesis was to develop a global empirical model of the dayside ionosphere of Mars. With this purpose and as it will be explained in next chapter, data from the full dataset of MARSIS AIS ionograms was analysed by using the MAISDAT software.

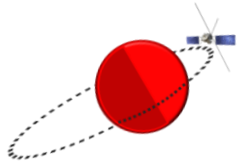

Chapter 3.

Development of the NeMars empirical model

3.1 General description

NeMars is an empirical model of the electron density in the dayside martian ionosphere (primary and secondary layers) developed during this thesis. The model is mainly based on MARSIS AIS data (Active Ionospheric Sounding from the Mars Advanced Radar and Ionospheric Sounding experiment aboard Mars Express mission) and to a lesser extent on radio occultation data from the NASA Mars Global Surveyor mission. The model is able to properly reproduce the main characteristics of the electron density profiles obtained with the two techniques by considering, as input parameters, the solar zenith angle, the solar flux $F_{10.7}$ as a proxy of the solar activity, and the heliocentric distance.

Several other empirical models have been previously published based on different available data-sets. Pi et al., (2008) developed a numerical model that adopts functions of two Chapman layers to compute Mars ionospheric electron densities at given local solar zenith angle and height from Mars Global Surveyor radio occultation. Mendillo et al., (2011) developed a model for the two main photochemical layers from several 1-dimensional iterations, constrained by radio-occultation data taken by MGS and MEX at the same time. Němec et al., (2011) published a study of electron density for the dayside of the main layer in the martian ionosphere. By using MARSIS AIS data, they studied the behaviour of the primary ionization layer in two different ionospheric regions, which are controlled by different physical mechanisms. The first one is a photochemical controlled region described by the basic Chapman theory, located in altitudes up to about 5 neutral scale heights above the peak of electron density. The second region is the diffusion zone, which is controlled by the induced magnetic fields originating from the interaction with the solar wind located at altitudes higher than about 10 neutral scale heights. NeMars models the martian ionosphere in the photochemical region which can reach altitudes up to about 200 km.

In the following sub-sections, the contribution of different parameters to the formation of each layer of the martian ionosphere is analysed step by step.

3.2 Data selection

Since June 2005, the topside sounder MARSIS on board Mars Express (MEX) has provided a large amount of data with much better coverage than previous missions. For this reason, the MARSIS AIS data set has been chosen to model

the ionosphere. As the sounding technique only permits the retrieval of the electron density profile from the maximum peak up to the satellite altitude, no information is available from MARSIS for the lower part of the Mars' ionosphere. Nevertheless, radio-occultation data from the radio science data of Mars Express and Mars Global Surveyor (MGS) missions have been used to study and model the lower layer, despite the fact that this kind of data has three shortcomings: the amount of data is smaller, their planetary coverage is reduced and the measurements are never, by design of the Mars Express mission, simultaneous with MARSIS.

In the next sub-sections, a summary of the characteristics of both kinds of data used is given. Data from Mars Express (MARSIS AIS and MaRS Radio Science) are available in the ESA's Planetary Science Archive (PSA) and data from Mars Global Surveyor (Radio Science) can be obtained from the NASA Planetary Data System (PDS).

3.2.1 MARSIS AIS data

Regarding the empirical modelling of the main ionospheric layer, a set of 1200 AIS ionograms from MARSIS instrument have been selected. At the time of writing, the available MARSIS data set corresponds to orbits 1844-9569 (June 2005 - July 2011). These data have been analysed using the MATLAB software called MAISDAT, developed by the European Space Agency for the Active Ionospheric Sounding Data Analysis (Bauer, 2008; Sánchez – Cano et al., 2012). The methodology used to analyse the ionograms follows exactly the same procedures explained in Gurnett et al., (2005), Morgan et al., (2008) and in the chapter 2 of this manuscript. As mentioned, the local electron density is derived from the plasma frequency harmonics (Duru et al., 2008), which are electrostatic plasma oscillations detected by the MARSIS receiver. The interpolation between data points used is exponential. As already commented, these data have an accuracy about ±2% in the electron density and an uncertainty about ±6.8 km in the altitude apparent range (Morgan et al., 2008 and 2013b).

The amount of available data is large for any condition like latitude, longitude, solar zenith angle, solar longitude, heliocentric distance, solar activity, etc. The ionograms have been selected one by one and all of them have been manually scaled. It has been preferable to limit the amount of data and to ensure the quality of information. Possible limiting assumptions in the results are discussed in the last section of this chapter. The considered criteria were the following:

☼ Ionograms that had been acquired when the spacecraft was above 600 km of altitude were not chosen because the plasma density in the vicinity of the spacecraft usually is quite low and therefore, the assumption of an exponential form in the gap between the spacecraft-local electron density and that at the first echo point becomes problematic. In this case, it is very difficult, if not impossible, to obtain the correct value of the harmonics of the local plasma frequency used to derive the local plasma frequency (Gurnett et al., 2005)-.

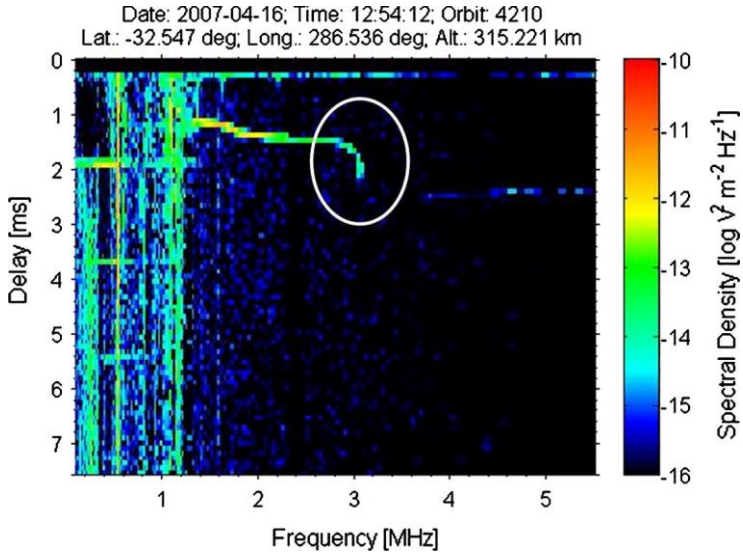

Figure 3.1: Example of a clean ionogram obtained from MARSIS instrument using MAISDAT tool. The white circle shows the last part of the trace with a well-defined vertical signature.

☼ Ionograms only in the dayside (solar zenith angle $\chi < 90^{o}$) were selected, as well as, over regions without presence of magnetic field anomalies on the martian surface to avoid any possible local magnetism effects in the ionospheric structure. These magnetic field anomalies were discovered and characterized by Mars Global Surveyor (e.g. Acuña et al., 1999, Langlais et al., 2004).

☼ As in this kind of ionospheric profile retrieval processes, the altitude is the parameter with larger scatter, clean ionograms with a well-defined trace were selected. It means that the lowest and the highest frequencies of the trace are the most critical areas to characterize the altitude of the full profile. At the lowest-frequency part, the trace is difficult to track

because of the noise and the overlap with the harmonic oscillations (Bauer, 2008). At the highest-frequency part, it is necessary to select a well-defined vertical signature of the trace in order to be sure that the values extracted are not affected by lack of definition in the ionogram and so, minimize the uncertainty of this parameter. An example of clean ionogram with a well-defined vertical signature is shown in Figure 3.1.

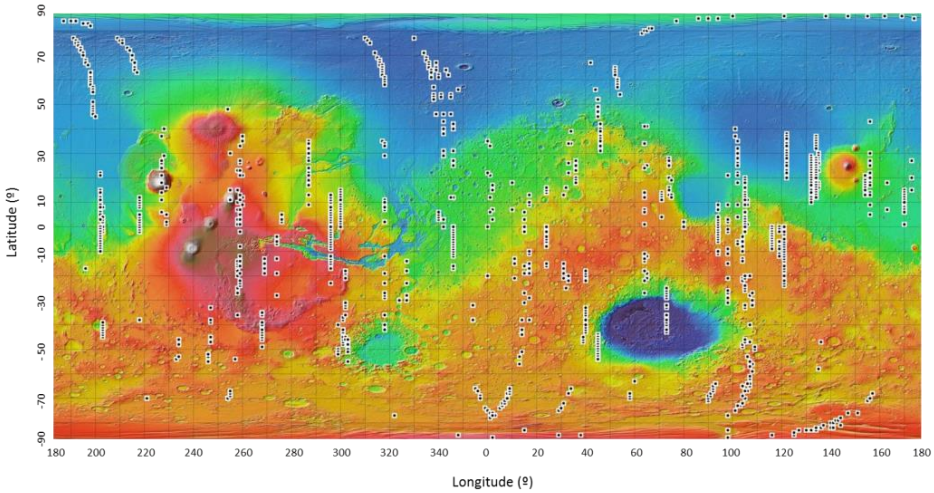

Figure 3.2: Global topographic map of Mars. Each black square corresponds to one of the 1200 AIS ionograms used to get the model.

Following this process, 1200 ionograms have been selected to model the main martian ionospheric layer. This sample offers a representative number of topside profiles in different conditions of latitude, longitude, solar zenith angle, solar longitude, Sun-Mars distance and solar activity (more info at Appendix I). Figure 3.2 shows the coverage and distribution of these data over the planet. Another sample of 500 selected ionograms, not previously used to develop the model, has been chosen to test the empirical equations of the main ionospheric layer. These ionograms also correspond to regions without presence of surface magnetic anomalies.

3.2.2 MGS and Mars Express radio occultation data

As mentioned before, radio occultation data have been selected to model the secondary ionization layer. Mars Global Surveyor spacecraft is the mission that

has provided most data of this nature: in total, there are 5600 electron density profiles measured between 24-12-1998 and 9-6-2005. Unfortunately, these measurements are restricted in solar zenith angle (70º-90º) and latitude (60º-85º North or South) due essentially to the observing geometry limitations between Mars and Earth orbits (Withers and Mendillo, 2005). A total of 500 electron density profiles have been selected, and as in the MARSIS AIS case, they have been chosen one by one. The selection was difficult because the lower layer is often embedded in the main layer and it is not easy to distinguish the precise location of the peak. In this case, as the objective was to build an empirical model, the localization of this peak is important to analyse its behaviour under different conditions and then, describe it with one equation. It means that if the peak behaviour is known for the visible cases, mathematically it can be extrapolated to the rest (see Appendix I). The two selection criteria were:

- Identifying clean profiles with a well-defined secondary ionization layer.
- Selecting profiles with different characteristics of heliocentric distance, solar longitude and solar activity.

The model equations have been tested with 50 radio occultation electron density profiles from Mars Express Radio Science (MaRS instrument), which were retrieved from PSA database and with 400 from Mars Global Surveyor, which were not used to develop the model because it has tried to give independent statistics. In the case of MaRS instrument, the number of available profiles is constrained by the special geometry needed for such experiment. This limitation in the amount of data is compensated because the coverage in solar zenith angle is much better than with MGS data. The period of these data spans from 2004 to now.

As can be seen in Acuña et al., (1998) or Krymskii et al., (2003), the formation of the secondary ionization layer is severely affected by the surface magnetic anomalies; therefore, only profiles over regions without surface magnetic anomalies have been chosen to avoid any possible contamination of the results due to this magnetic influence.

3.3 Peak characteristics

The Mars' ionosphere is assumed to behave under photochemical equilibrium in the region closest to the main ionization peak and the two main layers can be

represented by the α-Chapman equations. It means that the dissociation processes mainly are the dominant mechanisms of loss of ions.

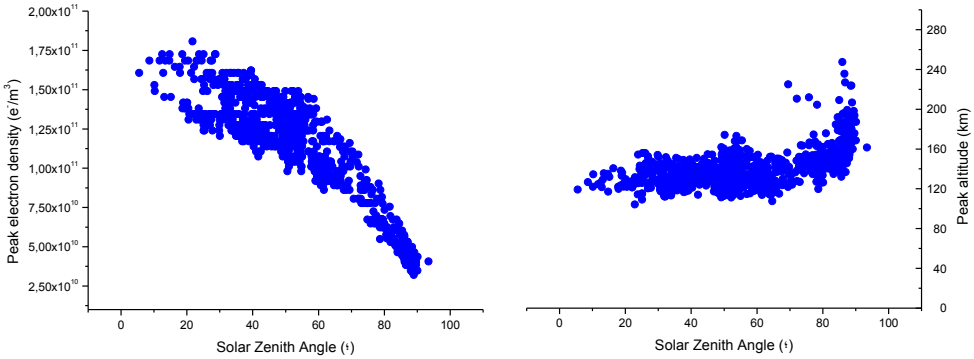

Figure 3.3: Martian ionospheric main peak variation with solar zenith angle. Electron density is represented in the left panel and altitude in the right one.

Following this theory, the electron density profiles of the primary and secondary layer can be represented, independently, with equation 1.8. For a Chapman layer, the electron density and peak altitude depend only on the solar zenith angle as is given in equations 1.5 and 1.9 (Hantsch and Bauer, 1990).

However, in order to represent more closely the observed behaviour of the martian ionosphere, it is necessary to introduce an altitude-variable scale height instead of a constant scale height and assuming the dependence on other parameters like heliocentric distance or solar activity. Figure 3.3 shows the behaviour of the electron density and altitude of the main martian peak.

3.3.1 Heliocentric distance versus solar longitude

Mars has an axial tilt of 25.19°, pretty close to the value of 23.44° for Earth, and thus Mars has four seasons as our planet does. *Solar longitude*, Ls, is the parameter that gives information about the seasons. It is the Mars-Sun angle measured from the Northern Hemisphere spring equinox (Ls=0º). In the Northern Hemisphere Ls=90º corresponds with the summer solstice, Ls=180º with the autumn equinox and Ls=270º with the winter solstice. As on Earth, seasons are the opposite for each hemisphere. Because Mars's orbit around the Sun is quite eccentric (distance varies between 1.38 and 1.66 AU), every Ls value corresponds to a specific heliocentric distance and in principle, the influence of

this parameter on the ionosphere could be expected. However, as it will be shown later, this influence has not been found.

The Solar Longitude parameter was used to represent the variation of the peak electron density in the primary layer along the martian year. The obtained plot (Figure 3.4, top panel) seems to indicate an increment of the electron density peak when the solar longitude increases. However, this tendency disappears when electron density peak data are normalized to the average Sun-Mars distance (Figure 3.4, bottom panel). To carry out this normalization, the well-known Chapman expression for the maximum electron density (N_m) in a plasma equilibrium situation was used (Schunk and Nagy, 2009):

$$N_m^2 = \frac{q}{\alpha} \qquad 3.1$$

where q is the ionization production rate and α the recombination coefficient. As q is directly proportional to the incident solar flux (I) which in its turn diminishes with r^{-2}, being r the distance from the Sun, the expression (3.1) gets:

$$N_m = \sqrt{\frac{q}{\alpha}} \propto \sqrt{\frac{I}{\alpha}} \propto \frac{1}{r}\sqrt{\frac{1}{\alpha}} \rightarrow N_{m2} = N_{m1}\frac{r_1}{r_2} \qquad 3.2$$

Therefore, the maximum electron density decreases with r^{-1}. Using these basic theoretical concepts, it has been possible to reduce the peak electron density data obtained from the MARSIS ionograms recorded at different heliocentric distances to the average Mars orbit, 1.52 AU (Astronomical Units). This normalization factor has been considered to obtain the bottom panel from the top one in Figure 3.4. As it can be observed, the apparent seasonal influence disappears when this normalization is introduced indicating that in ionospheric terms and for the electron density peak, the Mars orbit eccentricity effect is more important than the seasonal one. This result confirms those obtained by Lillis et al., (2010) which indicate that it is difficult to discern a clear correlation between the Total Electron Content (TEC) in the Mars ionosphere and the martian season. Therefore, with the amount of data analysed, it has been observed that the season influence in peak variations is pushed into the background by the Mars orbit eccentricity effect. This phenomenon is not so relevant for the Earth ionosphere due to its almost circular orbit around the Sun. Consequently, the Sun-Mars distance is one of the parameters that have been considered to develop the model as is detailed, layer by layer, in the following paragraph.

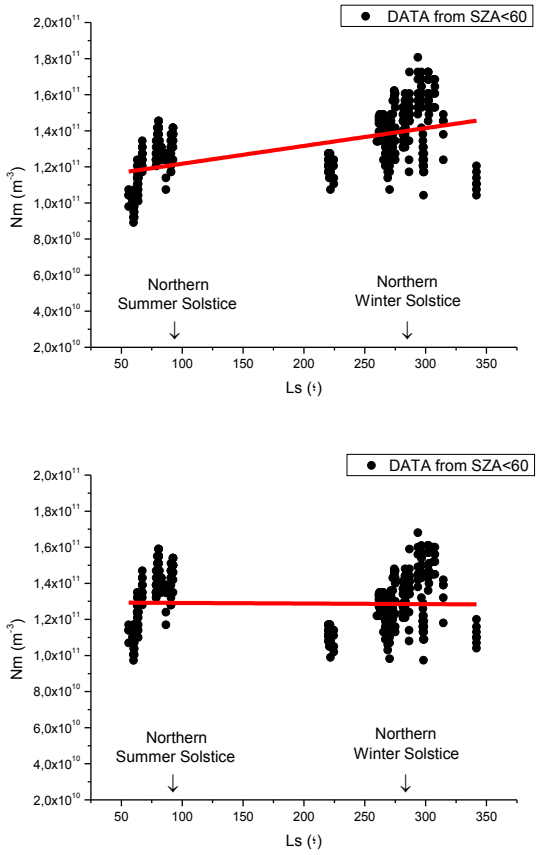

Figure 3.4: Relationship of the main electron density peak with seasons represented by solar longitude. In the top panel appear the raw data and in the bottom same data after the normalization for the Mars orbit distance to the Sun. It is possible to observe that the seasonal effect disappears when the distance between Sun and the spacecraft is considered.

Electron density of the main peak: In the case of the main layer, in a first step, each ionogram has been normalized to the average orbit (1.52 AU) following equation 3.2. Thus, the influence of the Sun-Mars distance disappears and solar flux and solar zenith angle effects can be studied in a more independent way (see next sub-section). **Electron density of the second peak**: In the case of the secondary layer, the process has been slightly different due to the lack of solar zenith angle data variation of the MGS mission. "Synthetic" data for the rest of solar zenith angle have been built under the assumption that the secondary layer can be represented by the Chapman function. Therefore, the synthetic data were obtained when the real data of the secondary peak were

introduced into the expression 1.8. After that, the procedure has been the same as for the main layer: each value has been normalized to the average orbit.

Height of both peaks: In the case of the peak altitude, and according to Němec et al., (2011), a dependence with the heliocentric distance was expected. However in this respect, this study is inconclusive and such dependence has not been noticed. It could be related to the fact that the data sample, based only on 1200 manually scaled ionograms, is much smaller than that from Němec et al., (2011).

3.3.2 Solar activity and solar zenith angle

The *solar zenith angle* (χ) is the angle between the incident solar radiation and the zenith at a specific place. This parameter is the main factor to be considered when the ionosphere is represented by the general Chapman function. As solar radiation reaching the upper atmosphere propagates into the ionosphere under a specific solar zenith angle, it is difficult to distinguish the solar activity effect on the electron density peak from that due to solar zenith angle. Therefore, it becomes necessary to analyse them together.

Mars receives less radiation than our planet because it is further away from the Sun. In addition, this radiation varies with the solar activity cycle. Despite its limitations, the $F_{10.7cm}$ *index* has been considered as the most adequate and practical solar activity index to be introduced into the empirical model to evaluate the solar flux. This index is a proxy for the number of sunspots and flares, and for the wavelength dependence of the EUV spectrum emitted by the sun. It's an integer whose unit corresponds to 10^{-22} $Wm^{-2}Hz^{-1}$. As the number of sunspots and the spectrum of solar radiation are the same for all objects in the solar system, it is not necessary to divide this number by the square of the distance from the Sun (Huestis et al., 2010). Therefore, $F_{10.7}$ cm is a proxy of the solar activity and evaluates the solar UV radiation in an easy and objective way. This index has been measured on a daily basis since 1947. Taking into account these parameters, the modelling construction continues as follow:

Electron density of both peaks: In the previous section, data were normalized to the average martian orbit (1.52 AU). At this point, to study the relationship between the peak electron density and the solar activity with no contamination of the solar zenith angle, data set has been initially split into small intervals of that angle. For every interval, the electron density has been fitted with the corresponding $F_{10.7}$ values taken from http://www.swpc.noaa.gov/ftpdir/

warehouse/ (Figure 3.5 and Appendix I). In each case, a linear relationship between the electron density peak and the solar activity for the same solar zenith angle has been observed. This result clearly differs from Němec et al., (2011) and Withers, (2009), who consider a root square relationship. However, in the $F_{10.7}$ range of 70-150, the usual $F_{10.7}$ values for the considered dates, the root square can be mathematically approximated by a straight line. Thus, residues obtained when these data were fitted to a line and to a root square show that both processes statistically are equivalent. Therefore, it was considered that a linear relationship can be accepted at least for the range of $F_{10.7}$ values considered.

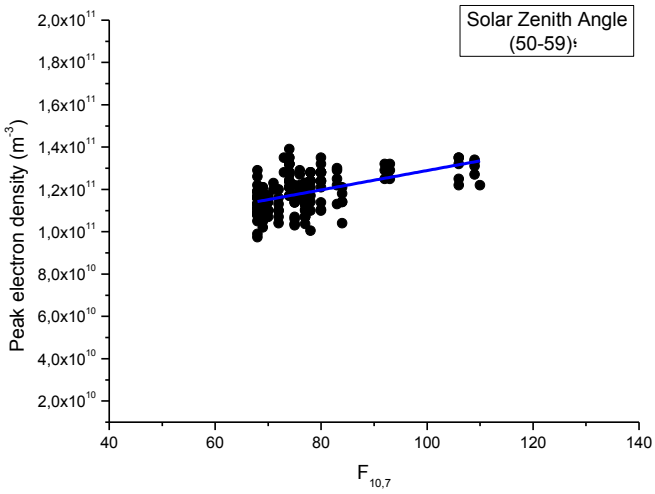

Figure 3.5: Example of peak electron density fitted with their corresponding $F_{10.7}$ for a specific solar zenith angle interval (this case, 50º-59º). A linear relationship has been found between the electron density peak and the solar activity. Similar graphics were obtained for the secondary layer (see Appendix I).

Now, to study the relationship between the peak electron density and the solar zenith angle with no contamination of the solar activity, different values of $F_{10.7}$ index (linearly equispaced between 70 and 150 for the main layer and between 70 and 180 for the secondary one) have been introduced in each Nm-$F_{10.7}$ equation obtained in the previous step. Therefore, from each Nm-$F_{10.7}$ equation (which is related to one solar zenith angle range), a new Nm($F_{10.7}$) data set is available for each solar zenith angle interval. Afterward, this last electron density, Nm($F_{10.7}$), has been fitted with their corresponding solar zenith angle value (the mean value of every interval). As result, a curve of electron density

peak versus solar zenith angle (Nm-χ) has been obtained for each value of solar flux (Figure 3.6 and Appendix I). In each case, an exponential-like decay relationship between the electron density peak and the solar zenith angle for each $F_{10.7}$ has been observed.

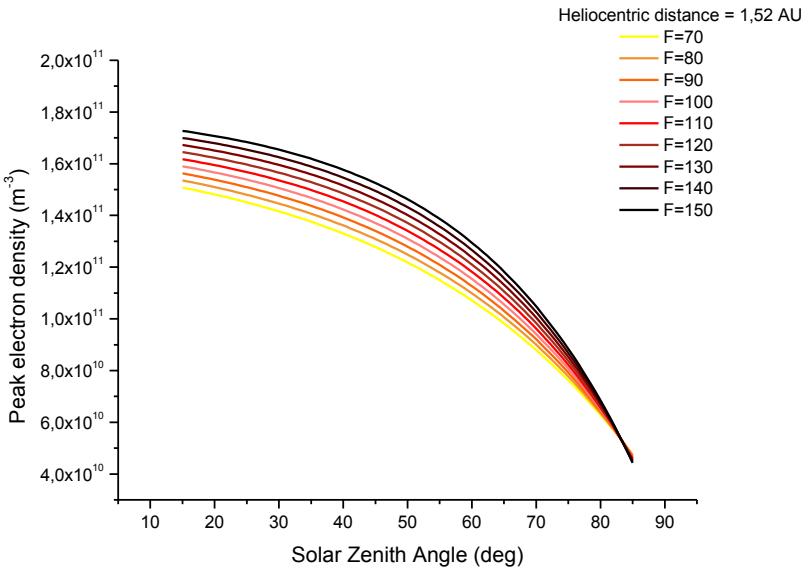

Figure 3.6: Electron density of the main peak versus solar zenith angle for different values of solar flux. In each case, a decay exponential relationship between the electron density peak and the solar zenith angle is observed. A similar graphic was obtained for the secondary layer (see Appendix I).

Finally, in order to obtain an unique expression able to relate Nm-$F_{10.7}$-χ, the following mathematical adjustment has been done: $Nm(F_{10.7} = XXX) - Nm(F_{10.7} = 70)$ versus $F_{10.7}(= XXX) - F_{10.7}(= 70)$, where XXX is the value of the solar flux of each equation and 70 represents the minimum value of solar flux considered in this study. The final step to find the electron density peak equation will be explained in the next sub-section.

Height of both peaks: According to Bougher et al., (2001) and Zou et al., (2011), the peak altitude is the parameter that has a major influence from the neutral atmospheric density. However at this stage, solar zenith angle and solar activity are the only parameters considered for the altitude peak. As it will be commented in the Chapter 5, devoted to the discussion of the results, this issue will be studied with more detail in the near future. On the other hand, it could

not find an altitude-$F_{10.7}$-χ relationship like in the electron density case. It observed that the peak altitude depends mainly on the solar zenith angle (exponential-like growth dependence, equations 3.7 and 3.8) and their variations with the solar flux can be masked by this angle. Despite considering that the altitude only varies with one parameter, the statistics (see model validation section and Figure 3.10) shows that the model reproduces fairly well the experimental data. Note that in the case of the secondary layer, data do not have a large variation with the solar zenith angle and as in the case of the electron density of the secondary layer, synthetic data from the real data were built considering the Chapman theory (equation 1.5): First, the h_{m0} (χ=0) value was obtained from the known hm and solar zenith angles and then, hm was retrieved for different solar zenith angles from the h_{m0} value (acquired in the first step).

3.3.3 Peak empirical equations

The general expressions for the peak empirical model can be written by combining all the above findings. Let us start with the analysis of the **electron density peak of both layers**. In this case, the relationship between electron density peak, solar zenith angle and solar flux is known but it is necessary to retrace the distance normalization previously done. To do this, the inverse of equation 3.2 is applied to the last obtained expression, Nm (χ,$F_{10.7}$).

The results are shown in equations 3.3 and 3.4 and constitute the empirical expressions obtained for the electron density of the main and secondary ionization peak, given in electron per m^3.

$$Nm(Main\ peak) = \frac{1}{r}\left[4.5 \cdot 10^8 \cdot F - 1.9 \cdot 10^{10} exp\left(\frac{\chi}{37.2}\right) + 2.3 \cdot 10^{11}\right] \quad 3.3$$

$$Nm(Second\ peak) = \frac{1}{r}\left[1.2 \cdot 10^8 \cdot F - 3.5 \cdot 10^9 exp\left(\frac{\chi}{32.9}\right) + 5.9 \cdot 10^{10}\right] \quad 3.4$$

where r is the heliocentric distance in AU and F is the solar flux index, $F_{10.7}$.

These expressions can be easily assimilated to the Chapman-shape (equation 1.9) by putting χ=0º and extended to χ>85º by introducing the Chapman grazing incidence function. In this way, equation 3.5 and 3.6 are obtained.

$$Nm(Main\ peak) \approx \frac{1}{r}[4.5 \cdot 10^8 \cdot F + 2.1 \cdot 10^{11}]\sqrt{cos\chi} \quad 3.5$$

$$Nm(Second\ peak) \approx \frac{1}{r}[1.2 \cdot 10^8 \cdot F + 5.5 \cdot 10^{10}]\sqrt{cos\chi} \quad 3.6$$

The results obtained with 3.3-3.4 and 3.5-3.6 are reasonably similar up to χ=85º, but only equations 3.3-3.4 empirically obtained are valid up to χ=90º. For the **peak altitude of both layers**, the results are shown in equations 3.7 and 3.8.

$$hm(Main\ peak) = 0.001exp\left(\frac{\chi}{8.3}\right) + 132.4 \quad 3.7$$

$$hm(Second\ peak) = 0.65exp\left(\frac{\chi}{22.8}\right) + 98.3 \quad 3.8$$

In a similar way to the electron density case, by doing χ=0º and extended to χ>85º by introducing the Chapman grazing incidence function, these expressions can be easily assimilated to the Chapman-shape (equation 1.5) with comparable results, as it is shown in equations 3.9 and 3.10.

$$hm(Main\ peak) = 132.4 + H_{\chi=0}(Main\ peak)Ln(sec\chi) \quad 3.9$$

$$hm(Second\ peak) = 98.9 + H_{\chi=0}(Second\ peak)Ln(sec\chi) \quad 3.10$$

where $H_{\chi=0}$ is the scale height defined in the next section for χ=0.

3.4 Scale height and full profiles

The basis of the empirical model is the α-Chapman expression (equation 1.8) and the parameter that allows describing the structure of the ionosphere is the *neutral atmosphere scale height*. This parameter is the vertical distance over which the pressure of the atmosphere decreases by a factor of e. In the vicinity of the maximum peak, its value is almost constant. Nevertheless, its variation with different parameters has been studied for both ionospheric layers. **Main layer:**

for the topside of the profile, when a constant scale height is considered, the deviation of the model with respect to the real profile is very small in the vicinity of the peak, but rapidly increases with the altitude and can reach huge differences at 15 km above the peak. For this reason and imitating several models for the Earth (Stankov and Jakowski, 2006, Kutiev et al., 2006, Liu et al., 2007), it has been introduced a linear variable scale height with altitude according to equation 3.11:

$$H = H_0 + m(h - h_0) \qquad 3.11$$

where H_0 is the scale height at the peak, h_0 the peak altitude and m is the normalization factor.

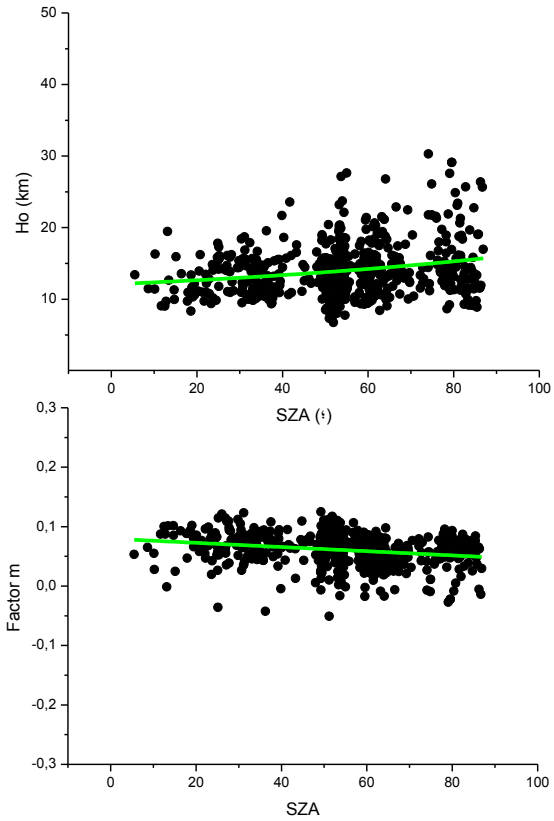

Figure 3.7: Variation with solar zenith angle of the scale height at the peak, Ho, (top panel) and the normalization factor, m, (bottom panel).

The value of H_0 and m parameters have been computed after doing the non-linear best-fitting of equation 1.8 to every ionogram electron density profile used in the model, by introducing equation 3.11 instead of parameter H. A significant variation with the solar zenith angle in these parameters has been observed. On

one hand, the parameter H_0 depends exponentially on the solar zenith angle (equation 3.12, Figure 3.7-top panel) like the peak altitude does (equation 3.7). On the other hand, the parameter m depends linearly on the solar zenith angle (equation 3.13, Figure 3.7-bottom panel). The relationship of these parameters with the solar activity was also studied, but in the case of the main layer no clear dependence has been found. So, the final scale height equation of the main martian ionospheric layer is obtained introducing the expressions 3.12 and 3.13 inside of equation 3.11. Therefore, H depends on the solar zenith angle and on the altitude.

$$H_0(Main\ layer) = 2.6exp\left(\frac{\chi}{100.5}\right) + 9.4 \qquad 3.12$$

$$m(Main\ layer) = 0.08 - 3.5 \cdot 10^{-4} \cdot \chi \qquad 3.13$$

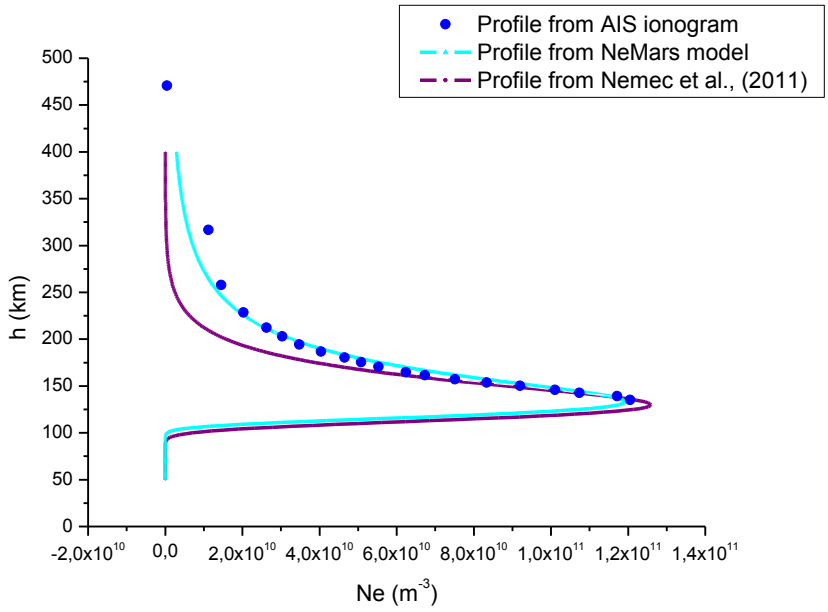

Figure 3.8: Comparison between a typical AIS ionospheric profile (blue dotted line) and the corresponding profiles obtained by the NeMars model which includes variable scale-height (cyan) and by equation used in Němec et al., (2011) (purple).

Figure 3.8 and the statistical analysis indicate that the dependency of the scale height with the solar zenith angle only in the region closest to the peak is not good enough and that an altitude dependence must be considered. As an example, this figure compares a typical AIS ionogram profile with the

corresponding profile obtained by the NeMars model which includes altitude variable scale-height and with the profile obtained by using the Němec et al., (2011) equation for the main layer. In this comparison, it is possible to see that in the vicinity of the peak, both expressions fit reasonably well. However, at 20 kilometres from the peak, differences begin to be noticeable and NeMars model better matches to the profile.

Secondary layer: In this case, it is not possible to consider a variation with the altitude because the topside of this layer is embedded in the main one. Nevertheless, after doing the best-fitting of equation 1.8 to each secondary layer of the radio occultation profiles, a constant value of the scale height has been obtained:

$$H(Second\ layer) = 12.0\ km \qquad 3.14$$

In this way, each parameter that can affect the general structure of the martian ionosphere has been studied and now, it is possible to get an empirical equation for each layer. As it has been mentioned several times, the basic equation of the NeMars model is the expression number 1.8 in which is necessary to replace:

- In N_{m0}, equations 3.3 or 3.5 in the case of the main layer and 3.4 or 3.6 in the case of the secondary layer, all of them with the condition χ=0.

- In h_{m0}, the expression 1.5. Where, for the main peak h_m corresponds to the expression 3.7 when χ=0 (or expression 3.8 for the secondary layer with χ=0) and H corresponds to the expression 3.11 when $h=h_m$ (h_m is also written like h_0) and χ=0 (or expression 3.14 for the secondary layer).

- In H, equations 3.11 for the main layer and 3.14 for the secondary peak.

3.5 Model validation

As most of the ionosphere is within the main layer, a large sample of 1200 MARSIS AIS ionograms was selected for this study. In order to see if this number of ionograms was large enough to represent the behaviour of the ionosphere, the empirical constants (peak electron density and peak altitude) of the NeMars model obtained with an increasing number of data points were represented and the results showed that the values remain essentially constant

from equations with more than 600 ionograms. For that reason, it was considered that the sample of 1200 ionograms can reliably represent the ionosphere. An example of that is presented in Figure 3.9, which displays the electron density of the main peak, for different solar zenith angles, calculated by the empirical model equations for the electron density peak using 200, 400, 600, 800, 1000 and 1200 ionograms. It shows that beyond 600 ionograms, the results converge for all solar zenith angles.

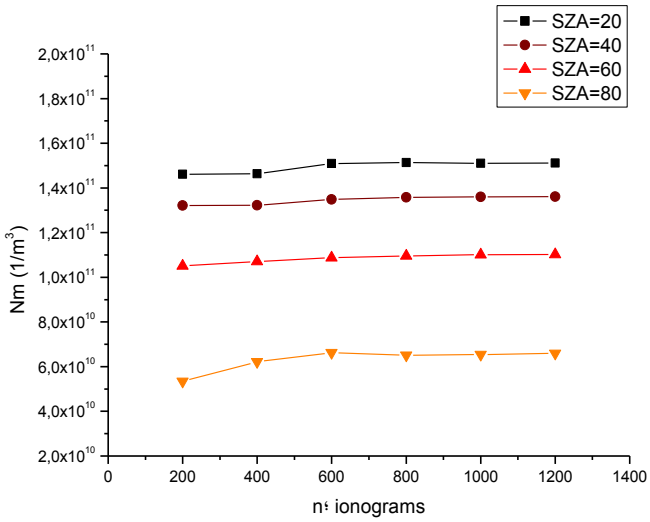

Figure 3.9: Example of the saturation in the main electron density peak equations. Every point corresponds to the electron density value obtained by the empirical equations with 200, 400, 600, 800, 1000 and 1200 ionograms for the same value of Sun-Mars distance and solar flux and different value of solar zenith angle. It is observed that the electron density value is saturated from equation with 600 ionograms onwards.

On the other hand, the model equations have been tested with two different and independent data sets from two missions to verify that they can well reproduce the behaviour of the Mars ionosphere. The results have been compared, first, with a broad set of ionograms from the ESA mission Mars Express not used previously to obtain the empirical model and, afterwards, with radio occultation data from Mars Express and Mars Global Surveyor. To check the model reliability, for the experimental data and for the absolute (±Ne, ±h) and relative (%) differences between the empirical model and the experimental data, the mean, median, standard deviation and interquartile range have been chosen as the best statistical parameters.

The electron density and peak altitude of the main layer have been tested with 500 independent ionograms not used to build the empirical model (Table 3.1,

Figure 3.10 and Appendix I) and which correspond to data of a wide range of solar zenith angle, solar activity and heliocentric distance. In particular, the mean and median for the electron density variation are below 3.5% and for the altitude below 1%. The standard deviation for the electron density variation is below 6 % and for the altitude variation is below 8%.

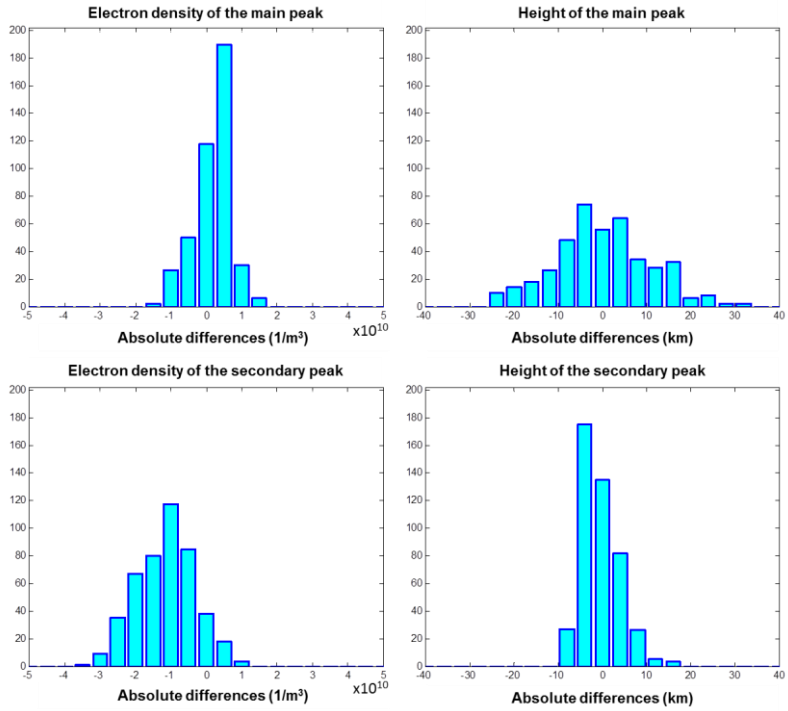

Figure 3.10: Histograms of the electron density (left panels) and peak altitude (right panels) differences between the empirical model and the experimental data for the main peak (up panels) and secondary peak (down panels).

	Electron density peak			Peak altitude		
	Real Value (m^{-3})	Absolute Difference (m^{-3})	Relative Difference (%)	Real Value (km)	Absolute Difference (km)	Relative Difference (%)
Mean	$1.00 \cdot 10^{11}$	$2.07 \cdot 10^{9}$	2.94	138.64	-0.07	0.36
Median	$1.14 \cdot 10^{11}$	$3.26 \cdot 10^{9}$	3.23	136.80	-0.68	-0.44
Standard deviation	$2.84 \cdot 10^{10}$	$5.27 \cdot 10^{9}$	5.99	12.24	10.88	7.76
Interquartile range	$5.32 \cdot 10^{10}$	$6.26 \cdot 10^{9}$	7.21	12.90	13.10	9.85

Table 3.1: Main layer: Statistics results of the electron density and peak altitude differences between the empirical model and the experimental data.

The same procedure has been applied to the secondary layer (Table 3.2, Figure 3.10). In this case, the secondary peak model results have been tested with 450 independent radio-occultation profiles (400 from Mars Global Surveyor and 50 from Mars Express).

	Electron density peak			Peak altitude		
	Real Value (m^{-3})	Absolute Difference (m^{-3})	Relative Difference (%)	Real Value (km)	Absolute Difference (km)	Relative Difference (%)
Mean	$3.83 \cdot 10^{10}$	$-7.96 \cdot 10^{9}$	-13.72	115.62	-0.75	-0.55
Median	$3.77 \cdot 10^{10}$	$-8.32 \cdot 10^{9}$	-21.51	115.67	-1.41	-1.21
Standard deviation	$1.11 \cdot 10^{10}$	$8.51 \cdot 10^{9}$	28.74	4.58	4.33	3.74
Interquartile range	$1.52 \cdot 10^{10}$	$1.16 \cdot 10^{10}$	22.59	6.23	6.23	5.46

Table 3.2: Second layer: Statistics results of the electron density and peak altitude differences between the empirical model and the experimental data.

It is noted that the altitude variation is quite small (mean and median below 1.3% and standard deviation below 4%) and that the electron density variation, although it is fairly acceptable, is bigger than for the main layer. This increment can be due to the fact that the density variation in the second layer is somewhat larger than in the main one because the secondary peak is sometimes embedded in the main layer, making it difficult to identify. However, in general terms, these deviations are not significant.

A variable scale height with altitude and solar zenith angle has been included in the NeMars model, as a very useful parameter to characterize the topside of the ionosphere. This particular shape-parameter allows us to consider that the topside behaviour practically follows the Chapman theory at least 60 km beyond the peak (i.e. about 200 km altitude) with a minimum error. In the top of the Table 3.3, the electron density relative differences (%) between the NeMars model and the real data for different heights are presented. This scale height shape fits reasonably well the ionospheric profiles retrieved from MARSIS data: at 10 km from the peak, the median relative difference (%) is below 0.5% and at 60 km, is less than 6%. In order to compare these results with those from Němec et al., (2011), in the bottom of the Table 3.3, the electron density relative differences (%) between their model and the real data for different heights are also presented. In this case, from 30 km up to the peak, the difference starts to be noticeable. Therefore, using a linear variable scale height with the altitude,

the NeMars model represents, in a very accurate way, the behaviour of the topside ionosphere.

Electron density at different altitudes. Relative Differences (%).

NeMars	h=hm+10 km (%)	h=hm+20 km(%)	h=hm+30 km (%)	h=hm+40 km (%)	h=hm+50 km (%)	h=hm+60 km (%)
Mean	1.23	6.85	8.55	8.55	8.54	7.68
Median	0.52	5.62	8.04	8.04	6.78	5.78
Němec et al., (2011)	**h=hm+10 km (%)**	**h=hm+20 km (%)**	**h=hm+30 km (%)**	**h=hm+40 km (%)**	**h=hm+50 km (%)**	**h=hm+60 km (%)**
Mean	-0.52	-0.63	-7.41	-17.43	-27.20	-37.56
Median	-1.00	1.96	-8.72	-18.27	-27.23	-37.90

Table 3.3: Ionospheric topside: Statistics of the electron density variations at different altitudes (relative differences, %) after considering a variable scale height for the NeMars model (top) and with the Němec et al., (2011) equations (bottom).

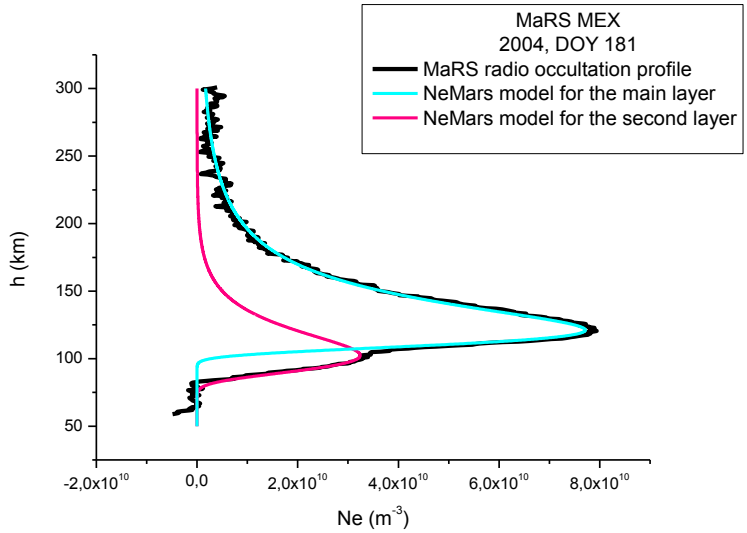

Figure 3.11: Example of typical MaRS radio-occultation profile (black line) and the corresponding curves obtained by the NeMars model for the main layer (cyan) and the secondary layer (pink).

In summary, NeMars model is able to reproduce the two main layers of the dayside ionosphere of Mars in a very quick way and high accurately, using the solar inputs only: solar zenith angle, solar activity and heliocentric distance. An

example is shown in Figure 3.11, where it can be observed how the NeMars curves (cyan and pink) reproduce pretty well the real data (radio-occultation profile from MaRS instrument).

3.6 Model comparison for extreme condition profiles

The main objective of this thesis was the elaboration of an empirical model able to reproduce the normal-condition ionosphere of Mars. As mentioned in the data section all data are representative of a quiet ionosphere without magnetic disturbances induced by the solar wind or originated by the planet itself.

However, the main open question is how reasonable is the response of this model when the ionospheric behaviour is contaminated by the presence of magnetic field or simply, affected by punctual external factors like small plasma instabilities. As the Figure 3.12, taken from Morel et al., (2004) shows, the magnetic field can influence the electronic distribution of the ionosphere and modify the shape of the electron concentration profiles. Figure 3.12 clearly shows how this shape at high altitudes can be completely different when an induced magnetic field with different intensities (here 0, 15 and 30 nT) penetrates the atmosphere. Trying to challenge the model, NeMars has been compared with a special set of electron density profiles from Mars Express MaRS instrument, which display a clear irregular vertical structure (Withers et al., 2012a).

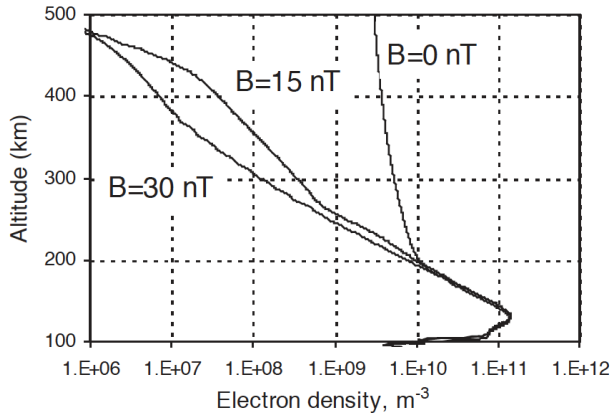

Figure 3.12: Vertical electron concentration profiles modelled for the daytime ionosphere of Mars with the model described at Morel et al., (2004). The three profiles are obtained for different values of the magnetic field at the top of the ionosphere: 30, 15 and 0 nT for the solar zenith angle of 0º (from Morel et al., 2004).

As these profiles are clearly different to those from a standard ionosphere, to get a further idea of the ionospheric variability behaviour, NeMars has been represented with two different approaches. First, assuming a scale height varying with both altitude and solar zenith angle (red curves in next figures) and then assuming a scale height depending only on solar zenith angle (pink curves in next figures). Similarly, to check the exactitude of the radio-occultation profile, two retrieval software have been used in the cases when it as possible: the software provided by the PI team of MaRS instrument (Paetzold et al., 2005) which drives to black curves, and that developed at ESA-ESTEC (cyan curves). Note that both curves come from the same raw data, and that the differences are only due to the different analysis software.

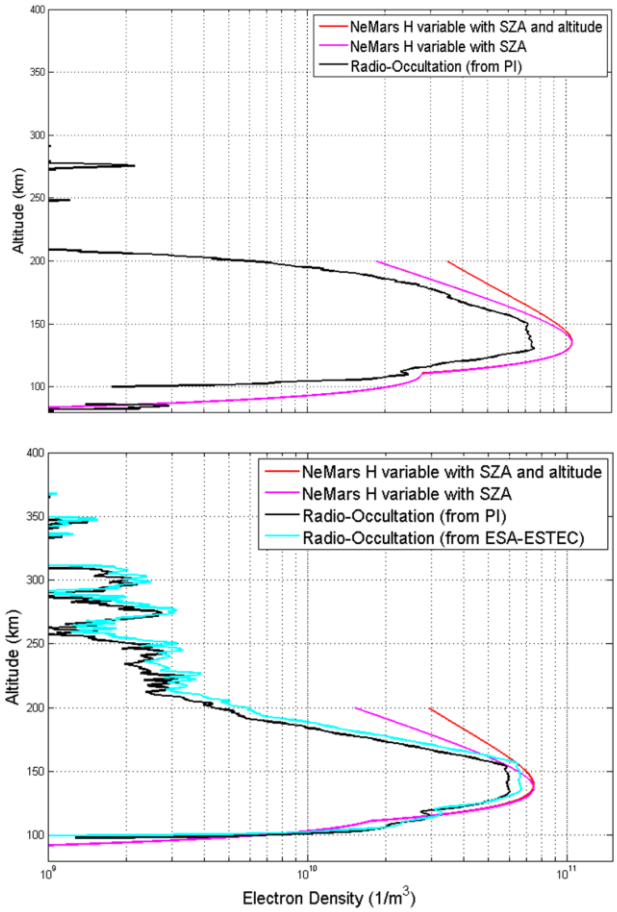

Figure 3.13: Two examples of profiles compressed by the magnetic field from the solar wind. Left-panel corresponds to profile 2A (latitude 42ºN, longitude 24ºE, χ=69º, orbit 1949, date 2005-07-22) and right-panel to profile 3B (latitude 67ºN, longitude 42ºE, χ=79º, orbit 2416, date 2005-11-30) at Withers et al., (2012a).

The first example is shown in Figure 3.13 where two profiles with a clear topside compression and flat peak shape are shown. These profiles correspond to those marked with 2A and 3B in Withers et al., (2012a). Taking into account the previous Figure 3.12, these shapes corresponds to a, relatively, strong magnetic field (higher than 30 nT) coming from the solar wind, probably after a coronal mass ejection in the Mars direction. In both cases, although the topside shape is not reproduced by NeMars model since it does not take into account the magnetic field contribution, the peak characteristics are not far from the real data. The model overestimates the main electron density peak in a factor of less than 25% while the peak altitude is properly reproduced for both layers.

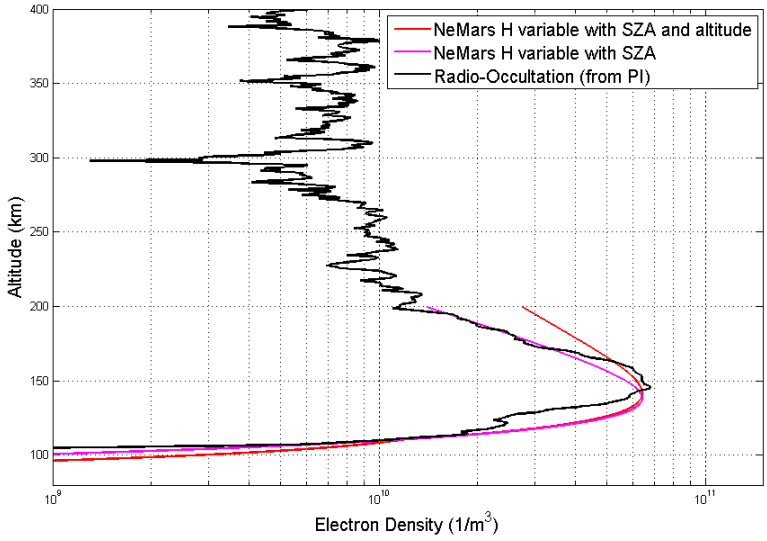

Figure 3.14: Examples of profile affected by crustal magnetic field. It corresponds to profile 2B (latitude 82ºS, longitude 180ºE, χ=82º, orbit 9613, date 2011-07-14) at Withers et al., (2012a).

On the other side, Figure 3.14 shows a profile with a strong contribution of magnetic field from the Mars surface (profile 2B at Withers et al., 2012a), 220 nT at 150 km (Arkani-Hamed, 2004). In general terms, the shape-profile in the Chapman region (up to 200 km) is reasonably reproduced by NeMars with a constant scale height. Interestingly, the behaviour is just the opposite as in the previous case: the main peak electron density is almost perfectly reproduced while the peak altitude is slightly underestimated. These comparisons clearly show the need of an improvement of the model in the near future, in such a way

that NeMars can include the plasma transport in the diffusion region, where currently it is not well described.

As it was already explained in the first chapter, there are other factors not related to magnetic field that can alter the undisturbed ionosphere. Small plasma instabilities due to dust, meteoroids, gravity waves, topography, cosmic rays, etc., can produce a huge variability in the electron density profile shapes.

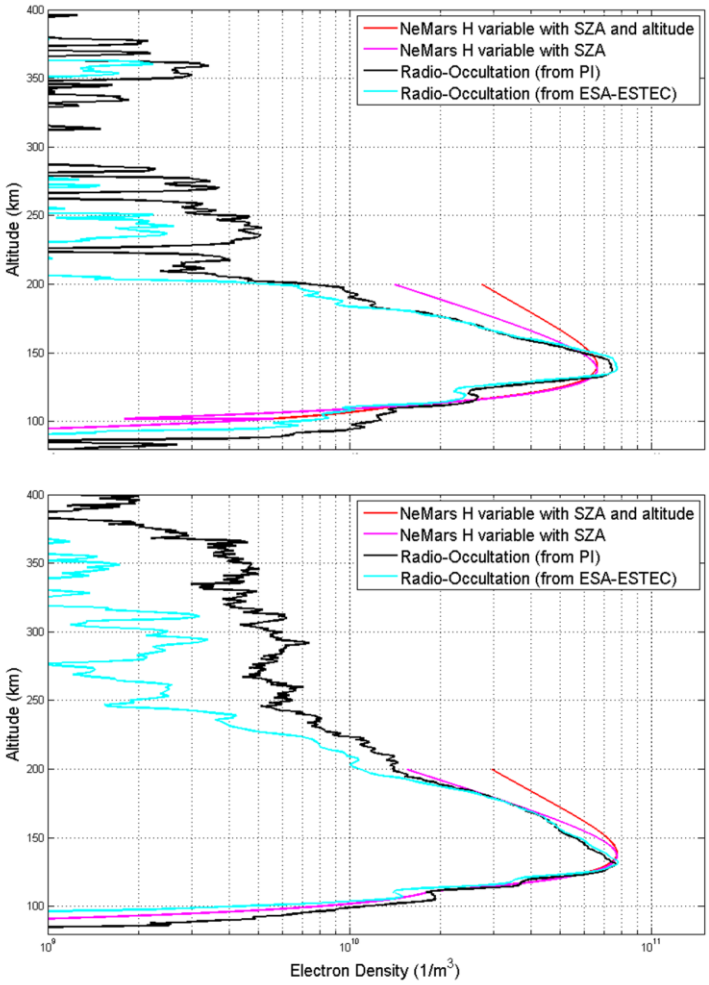

Figure 3.15: Two examples of profiles with presence of a third layer below the main peak. Left-panel corresponds to profile 1B (latitude 66ºN, longitude 341ºE, χ=81º, orbit 2402, date 2005-11-26) and right-panel to profile 3D (latitude 67ºN, longitude 333ºE, χ=78º, orbit 2435, date 2005-12-05) at Withers et al., (2012a).

One case, which is very common to find in the martian ionosphere, is the presence of a third ionospheric layer below the main peak (Paetzold et al., 2005). By definition, NeMars is not able to reproduce this third layer, although, as it is seen in Figure 3.15 that displays two samples (profiles 1B and 3D at Withers et al., 2012a), the result is not far from the measurements. Both samples are well reproduced by NeMars model with a constant scale height. In other words, the slope of the profile does not vary the altitude. Similarly, the peak characteristics (both, altitude and density) are quite close.

To summarize, NeMars can reproduce the ionosphere of Mars in a very accurate way for quiet conditions. However, faced with the challenge of being compared to extreme cases, the model capabilities perform much better than expected. Nevertheless, for greater accuracy and more precise variability profile-to-profile, further improvements are necessary. This will be discussed in the last chapter of this Thesis.

3.7 Discussion and summary

NeMars is an empirical model for the martian dayside ionosphere (primary and secondary layers) based on MARSIS AIS data from Mars Express and on radio-occultation data from Mars Express and Mars Global Surveyor.

Ionograms and radio-occultation profiles were carefully chosen one by one following the selection process described in the data section. It was considered that the limiting assumptions of this selection procedure are reasonably acceptable if they are compared with other factors like data error, harmonic identification at the spacecraft altitude or correct detection of the ionospheric trace at low frequencies.

Possible overestimation errors can be introduced when the secondary layer is studied. As described before, this layer has been analysed in the most prominent case (when the secondary peak was clearly visible). It does not mean that the rest of data are wrong, but if the peak behaviour is known in the visible cases, mathematically it can be extrapolated to the rest. Therefore, the NeMars equations can describe the behaviour of this layer also when is embedded in the main one. To reduce the possible overestimation of this layer, the equations could be improved, as soon as new data with greater variability become available. Anyway, it can be expected that these limiting assumptions would be small and not affecting much the results. About the slight range of variation of solar zenith angle in the data used for defining the secondary layer, further

improvements of the equations will be held as soon as new with greater variation of this parameter will be available. On the other hand, special attention is required by the mixture of different types of ionospheric profiles (from ionograms and from radio-occultation). Due to the design of Mars Express, radio-occultation data and AIS ionograms cannot be acquired at the same time. Similarly, Mars Global Surveyor and Mars Express only took data for few months at the same period. Although AIS ionograms and radio science data are qualitatively different and do not overlap significantly in time, previous chapter has shown that the electron density profiles obtained from MARSIS soundings and the electron density radio-occultation profiles show similar results under similar conditions of solar zenith angle, solar longitude, martian latitude and solar activity ($F_{10.7}$ index), especially in the region of maximum ionization.

The whole model is based on the consideration that the martian ionosphere is in photochemical equilibrium and the two main layers can be represented by the α-Chapman theory. However, other contributions like solar activity or heliocentric distance have been considered.

Regarding the **main layer**, the electron density peak is calculated with high precision (standard deviation relative differences (%) below 6 %) from the inputs solar zenith angle, solar flux index $F_{10.7}$ and heliocentric distance. However, the altitude of the main peak cannot be calculated from the same inputs because the large height variation of the AIS data and their slight variation with the solar activity hide the possible variation of the height peak with the $F_{10.7}$ index. Nevertheless, there is an important dependence with the solar zenith angle and the statistics shows that with this unique dependence, the model adjusts reasonably well (standard deviation relative differences (%) below 8%). As the NeMars main objective is to reproduce physically the martian ionosphere in the most accurate way, special attention was given to the topside shape profile. The scale height is the most important parameter to describe this shape, so, this factor has been analysed in MARSIS AIS data to study the profile behaviour above the maximum electron density. The MARSIS AIS data shape is reproduced better when a scale height linearly variable with the altitude and the solar zenith angle is considered. Accepting this kind of scale height, the median relative differences (%) between the real and the model profiles are lower than 6% even at altitudes about 60 km over the maximum peak. Figure 3.8 indicates that this result differs from Němec et al., (2011) who studied the behaviour of the primary ionization layer under the condition of a constant scale height for each solar zenith angle. In that figure, it can be observed how this new scale height hypothesis works better even at high altitudes.

Concerning the **secondary layer**, the shape of the electron density peak equations is similar to the main one.

It is clear that the solar zenith angle is one of the most important parameters in the description of the ionosphere. When Mars Global Surveyor radio occultation data are considered, this parameter suffers a strong limitation due to its small variation. This disadvantage, although partially solved with the theoretical study of the solar zenith angle described in this chapter, can be an error source. However, these differences are not significant because the variations are always one order of magnitude lower than those of the maximum ionization area. Nevertheless, the peak altitude is much better defined and the confidence interval is quite large. A typical MaRS Radio-occultation profile with the corresponding NeMars curves is shown in Figure 3.11.

In the future, other issues as the secondary production (Nicholson et al., 2009), the chemistry and the temperature of the martian upper atmosphere (Forget et al., 2009), the dependence of the height on the neutral atmospheric density (Bougher et al., 2001 and Zou et al., 2011) and the ionospheric effect of the crustal magnetic field on the Southern hemisphere (Nielsen et al., 2007) will be considered to improve the model.

Once the model is run, several by-products can be retrieved. One of the most interesting is the total electron content (TEC). This parameter can be used to validate the model by comparing the observational TEC values given by MARSIS with the estimates obtained with NeMars. This topic is discussed in detail in the next chapter.

NeMars is a model developed to provide quickly and accurately the electron density profile of the "normal and quiet" dayside ionosphere of Mars for any location and time. As shown in the statistics section, the model represents the actual behaviour of the ionosphere quite well. Besides, when the NeMars model is compared with extreme conditions profiles, the results are better than expected. New improvements will be introduced in the near future.

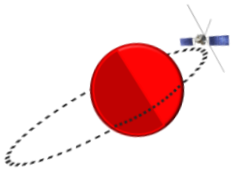

Chapter 4.

Study of the Total Electron Content in the martian atmosphere: a critical assessment of multiple data sets

4.1 Context

The total electron content (TEC) in the atmosphere is defined as the total number of free electrons contained in a column with the cross-section of one square meter along a propagation path between two points. It means the integral of the electron density along a path in the ionosphere (equation 4.1, Figure 4.3) whose units are electrons per square meter and 10^{16} electrons per m^2 correspond to one TEC unit (TECu). On Earth, typical vertical TEC value range is between 10^{17} and 10^{18} e^-/m^2. Earth TEC varies with geomagnetic location, local time, season, solar EUV flux, and magnetic activity. It has to be noted that TEC values for the ionosphere of Mars are lower than those of the Earth by one order of magnitude or more.

$$TEC = \int_{h_i}^{h_f} Ne\, dh \qquad 4.1$$

Furthermore, TEC can be determined by measuring the travel time difference for two signals with different frequencies f_1 and f_2 along the same propagation path in the ionosphere (e.g. on Earth, GPS receivers basis). Due to the dispersion of the ionospheric plasma the two signals are affected differently and arrive at different times ($\Delta\tau$) at the receiver. Therefore, TEC can be also calculated using the following equation:

$$TEC = \frac{c\Delta\tau}{40.3}\frac{f_1^2 f_2^2}{(f_2^2 - f_1^2)} \qquad 4.2$$

TEC constitutes a very useful parameter to characterize or monitor the ionosphere. In the case of Earth (Figure 4.1), TEC is the ionospheric parameter that affects satellite communications and position determination with Global Navigation Satellite Systems. TEC measurements are essential to Ionospheric studies like the analysis of solar activity effects and ionospheric equatorial anomaly monitoring. Any operating or potential system which involves radio waves propagating through the ionosphere and requires time delay measurements with accuracy of the same order as the ionosphere time delays errors, demands knowledge of TEC to correct for these errors (Klobuchar and Aarons, 1973; Budden, 1985).

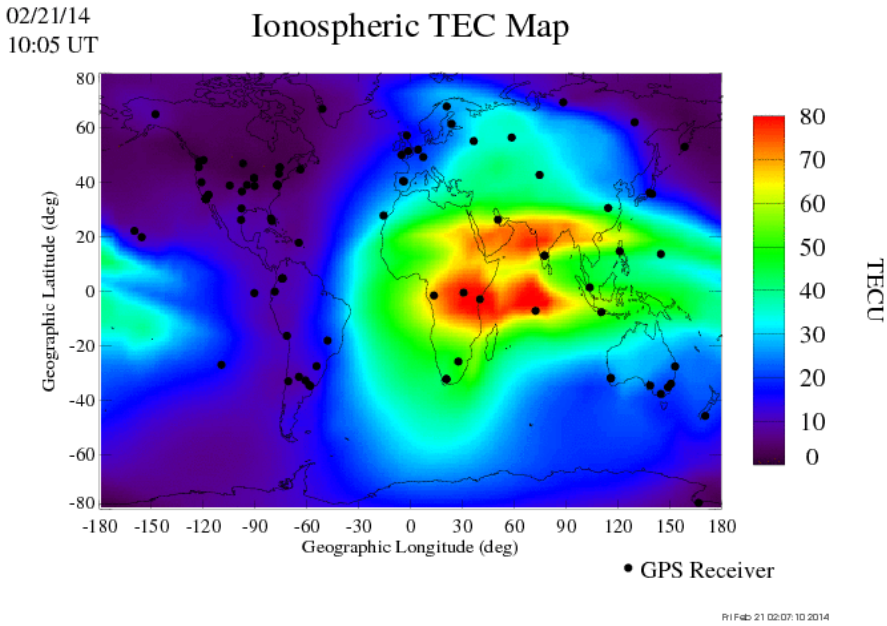

Figure 4.1: Earth global maps of ionospheric total electron content (TEC) produced in real-time (RT) by mapping GPS observables collected from ground stations (day: 21-2-2014 at 10:05 UT). These maps are produced to test real-time data acquisition, monitoring facilities, and mapping techniques. The RT TEC mapping can provide accurate ionospheric calibrations to navigation systems. These maps are also used to monitor ionospheric weather and to nowcast ionospheric storms that often occur responding to activities in solar wind and Earth's magnetosphere as well as thermosphere (source: http://iono.jpl.nasa.gov/latest_rti_global.html).

On Mars, the best example of TEC measurements is given by the radar MARSIS on board Mars Express when it works in its SubSurface (SubS) mode (Picardi et al., 2004). As the signals cross the ionosphere below the spacecraft, they are affected, sometimes very strongly, and an ionospheric correction is unavoidable to properly interpret the data. These corrections lead to sharper radargrams of the Mars' surface and subsurface (Figure 4.2). As a by-product of these corrections, TEC values are available for the benefit of ionosphere physicists.

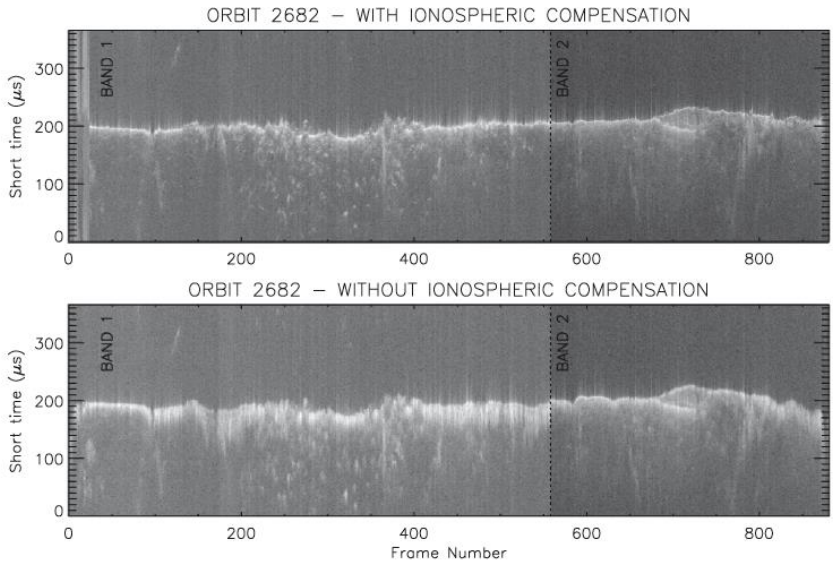

Figure 4.2: Radargram of the orbit 2682. Vertical axis: short time corresponding to the depth penetrated by the signal. Horizontal axis: MARSIS successive measurements. The white first line is the surface echo followed by the subsurface signal. The top radargram displays the signal after correction. The bottom one corresponds to the same signal before correction (adapted from Mouginot et al., 2008).

This parameter can be evaluated at Mars from different techniques, models and instruments, as will be explained in next sub-sections.

4.1.1 TEC from measured electron density profiles

Obviously, TEC can be easily computed from equation 4.1 directly from the vertical electron density profile (Figure 4.3).

As mentioned in Chapter 2 of this doctoral thesis, there are different kinds of data that allow obtaining the vertical electron density profiles. It should be pointed out that the radio-occultation technique provides an extended profile around the main ionospheric peak. This profile ranges between 80 and 220 km in the case of Mars Global Surveyor and between 80 and 1000 km in the case of Mars Express. The difference is due to the different orbital characteristics. In its turn, when MARSIS operates in its Active Ionospheric Sounding (AIS) mode provides the topside part only.

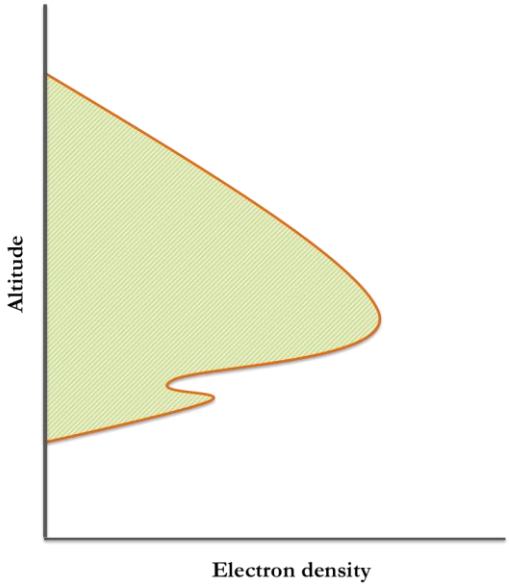

Figure 4.3: Schematic view of the characteristic martian electron density profile. The green colored area is the graphic solution of equation 4.1 and corresponds to the total electron content (TEC) for such electron distribution.

Nevertheless in order to analyse a more realistic MARSIS AIS profile, some authors as Gurnett et al., (2008) proposed different methods to combine topside AIS electron density profiles (real data) with a reconstructed bottomside. On one hand, this could be done with a combined analysis of both ionospheric echo and surface reflection trace, although in practice the accuracy is not good enough (see sub-section 4.1.3). On the other hand, for the main layer, it could be done with a comparison of the real topside AIS profile with a Chapman theoretic profile by doing the best least-square fit of equation 1.8. Although the Chapman theoretical model fits the locally measured electron density profile very well, the parameters are somewhat sensitive to the profile used to interpolate across the gap between the local plasma frequency and the lowest frequency at which the ionospheric echo trace can be measured (for a more detailed explanation see Gurnett et al., 2008).

4.1.2 TEC from models

Models are another method to compute the TEC. Instead of using the measured electron density (previous sub-section), equation 4.1 can give the TEC by

considering the electron density profile computed by a model. In this case, the altitude extension depends on the model limitations.

Several models of the ionosphere of Mars have been developed in the last 40 years, and it is clearly out of the scope of this thesis to provide a complete view of these modelling efforts. Thus, this manuscript only present a selection of the most recent ones:

Empirical models reproduce the Mars' ionosphere from direct and indirect observations, while respecting some physical and mathematical properties of the general plasma theory. NeMars (chapter 3 and Sánchez – Cano et al., 2013) is a clear example of such model. Since electron density is the main output of the model, TEC can be retrieved as a direct by-product by using equation 4.1. This value is reasonably precise and representative of the entire martian ionosphere on the dayside, as shown in the validation section of the previous chapter. The main and useful advantage, as will be commented later, is that the NeMars TEC can be calculated in any selected altitude range in a very quick way.

Another empirical model worth to be mentioned is the one developed by Němec et al., (2011). This model (based on a large amount of MARSIS AIS data) is able to reproduce the electron density profiles only for the main ionospheric layer. Therefore, the TEC comes only from the main layer without any information of the secondary ionization layer. An advantage of this model is that the electron density is also calculated above the photochemical region where transport can occur, either via diffusion or due to the presence of the induced magnetic fields originated in the solar wind.

On the other hand, the most recent efforts of the global scientific community are directed towards creating an International Reference Model for Mars ionosphere -called MIRI- taking advantage of the large available amount of Mars' ionosphere data and of the large scientific experience with the International Reference Model (IRI) for the Earth ionosphere. This reference model is an international project sponsored by the Committee on Space Research (COSPAR) and the International Union of Radio Science (URSI). These organizations formed a global Working Group in the late sixties to produce an empirical standard model of the ionosphere, based on all available data sources. For a given location, time and date, IRI provides monthly averages of the electron density, electron temperature, ion temperature, and ion composition in the altitude range from 50 km to 2000 km. Additionally parameters given by IRI include the total electron content, the occurrence probability for Spread-F and also the F1-region, and the equatorial vertical ion drift (more info at http://iri.gsfc.nasa.gov/). The initiative of MIRI (Mendillo et

al., 2013b) is under COSPAR sponsorship, whose next meeting will have a special session for "References Atmospheres of Venus and Mars (VIRA and MIRA)". The work carried out in this thesis will most likely contribute to this model.

Photochemical models compute the Mars' ionospheric composition assuming photochemical equilibrium (chemical losses equal to chemical and photo-production). One of these recent models is the IonA model (Peter et al., 2014), a fast and flexible ionospheric model suited to reproduce the behaviour of the dayside ionosphere of Mars. Another recent and similar model is Mendillo et al., (2011). The model calculates the density, velocity and temperature of the chemical ionospheric species as a function of the altitude, latitude and time. As shown later, this model agrees well with another TEC data set from MARSIS.

There is another kind of model called TRANSMARS, which is a *numerical/physical model*. It is a 1D-model, based on a coupling between a kinetic part and a fluid code (Witasse, 2000, Witasse et al., 2002, Morel et al., 2004, Bertaux et al., 2005, Leblanc et al., 2006). The kinetic part is a stationary Boltzmann approach that describes the energetic electron flux whose source may be either the incoming solar wind electrons or the photoelectrons. The fluid code is an 8-moment time-dependent model that solves the transport equations of the different charged species. This code has been extensively and successfully used to describe the Earth ionosphere, as well as for Mars, Titan (Gronoff et al., 2009a and 2009b), Jupiter (Menager et al., 2013) and Venus (Gronoff et al., 2008).

4.1.3 TEC from surface reflexion: MARSIS instrument

There are other techniques that, as indirect measures, allow estimating the absolute value of the total electron content. One of them is the analysis of the martian surface echo in the MARSIS AIS data, which is common to find in the ionograms (Figure 4.4). At frequencies above ionospheric plasma frequency (f_P), a weak but easily detectable surface reflection can be detected in some cases when there is no ionospheric absorption. This reflection becomes progressively more intense and better defined as the frequency increases toward the upper limit of the sweep. However, there is a considerable variation from orbit to orbit, and sometimes disappears completely during periods of intense solar activity due to enhanced absorption near and below the peak in the density profile.

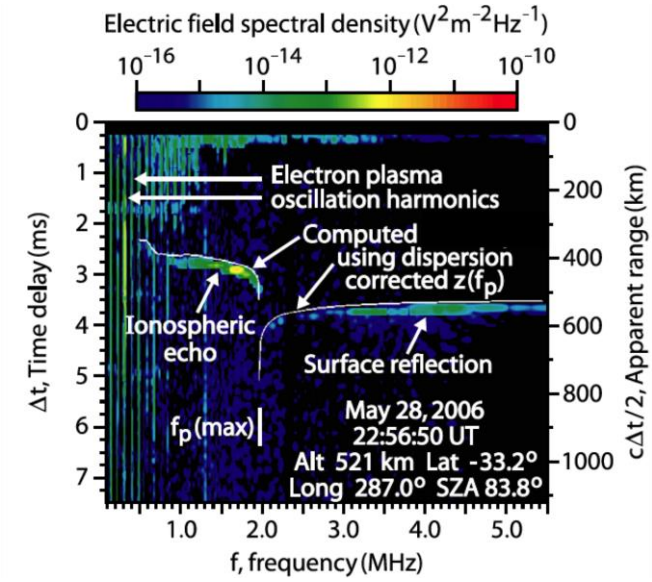

Figure 4.4: MARSIS ionogram where white line represents the computed ionospheric echo and the computed surface reflection to obtain TEC values (adapted from Gurnett et al., 2008).

In principle, this feature should be significant to reconstruct the bottomside electron density profile from a combined analysis of both the ionospheric echo trace and the surface reflection trace. However, in practice the accuracy is not good enough to provide a reconstruction of the bottomside part (Gurnett et al., 2008). Nevertheless, this element can provide additional information like the total electron content integrated through the ionosphere by fitting the surface reflection to polynomial. In the case of Figure 4.4, the best fit to the dispersion of the surface reflection gives TEC=$3.06 \cdot 10^{15}$ m^{-2}, which is a typical value at this solar zenith angle, 83.8º (Gurnett et al., 2008). Conversely, since the surface reflection can be very weak in most of the cases -even not easily detectable-, or detectable but with a high dispersion, the accuracy of this TEC is not good.

To give an example of that, different TEC values for the same ionospheric measurement by MARSIS can be seen in Figure 4.5 (Morgan, 2013a). For the AIS MARSIS measure at 05:06:40.356 UT of the orbit 7964 (21-03-2010), it can be seen that the straight integration from the ionospheric topside electron density profile gives TEC=2.54×10^{15} m^{-2}. When a Chapman best-fitting is included in the profile (TEC=3.01×10^{15} m^{-2}), the bottomside Chapman fit can be easily derived: TEC=1.03×10^{15} m^{-2}. Therefore the TEC for the main layer is a sum of the straight topside profile integration and this Chapman bottomside: TEC=3.57×10^{15} m^{-2}. If this result is compared with that obtained by the

polynomial fit to the ground trace (TEC=5.17x10^{15} m^{-2}), it is clearly seen that MARSIS AIS surface reflections yield TECs too high.

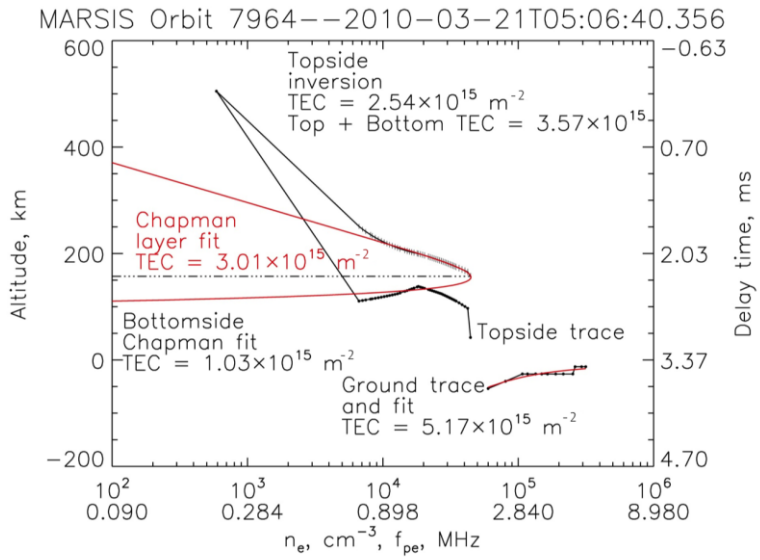

Figure 4.5: Different TEC values obtained for the same ionospheric measurement by MARSIS AIS mode (Morgan, 2013a). The straight integration of the topside ionospheric electron density profile gives TEC=2.54x10^{15} m^{-2}. In red, a Chapman best fit of the profile (TEC=3.01x10^{15} m^{-2}). The bottomside Chapman fit is TEC=1.03x10^{15} m^{-2}. Therefore, TEC for the main layer is a sum of the straight topside profile integration and the Chapman bottomside: TEC=3.57x10^{15} m^{-2}. If this result is compared with that obtained by the polynomial fit to the ground trace (TEC=5.17x10^{15} m^{-2}), it is clearly seen that MARSIS AIS Surface reflections yield TECs too high.

4.1.4 TEC from MARSIS SubSurface data

Another technique to retrieve TEC is the MARSIS radar in its SubSurface (SubS) mode. MARSIS SubS is a nadir-looking pulse limited radar sounder. In this mode, MARSIS transmits radar pulses that penetrate through the planetary surface and are reflected by any dielectric discontinuity in the martian subsurface (Cartacci et al., 2013). This means that the radar signals pass thorough the martian ionosphere twice (from spacecraft to ground and vice versa). As the ionosphere is a dispersive medium, the MARSIS pulses are distorted due to the fact that their frequencies are close to the ionospheric plasma frequency, which can range from about 3.9 MHz during day to less than 1 MHz on the nightside (Gurnett et al., 2005; Mouginot et al., 2008). As a result, the radargrams are

defocused by the frequency-dependent phase shift because of the ionosphere (Figure 4.2).

MARSIS SubS pulses consist of wave packets of duration T=250 μs, which are linearly modulated in frequency over a bandwidth B=1 MHz around a central frequency of 1.8, 3, 4 and 5 MHz (Picardi et al., 2005). MARSIS usually alternates two frequencies at every pulse step to increase the probability that at least one of them propagates above the plasma frequency. One additional feature of MARSIS is that it is equipped with a tracking loop that allows the radar to keep echoes within the receiving window regardless of the presence of any additional ionospheric delay. As the penetration depth of radar signals in the subsurface is approximately proportional to their wavelength (with the exception of ice), MARSIS operates at the lowest possible frequencies capable of propagating through the martian ionosphere, i.e. just above the local plasma frequency, f_p. As the electron density is known to be definitely lower in the nightside, this constraint implies that the MARSIS subsurface sounder works better for solar zenith angles higher that 90º. However, as the ionospheric layer extends between 100 and 200 km, the true nightside is usually considered to correspond to solar zenith angle higher than 105º-110º, so that the Sun light cannot reach the ionosphere at all (Cartacci et al., 2013).

The propagation of an electromagnetic wave of frequency f in the martian ionosphere is characterized by the refraction index:

$$n(z) = \sqrt{1 - \frac{f_P^2(z)}{f^2 - jf\nu}} \cong \sqrt{1 - \frac{f_P^2(z)}{f^2}} \qquad 4.3$$

where f_P is the plasma frequency, ν the electron-neutral collision frequency and z is the altitude above the ground. If a typical MARSIS operation frequency is considered (e.g. 1.3-5.5 MHz range), the imaginary term in the denominator of equation 4.3 can be neglected because $\nu \sim 10.60$ KHz. The plasma frequency, in Hz, can be written as:

$$f_P(z) = 8.98\sqrt{N_e(z)} \qquad 4.4$$

where N_e is the electron density in m^{-3}. The maximum value of f_P corresponds to the maximum value of the electron density.

As a consequence of equation 4.3 all frequencies lower than f_P will be reflected regardless of the incidence angle. Moreover, if the radar signal has a wide band, the propagation speed is not constant through the band and a frequency dependent phase shift arises. It means that frequencies higher than f_P will be attenuated, delayed by an average delay (group delay) in signal travel time and dispersed depending on the electron density values encountered along the path (Cartacci et al., 2013).

The phase shift induced by the ionosphere in a radar signal of frequency f can be written as:

$$\Delta\phi(f) = \frac{4\pi}{c} f \int_0^L [n(z) - 1] dz = \frac{4\pi}{c} f \int_0^L \left[\sqrt{1 - \left(\frac{f_P(z)}{f} \right)^2} - 1 \right] dz \qquad 4.5$$

where L is the ionosphere thickness and c is the speed of light in vacuum.

There are several methods to correct the ionospheric distortion of MARSIS SubS echoes: Ilyushin and Kunitsin (2004), Mouginot et al., (2008), Picardi et al., (2008) or Zhang et al., (2009). However, this doctoral thesis focuses on two of them, which were developed by two groups in charge of analysing and correcting the MARSIS SubS instrument data: the so-called "Grenoble" group (Safaeinilli et al., 2007, Mouginot et al., 2008) and the so-called "Rome" group (Picardi et al., 2008, Cartacci et al., 2013). Both names come from the geographical localization of the groups.

4.1.3.1 "Grenoble" group method

The method of the "Grenoble" group is based on the method explained in Safaenili et al., (2003), Safaeinili et al., (2007) and Mouginot et al., (2008), where the estimation of the TEC was improved by introducing an additional constraint: to match the surface echoes position at real surface altitude. This method corrects the signal by matching the surface echo to the filter (surface altitude), while also taking the ionosphere into account. The correction of phase of signals is done using the limited series expansion of the plasma refractive index. This correction permits a good detection of surface and subsurface echoes. The main by-product from the corrections of ionosphere effect is the total electron content of the ionosphere. These TEC data are available in the European Space Agency Planetary Science Archive (ESA PSA, http://www.rssd.esa.int/ index.php?project=PSA).

As described before, the ionosphere induces a frequency-dependent phase shift that results in the defocusing of the radargram (Figure 4.2). The phase shift term $\Delta\phi$ is described by equation 4.5. Doing a third order Taylor expansion of the refractive index and taken into account the expression 4.4 for the plasma frequency, the phase shift can be written as:

$$\Delta\phi(f) = \frac{4\pi}{c}\left[\frac{40.32}{f}\int_{h1}^{h2} n_e dh + \frac{812.851}{f^3}\int_{h1}^{h2} n_e^2 dh + \frac{32774.2}{f^5}\int_{h1}^{h2} n_e^3 dh\right] \quad 4.6$$

As MARSIS SubS operates primarily for solar zenith angles higher than 60º, and in the case of 60º-90º the radar is operated with the band frequency of 3 MHz and above, the attenuation due to electron-neutral collisions in the ionosphere (Safaeinilli et al, 2003; Nielsen et al., 2007) and the Faraday rotation can be considered negligible to first order.

Since a priori the necessary coefficients to correct the signal are unknown, an optimization method is used. The set of parameters (integrals of n_e, n_e^2 and n_e^3) are explored to obtain the maximization of the amplitude of the signal reflected by the surface at the output of matched filter. To make this procedure efficient, some physical constrains are introduced.

- The first constraint is the altitude of the spacecraft and the propagation time corresponding to this altitude. This altitude is estimated from the Mars Orbiter Laser Altimeter (MOLA) data (Smith et al., 2001).
- The second constraint is considering a simplified electron density profile as initial condition to start the optimization procedure. The choice is a Gaussian profile, whose integral solution is well known.

Once the optimization procedure is concluded, the ionospheric behaviour of the resultant data is studied by using Chapman-based density profiles to model every member of equation 4.6. Then, the measured parameters are fitted. The Chapman function used corresponds to equation 1.8, including grazing incidence (equation 1.13). In this approach, it is assumed that the maximum electron density when the Sun is overhead (χ=0), N_{m0}, and the neutral atmospheric scale height, H, are constant parameters of the ionosphere. In particular, $N_{m0} = 2x10^{11}\ m^{-3}$ and H varies from 5 to 30 km. The H range was chosen arbitrarily and covers a range larger than the expected values for the martian ionosphere. The parameter N_{m0} is just a factor whereas H appears also

in Chapman incidence function *Ch* (equation 1.13). Nevertheless, the effect of both N_{m0} and H on TEC looks very similar. The main difference comes from the behaviour of TEC during sunrise and sunset at solar zenith angles near 90º. H variation has a bigger impact for solar zenith angles between 80º and 100º.

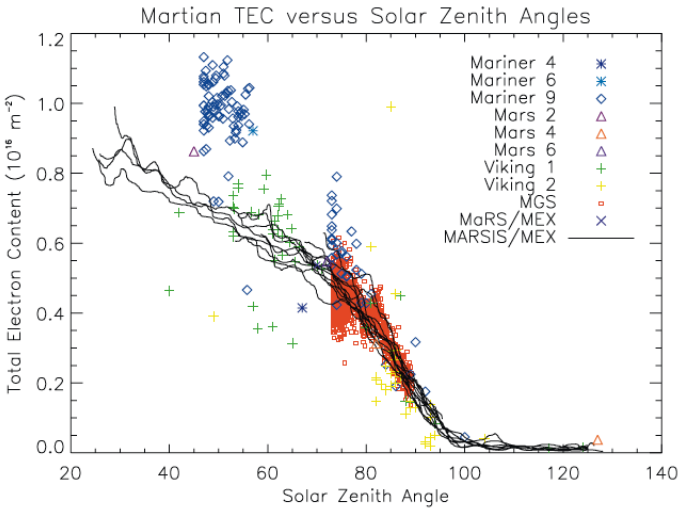

Figure 4.6: Total electron content as a function of the solar zenith angle. Each dot corresponds to TEC measurements by other instrument and solid lines to MARSIS TEC measurements in surface sounding mode (Mouginot et al., 2008).

Figure 4.6 shows the TEC computed by the "Grenoble" group compared with measurements obtained during other missions. Red points correspond to data from the last period of Mars Global Surveyor (MGS) (January 1, 2005–June 9, 2005) which is the closer period to MARSIS (at time of Mouginot et al., (2008) work: November 2005–January 2006). Both data samples belong to relative low solar activity periods. A good agreement between MARSIS and MGS data can be found at high solar zenith angles. On the other hand, Mariner 9 radio-occultation data were obtained during moderate solar activity. As expected, on the first order, TEC values increase with the solar activity and those obtained from Mariner 9 are larger than the MARSIS ones.

4.1.3.2 "Rome" group method

The method of the "Rome" group to estimate the total electron content is based on the so-called Contrast Method (Picardi and Sorge, 2000), which allows

correcting the phase distortion of the echoes recorded by MARSIS in its subsurface mode. The basis of the procedure is described in Cartacci et al., (2013) and the physical principles are the same as in the case of the "Grenoble" group: the ionosphere produces a variation of the refraction index which values are greater than one, and induces radar signal phase changes in the bandwidth through the path. The mismatch between the transmitted and the received signal phases does not allow a correct range compression and produces a degradation of the radar performances.

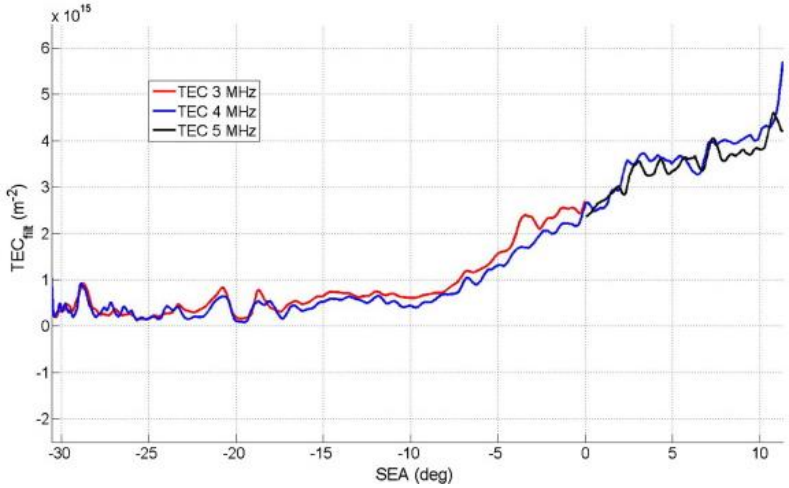

Figure 4.7: Total electron content evaluated through the "contrast method" at three frequencies (3, 4 and 5 MHz, as red, blue and black lines) versus solar elevation angle (SEA, complementary angle to solar zenith angle) for orbit 6001 (Cartacci et al., 2013).

An important assumption of this method is to consider a simplified ionosphere with a constant plasma frequency and an equivalent slab thickness. The phase shift induced by the ionosphere in a radar signal of frequency f is given by equation 4.5. If f_0 is the central frequency of the radar signal band, it can perform a Taylor expansion of the integrand of equation 4.5 and then integrate each term of the expansion, obtaining:

$$\Delta\phi(f) \cong a_0 + a_1(f - f_0) + a_2(f - f_0)^2 + a_3(f - f_0)^3 + a_4(f - f_0)^4 + \cdots \qquad 4.7$$

where a_i depends on frequency f, plasma frequency f_P and slab thickness L. The term a_0 is negligible and does not introduce any distortion. Something alike

happens with the term a_1 that only introduces a time displacement (group delay). Therefore, the expression 4.7 becomes:

$$\Delta\phi(f) = a_2(f - f_0)^2 + a_3(f - f_0)^3 + a_4(f - f_0)^4 \qquad 4.8$$

The "contrast method" was developed to correct, or at least reduce, the effects due to such a phase shift. The method consists in iterating the range compression of the radar echoes. Therefore, it is a loop in which the received signal undergoes range compression, after the azimuth compression, "n" times, using a different phase compensation term. The contrast method is applied to all frames collected by MARSIS and for each frequency, obtaining as final products: a_2, a_3 and a_4.

In this case, the most important coefficient of the equation 4.8 is the term a_2, which is directly related to the TEC.

$$a_2 = \frac{-2\pi}{cf_0^3}(8.98)^2 \int_0^L N_e(z)dz - \frac{3\pi}{cf_0^5}(8.98)^4 \int_0^L N_e^2(z)dz \qquad 4.9$$

Here, the first integral in the right-hand side is the total electron content along the path between the spacecraft and the martian surface. The relevance of the second integral in the right-hand side is negligible during the nightside, consequently can be omitted. This approximation yields an overestimate of the absolute value of a_2 of the order of $1.5(f_P/f_0)^2$, which for f_P=1MHz and f_0=4MHz, is about 10%. This implies a TEC overestimation during dayside. Therefore, this parameter can be written as:

$$TEC \cong -\frac{a_2 cf_0^3}{2\pi(8.98)^2} \qquad 4.10$$

4.1.4 TEC from SHARAD SubSurface data

There is another instrument able to obtain TEC values as by-product. It is the SHARAD (Shallow Radar sounder) radar on the Mars Reconnaissance Orbiter (MRO) spacecraft. The sounder is similar to MARSIS SubS mode although the emitted signal is a swept of higher frequencies: from 15 to 25 MHz (Campbell et al., 2011). Although the frequencies are considerably higher than the martian plasma frequency, changes in the ionosphere of Mars can however substantially affect the image quality and radiometric consistency of SHARAD radargrams.

The most obvious effect is phase distortion, which leads to blurring of the range-compressed signal. Secondary effects include variations in both the round-trip delay and the attenuation of the sounder signals with ionospheric TEC (Campbell et al., 2013 and reference there).

Although there are several methods proposed to compensate for ionospheric effects on the received echoes, Campbell et al., (2011) proposed using a form of the frequency-dependent phase-distortion function for rapid single-parameter autofocus correction. The phase distortion of SHARAD signals by the ionosphere is a function of the sounder frequencies f and progressively higher order terms of the vertical distribution of electrons (electron density profile). This relationship is described by equation 4.6. The autofocus approach yields a single parameter, which is termed *E*, as the scaling factor for a representation of the phase distortions, $\Phi(f)$, is given by:

$$\Phi(f) = \frac{E}{f^{1.93}} \qquad 4.11$$

where *f* is the instantaneous frequency along the sounder chirp. There is a linear relationship between this parameter and TEC. Ionospheric delay offsets arise due to a linearly varying phase shift over the spectrum of an echo record. Given the dominance of the first term in 4.6, it is possible to approximate the phase error at the 20-MHz centre frequency as:

$$\Delta\varphi = 2\pi(1.344x10^{-14}TEC) \qquad 4.12$$

Each delay shift Δt of one resolution cell (0.0375 μs) along a sounding record requires a 2π shift in phase over the spectrum. Therefore, E and TEC can be linked by comparing the magnitude of observed delay offsets with the corresponding value of E from the autofocus processing. The delay offsets are measured by comparing SHARAD observations of the identical footprints (i.e. at orbit crossings) with the data collected at different values of solar zenith angle, and thus, different ionospheric TEC.

4.2 TEC data discrepancy: description of the problem

Regardless of the method or technique used, they should all, in principle, give similar results, at least within the error bars. However, in reality, large discrepancies in the results have been observed in the recent years.

Experimental data do not agree among themselves, and supporting models do not help to solve the problem.

To illustrate the difficulty of the situation, Figure 4.8 shows a clear example of this disagreement. Using the NeMars model, TEC (of the full ionosphere) is calculated by numerical integration of the NeMars electron density (equation 4.1). On the other hand, as it has been already mention several times, MARSIS can operate in two modes, not simultaneously. It is common to find, for the same orbit, ionospheric and subsurface consecutive measurements, i.e. AIS for 10 minutes, then subsurface mode for 20 minutes and then AIS again for 10 minutes. This characteristic is very useful as from both modes, TEC can be derived. Thus, it is possible to compare the TEC calculated by the NeMars model with the TEC deduced from both MARSIS modes of operation (SubS and AIS) and to study and analyse the evolution of this parameter for the same orbit.

Two examples, Mars Express orbits 4210 and 4215, are presented in Figure 4.8. The TEC value from the MARSIS subsurface mode (corresponding to the "Grenoble" group and archived in the ESA Planetary Science Archive) and the MARSIS ionogram TEC that corresponds to the ionospheric topside of the electron density profile (ionogram integral, equation 4.1) have been plotted. It can be observed that TEC estimates based on MARSIS AIS data are not consistent with those obtained from MARSIS subsurface sounding data: this is obviously due to the fact that MARSIS in AIS mode is a topside sounder, measuring only the properties of the ionosphere above the maximum plasma frequency, while in subsurface mode it provides an integral information on the TEC for the entire ionosphere. Furthermore, the NeMars modelled TEC for the topside ionosphere and for the entire ionosphere are also presented with similar results. From the figure, it appears that derived TEC from AIS ionogram for the topside is reasonably well represented by the model topside TEC.

Another example is shown in Figure 4.9. In this case, the discrepancy appears among different methods applied to the same data set. Blue and black data show the same fact described above: AIS TEC from the topside ionosphere (in blue) and SubS TEC from "Grenoble" retrieval method (in black). Furthermore, in this case "Rome" data have been added (in red) for the same orbit. Although the raw data are identical for both groups, the derived TEC values differ. Close to the terminator both kinds of data seem to match well. However, a significant discrepancy is visible in the dayside; in this figure the difference is up to 40 % at χ=65º and up to 20% at χ=80º. This disagreement is clearly higher for lower solar zenith angles.

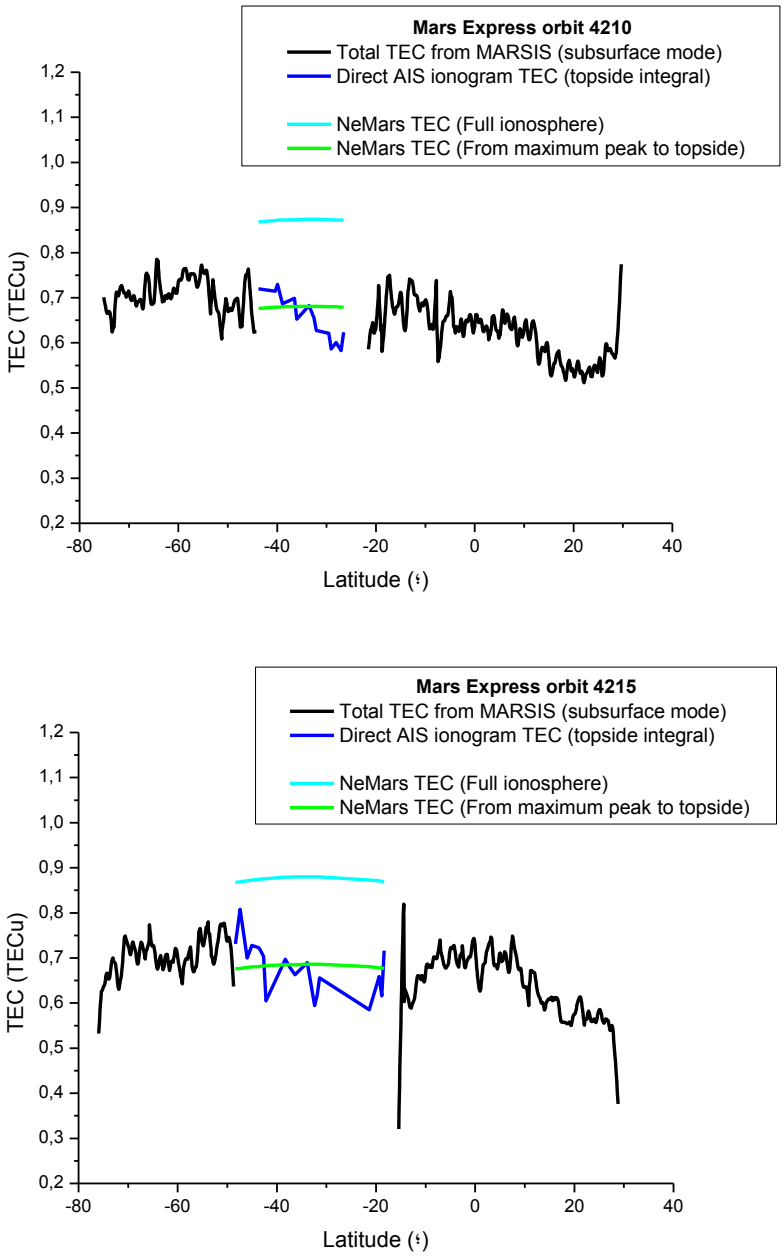

Figure 4.8: TEC-latitude variation for Mars Express orbits 4210 and 4215 (16-4-2007 and 17-4-2007 respectively). The full ionosphere TEC resultant from MARSIS subsurface mode (black) has been represented with the real topside integral MARSIS ionogram TEC (blue). In addition, the comparison of TEC retrieved from the NeMars model for the topside ionosphere (green) with the full ionosphere (cyan) indicates that the results given by NeMars are consistent.

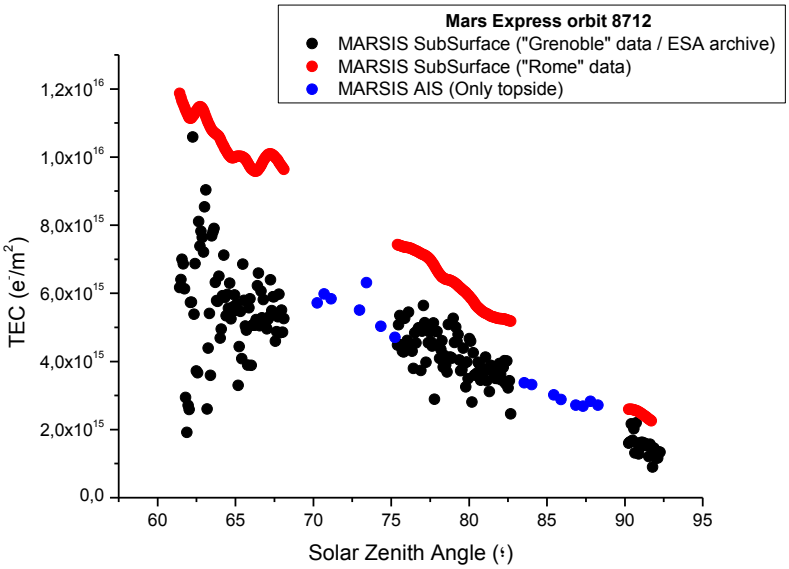

Figure 4.9: TEC-solar zenith angle variation for orbit 8712 (27-10-2010). The full ionosphere TEC retrieved from MARSIS subsurface mode (black from Grenoble method and red from Rome method) have been represented with the real topside integral MARSIS ionogram TEC (blue). Again the comparison shows practically the same value between AIS and SubS Grenoble data although it is not physically possible. However, SubS Rome in first approximation seems to be more consistent.

All in all, the values obtained from the subsurface mode by "Grenoble" method appear to be low for a reason still to be determined. Moreover, different data and techniques provide different results for the TEC, leading to a substantial misunderstanding of what the real value should be. Figure 4.10a is a good example of this unfortunate situation. Data from most of the techniques explained in the previous sub-sections have been plotted here, corresponding to the Mars Express orbit 8712. In particular, there are TEC data from MARSIS SubS: "Grenoble" method (in black dots) and "Rome" method (in red dots); from MARSIS AIS: retrieve with the method explained in chapter 2 (in blue stars) and from "Iowa group" main layer (combination of the topside with a reconstructed Chapman-bottomside, in pink triangles); from NeMars model for the entire ionosphere (in cyan dots) and only topside ionosphere (in green triangles).

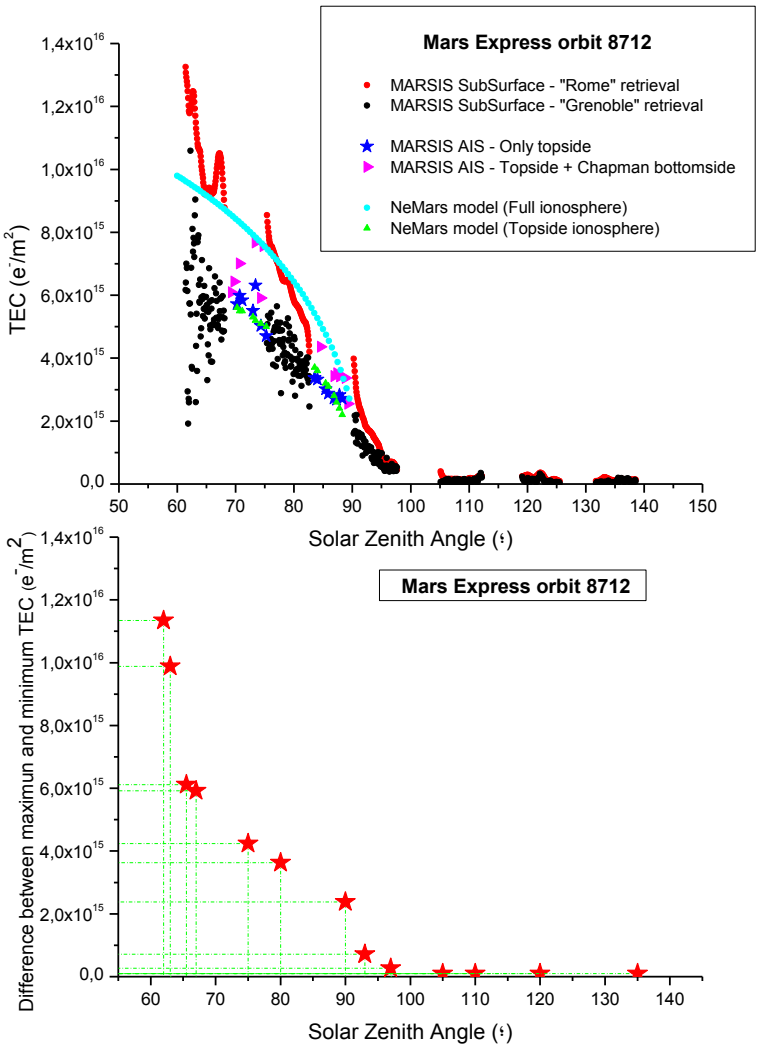

Figure 4.10: Mars Express orbit 8712. Up-panel: TEC data versus solar zenith angle from MARSIS SubS: "Grenoble" method (in black dots) and "Rome" method (in red dots); from MARSIS AIS: straight topside profile integration (in blue stars) and from "Iowa group" main layer (combination of the topside with a reconstructed Chapman-bottomside, in pink triangles); from NeMars model for the entire ionosphere (in cyan dots) and only topside ionosphere (in green triangles). Bottom-panel: Absolute differences between the maximum and minimum TEC value among all of these techniques and for different solar zenith angles.

The absolute differences between the maximum and minimum TEC value among all of these techniques and for different solar zenith angles are plotted in Figure 4.10b, where the data scatter clearly is increased in the dayside. All methods practically converge at nightside and terminator and during dayside, the

discrepancy can be up to one unit of TEC at χ=60º. This means that dispersion among all technique data at χ=60º, is equal to the average value of data at this solar incidence value.

It is important to note that the martian TEC values are quite small comparing with those from Earth ionosphere. In fact, few TEC units are the typical uncertainty expected for the terrestrial atmosphere. It means that the martian TEC is lower than the TEC Earth confidence interval. However, this uncertainty in the case of Mars cannot be considered as such, since it is a value that depends on instrument, on measurement and on data. This chapter will give a critical analysis of the datasets.

At this stage, the following preliminary conclusions can be drawn:

1. The maximum difference of TEC among all the dataset and techniques can be easily up to one unit of TEC on the dayside. However, on the nightside all of them are considerably more consistent.

2. The discrepancy in the results processed from the same data set with two different techniques is of concern. The "Grenoble" method seems to be more physically and ionospherically correct; however a first comparison with the topside sounder data indicates that the results are underestimated. On the other hand, the "Rome" method is expected to overestimate the results (especially on the dayside). Nevertheless, a first comparison with the topside sounder data seems to give more credits to this method.

However, some authors do not agree with those inferences. Lillis et al., (2010) showed that "Grenoble" data behaviour could be reproduced fairly well with the general Chapman theory. Mendillo et al., (2013a), with the aim of studying the ionospheric variability, compared a two-year sample of this dataset with the TEC results obtained using the 1-dimensional (vertical) Boston University Mars Ionosphere Model described in Mendillo et al., (2011). The main conclusion of this work is that model-data comparisons are reasonably successful when model's conditions best approximate observational conditions. Moreover, Campbell et al., (2013) affirm that the SHARAD instrument is well calibrated since the maximum average TEC value obtained in the calibration of the SHARAD observations agrees well with estimates of the TEC at similar solar zenith angles from the MARSIS instrument in Safaeinili et al., (2007).

With the main objective of understanding these differences, which in principle could be due to the data processing methodology, the Mars Express project decided to conduct a special campaign where for one orbit, ionospheric and subsurface measurements would be acquired alternately every few minutes.

These orbits are known with the name "*interleaved MARSIS mode orbits*" and there are 26 between orbit 7964 -21 March 2010- and orbit 9531 -20 June 2011-.

The next sections will address the question of this disagreement and to identify the potentially wrong data set or technique. Firstly, data differences will be quantified with a statistical study and then, the NeMars model will be used as a diagnostic tool. The main objective is to identify the source of the problem, and eventually to propose a way forward.

4.3 Objective statistical analysis

In order to try to understand the possible discrepancy in data, an objective statistical analysis has been done. Taking advantage of the large number of Mars Express orbits with ionospheric and subsurface data from which are possible to retrieve TEC by, at least, three different methods (as mentioned before), a comparison with no a-priori has been done.

Orbit number	Date	F10.7 (sfu)	d_{M-S} (AU)	Ls (º)
4210	16-04-2007	69	1.3983	220.2
4214	17-04-2007	69	1.3976	220.9
4215	17-04-2007	69	1.3974	221.1
4219	19-04-2007	68	1.3967	221.8
4221	19-04-2007	68	1.3963	222.1
4223	20-04-2007	69	1.3960	222.5
5295	15-02-2008	70	1.6290	32.3
5299	16-02-2008	70	1.6300	32.8
6458	12-01-2009	69	1.4450	190.0
6461	13-01-2009	71	1.4440	190.5
6462	13-01-2009	71	1.4437	190.7
6581	16-02-2009	70	1.4095	211.1
6587	18-02-2009	70	1.4081	212.1
6592	19-02-2009	69	1.4069	213.0
6598	21-02-2009	71	1.4055	214.1
8712	27-10-2010	88	1.4869	169.7
8761	10-11-2010	86	1.4687	177.6
9466	04-06-2011	103	1.4319	303.4
9498	14-06-2011	99	1.4422	308.9
9528	23-06-2011	96	1.4523	314.0
9531	23-06-2011	96	1.4534	314.5

Table 4.1: Information related to the 21 Mars Express selected orbits. Orbit number is marked in first column, terrestrial date of the measurement in second column, F10.7 index as proxy of the solar activity in third column (1sfu=10^{-22} $Wm^{-2}Hz^{-1}$), Mars heliocentric distance in fourth column and solar longitude (This angle provides a measure of season) in fifth column.

Since the temporal coverage of the "interleaved mode orbits" is not very large, other orbits previous to this special campaign with data in both modes (as for example figure 4.8) have been selected to extend the temporal data range. In this way has been possible to cover a reasonable range in heliocentric distance, solar longitude, solar zenith angles, solar activity, etc., and therefore, have a broader control of the statistics. Twenty-one Mars Express orbits with data in both operational modes were selected, 6 of them belong to the special interleave campaign. The full orbit list is available in Table 4.1.

4.3.1 "Grenoble" and "Rome" data versus MARSIS AIS data

For one orbit, the heliocentric distance, solar longitude, and solar activity values are the same; latitude and solar zenith angle are the only parameters that vary. For these orbits, ionospheric and subsurface measurements are consecutive, i.e. they never are taken at the same time. This characteristic, although useful to examine visually the data, can be a weakness in the statistical comparisons. Therefore, to compare data acquired in subsurface and ionospheric modes at exactly the same position, it has been decided to compute the best fitting of the subsurface data. Then, an interpolation/extrapolation of this best-fitting curve was done for the solar zenith angle or latitude condition of every ionospheric data (e.g. Figure 4.11).

In order to minimize the error introduced in the comparisons doing the data best fit, every case has been analysed carefully. Since the only two parameters that vary along one orbit are solar zenith angle and latitude, the same study has been done for both configurations: TEC versus solar zenith angle and TEC versus latitude (Figure 4.11 and Appendix I). This approach ensures that the results are consistent regardless of the graphical representation. Every orbit has been fitted to a second-degree polynomial. However in some particular cases (e.g. orbit 9531, Figure 4.11), where there are data from deep night, fittings have only considered data with the same trend. For example, in the case of the orbit 9531, as the nightside trend is very different to the dayside one and AIS data belong to dayside, the fit has been done only for solar zenith angles smaller than 100º.

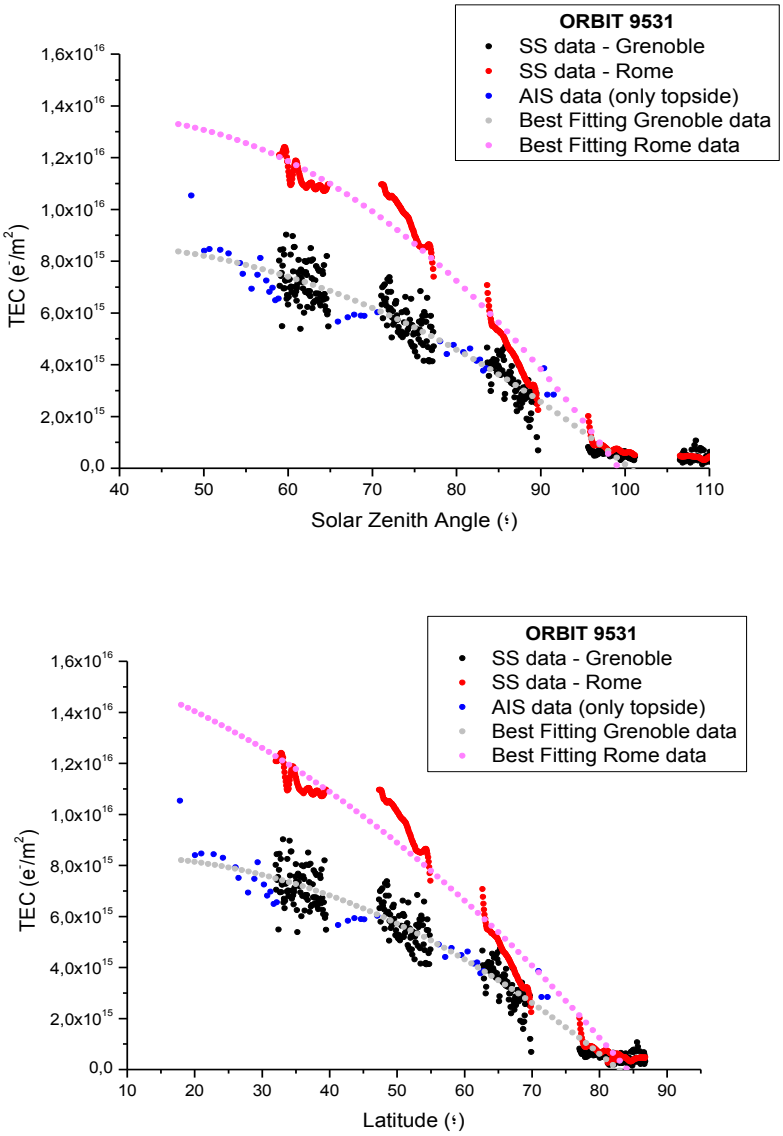

Figure 4.11: TEC-solar zenith angle variation (top-panel) and TEC-latitude (bottom panel) for orbit 9531 (26-6-2011), which belongs to the Mars Express "interleaved mode" campaign. The full ionosphere TEC derived from MARSIS subsurface mode (black from "Grenoble" method and red from "Rome" method) has been represented with the real topside integral MARSIS ionogram TEC (blue). Moreover, the best-fitting curves for "Grenoble" method (grey) and for "Rome" method (pink) have been plotted.

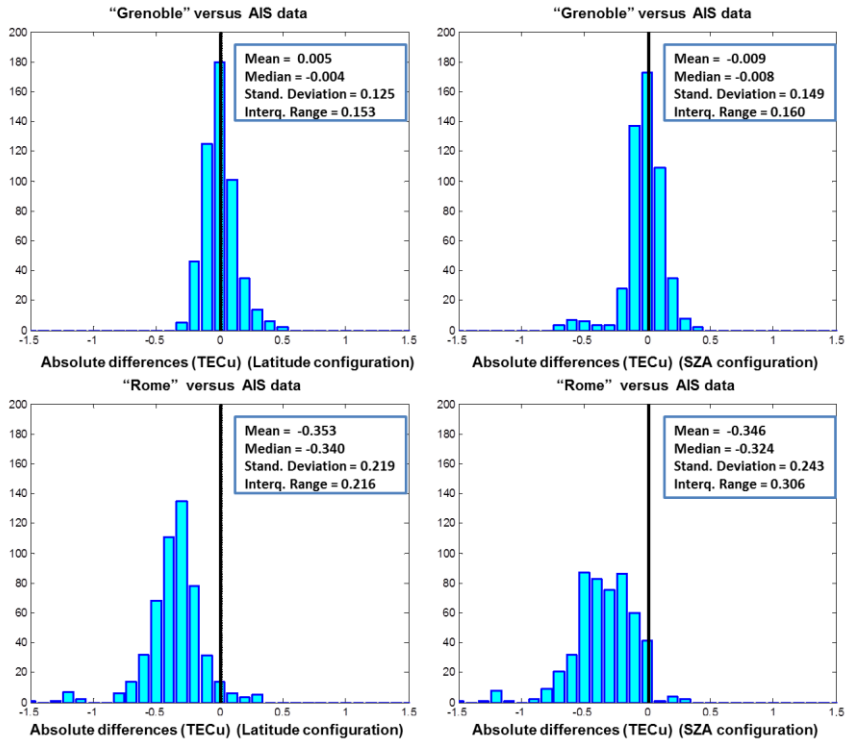

Figure 4.12: Objective statistics between the full ionosphere TEC retrieved from MARSIS subsurface mode (top-panel from "Grenoble" method and bottom-panel from "Rome" method) with the real topside integral MARSIS ionogram TEC. Total number of data 514 (21 orbits). Left-panels: Histograms of the absolute differences in TECu for the latitude configuration. Right-panels: Histograms of the absolute differences in TECu for the solar zenith angle configuration. The vertical black line marks the null difference.

Figures 4.12 and 4.13 show the results of these comparisons. The same procedure has been performed with subsurface data from "Grenoble" and "Rome" methods. In total, there were 514 data belonging to the 21 selected orbits (Table 4.1). The analysis confirms that the absolute and relative differences between "Grenoble" subsurface data (data archived in the ESA science archive) and ionospheric data from the AIS mode are very small (practically null), both for latitude and solar zenith angle configurations. Note that for studying the accuracy of subsurface data, AIS data have been taken as the most reliable based on a large sounding experience on Earth routinely, and therefore, constitutes a well-known technique. The mean and median absolute differences are less than one-hundredth of a unit of TEC, equivalent to a mean relative difference less than 5% and a median relative difference less than 1.5%. It means that clearly "Grenoble" method is underestimating the real value of the martian TEC, since it is not physically possible because the first mode calculates

the TEC of the entire ionosphere and the second one only of the topside. On the other hand, the absolute and relative differences between "Rome" subsurface data and ionospheric data from the AIS mode are higher (two order of magnitude, ~-0.35 TECu of absolute difference, equivalent to ~ 35% of relative difference).

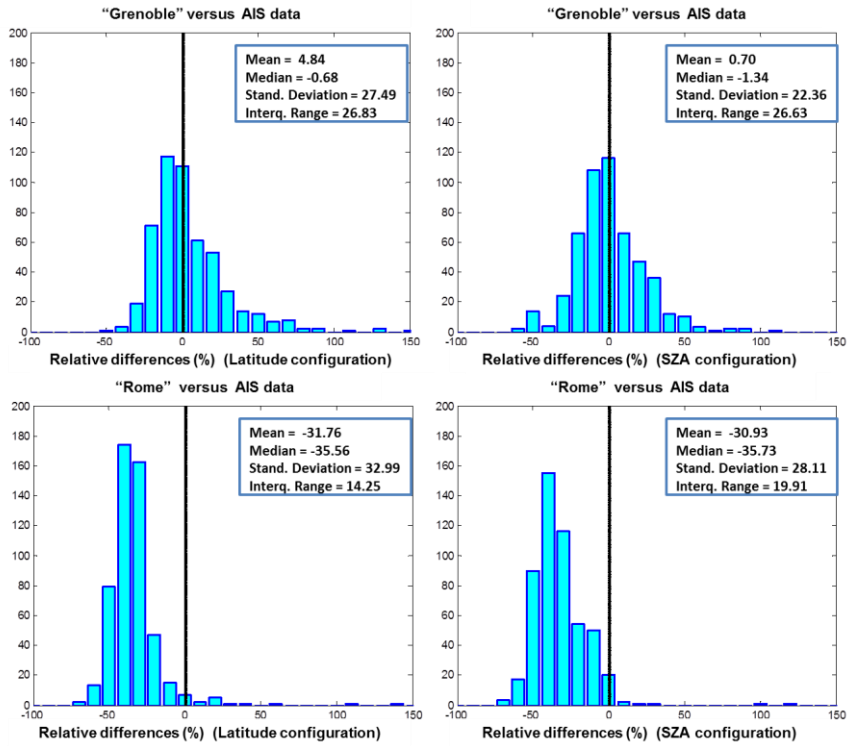

Figure 4.13: Objective statistics between the full ionosphere TEC retrieved from MARSIS subsurface mode (top-panel from "Grenoble" method and bottom-panel from "Rome" method) with the real topside integral MARSIS ionogram TEC. Total number of data 514 (21 orbits). Histograms of the relative differences in percentage for the latitude configuration are plotted in the left-panels, and histograms of the relative differences in percentage for the solar zenith angle configuration are plotted in the right-panels. The vertical black line marks the null difference.

This result is consistent with the ionospheric data, being the contribution of the bottomside of the main layer plus the secondary layer in average about a third part of the ionospheric TEC (see statistics before). At this point of the study, it is not possible to ensure that this subsurface TEC is totally correct since the authors themselves indicate that the TEC at lower solar zenith angles could be about 10% overestimated (Cartacci et al., 2013). It is important to note that both

ionospheric and subsurface dataset are characterized by a different sampling rate (2 seconds for subsurface and 7 seconds for the ionospheric sounding). In principle, since the comparison only takes into account the TEC value of the best-fitting at each AIS latitude/solar zenith angle value, the sampling rate is not important.

4.3.2 "Grenoble" versus "Rome" data

One of the main problems of MARSIS SubS mode is the signal distortion due to the ionosphere. As consequence, measures in the plain dayside ($\sim\chi$<60º) are avoided. Nevertheless, 60º is still dayside and although the MARSIS frequencies are higher than the plasma frequency, the signal distortion and absorption could be an essential factor to consider in the TEC SubS retrieving. For that, "Rome" and "Grenoble" data have been split up into three different solar zenith angle intervals: dayside (60º< χ<75º), dayside terminator (75º< χ<90º) and nightside (χ>90º).

Figure 4.14 corroborates this assessment: during nightside, the differences between both methods are practically null (mean and median values less than 0.02 units of TEC), indicating that both methods are very accurate during the night when the ionosphere is almost non-existent and the signals are transmitted without any distortion. However, close the terminator where the day-to-night ion transport is significant, differences appear between both methods: 0.12 TECu in average of mean and median. That implies that close to the terminator, the differences have increased by one order of magnitude due to the weak ionosphere at dawn/dusk. This discrepancy in the results is much higher in the dayside (mean differences 0.57 TECu and median differences 0.29 TECu) where the ionosphere clearly affects the propagation of the electromagnetic signals. This discrepancy is significant, and can be higher than half of one unit of TEC, which is 50% of the typical TEC value on the dayside. Also, the ionospheric distortion in the electromagnetic signals can also be observed on the data spread: the standard deviation parameter is considerably higher in the case of the dayside than in the nightside (a unit of TEC of difference). Finally, these data have been compared by plotting their ratio (Figure 4.15), which can be useful to look for systematic trends. Obviously, the ratio departs from the 1:1 dependence (black line). A ratio of about 1.4 has been found between the 2 sets, with a larger scatter on the dayside. If, in the future, comparison between the two techniques is carried out, from a theoretical or simulation point of view, it would be useful to see whether a similar ratio can be found.

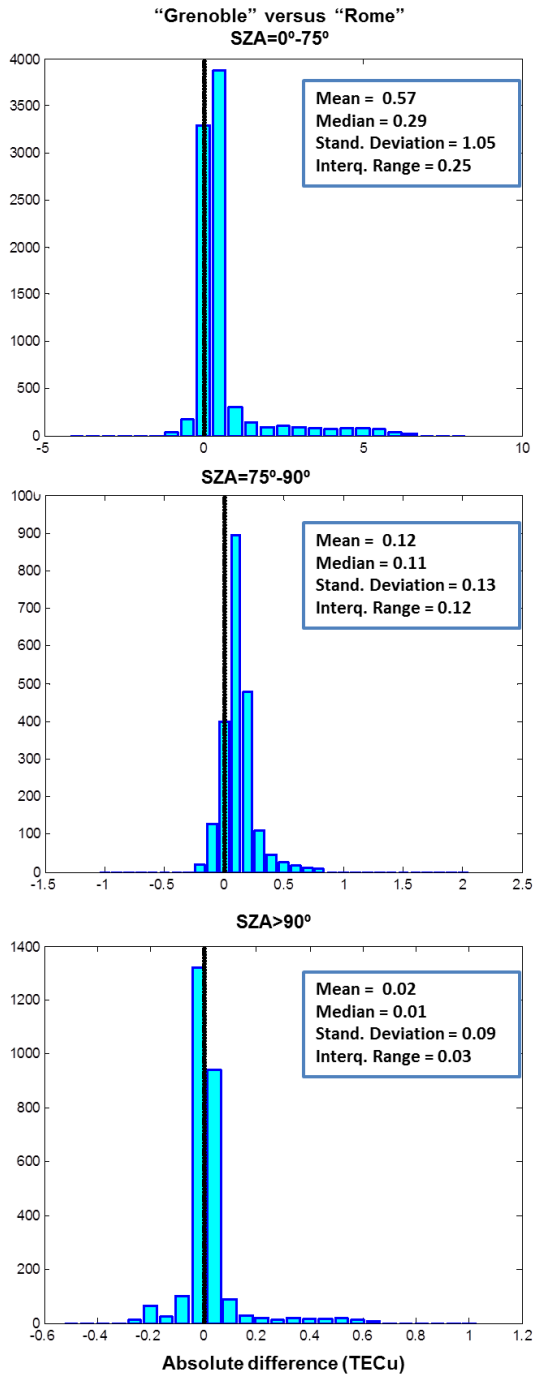

Figure 4.14: Objective comparison between "Rome" and "Grenoble" data for three different solar zenith angle intervals: dayside ($60^o < \chi < 75^o$) (top), dayside terminator ($75^o < \chi < 90^o$) (medium) and nightside ($\chi > 90^o$) (bottom). Note that the figure scales are not the same for the three cases. The vertical black line marks the null difference.

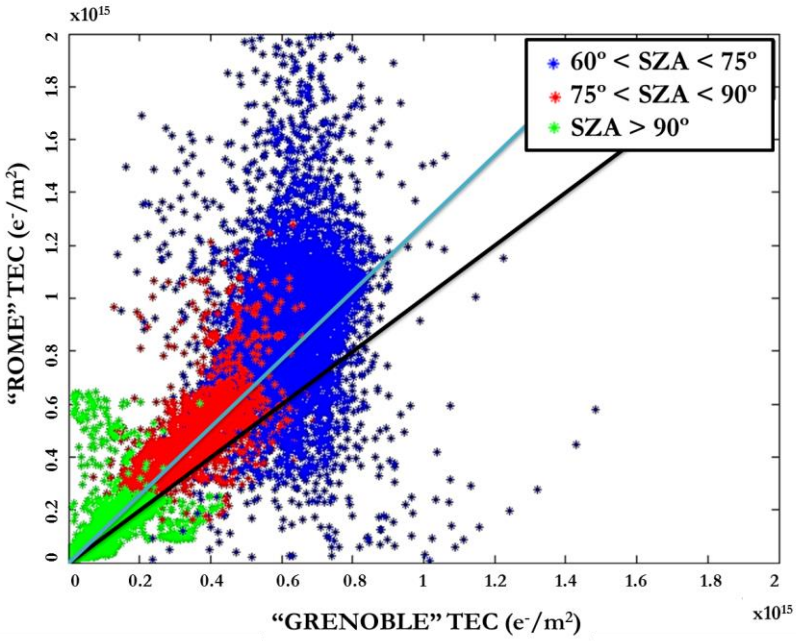

Figure 4.15: "Rome" versus "Grenoble" TEC representation. Data have been split up into three different solar zenith angle intervals: dayside in blue (60º< χ<75º), dayside terminator in red (75º< χ<90º) and nightside in green (χ>90º). The solid black line shows the 1:1 dependence, while the solid blue line represents a ratio of 1.4 between the two data sets.

4.4 Model comparison statistical analysis

The use of a model as a diagnostic tool to possibly identify the source of the problem is another way to quantify and evaluate the discrepancy in the MARSIS data set. Following the spirit of this doctoral thesis, the model developed in this frame (chapter 3) has been selected for this task. The main reasons are:

- NeMars reproduces quite accurately AIS MARSIS data (see validation section of Chapter 3).
- It allows a direct comparison with subsurface data.
- It is very quick and pretty flexible to run, therefore, it constitutes a manageable and useful tool to analyse the TEC at different altitude ranges.

The dayside TEC from NeMars model has been calculated with the conditions of solar zenith angle, solar activity and heliocentric distance (inputs of the model) of every orbit. An example is shown in Figure 4.16, where the same orbit than in Figure 4.11 is plotted adding the dayside NeMars TEC (more info at Appendix I). Visually, again the important discrepancy in dayside is perceived. At every epoch NeMars TEC values are higher than subsurface TEC from the ESA archived "Grenoble" method. Regarding "Rome" subsurface TEC data, it is observed that close the terminator these and NeMars data match almost perfectly, although they diverge after sunrise. Here is where the overestimation of the "Rome" data can be observed.

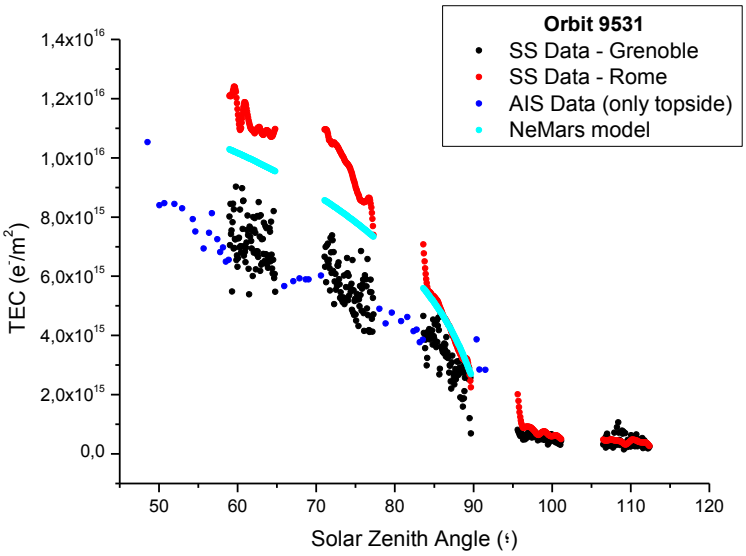

Figure 4.16: TEC-solar zenith angle variation for orbit 9531 (26-6-2011, same as Figure 4.11), which belongs to the Mars Express interleave campaign. The full ionosphere TEC derived from MARSIS subsurface mode (black from "Grenoble" method and red from "Rome" method) have been represented with the real topside integral MARSIS ionogram TEC (blue). Moreover, the NeMars TEC for the dayside ionosphere (cyan) has been plotted. Additional material is shown at Appendix I.

These discrepancies have been quantified with a new statistical study of the differences between both subsurface data and modelled TEC data (Figure 4.17). The statistic considers the total amount of data in each orbit and shows that TEC from NeMars model is fairly close to "Rome" subsurface data: the absolute difference of the mean and median is less than 0.09 units of TEC while compared with "Grenoble" data, these differences are about 0.32 units of TEC.

This statement constitutes a further confirmation of the underestimation of "Grenoble" retrieval while on average, the "Rome" retrieval seems visibly consistent with the model and with other measurements.

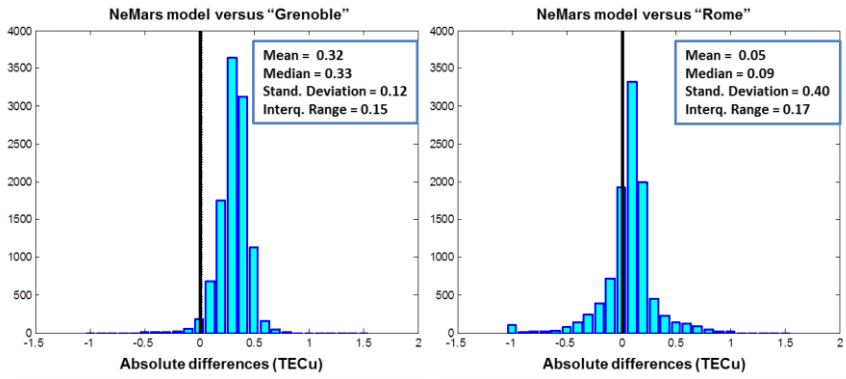

Figure 4.17: Comparison between TEC from NeMars model and "Grenoble" (left panel) / "Rome" (right panel) TEC. The statistic shows that "Rome" data match practically perfect with NeMars TEC, while the "Grenoble" data seems underestimated. The vertical black line marks the null difference.

However, as mentioned before, the "Rome" technique seems to overestimate the TEC on the dayside. For that reason, data have been again split into three solar zenith angle intervals in the same way as in the previous section. The objective is to analyse and quantify the possible overestimation of the Rome data as a function of solar illumination. Therefore, this comparison has been carried out between "Rome"/"Grenoble" data and TEC from NeMars model, in two of the three solar zenith angle intervals as previously: dayside ($60^o < \chi < 75^o$) and dayside terminator ($75^o < \chi < 90^o$). Comparisons for the nightside ($\chi > 90^o$) were not possible since NeMars works only for the dayside. Figure 4.17 shows the histograms and results of the comparisons. At the interval $75^o < \chi < 90^o$ the match between "Rome" and NeMars data is almost perfect (mean and median of the absolute difference 0.08 and 0.1 TECu respectively). However, the match between "Grenoble" and NeMars data although reasonable, it shows a difference between the two sets of data (mean and median of the absolute difference less than 0.19 units of TEC). These results corroborate the one obtained in the previous section (Figure 4.14), giving again clear evidence that close to the terminator, all kind of data give a consistent value of the total electron content. This is most likely due to the low ionospheric densities in this region. Nevertheless, it can be noticed that the

"Grenoble" data are a bit below the "Rome" data meaning that the ionosphere at low-density can still has a noticeable effect on the TEC retrieval.

At the interval 0º<χ<75º, full dayside, the ionosphere has obviously a significant effect on the signal dispersion. This is corroborated statistically on Figure 4.18 where both kinds of subsurface retrievals do not match the model results. On one hand, "Grenoble" underestimates model data in a factor of 0.35 TECu (same difference as in the previous section "Rome" had with respect to topside AIS data). On the other hand, "Rome" overestimates model data in a factor of 0.21 TECu for the mean and a bit underestimation of 0.08 TECu is marked for the median absolute value with a high standard deviation of 1 TECu. Therefore, after combining the results from Figures 4.14 and 4.18, the main conclusion of this statistical study is that "Rome" data processing is quite consistent with the MARSIS AIS data.

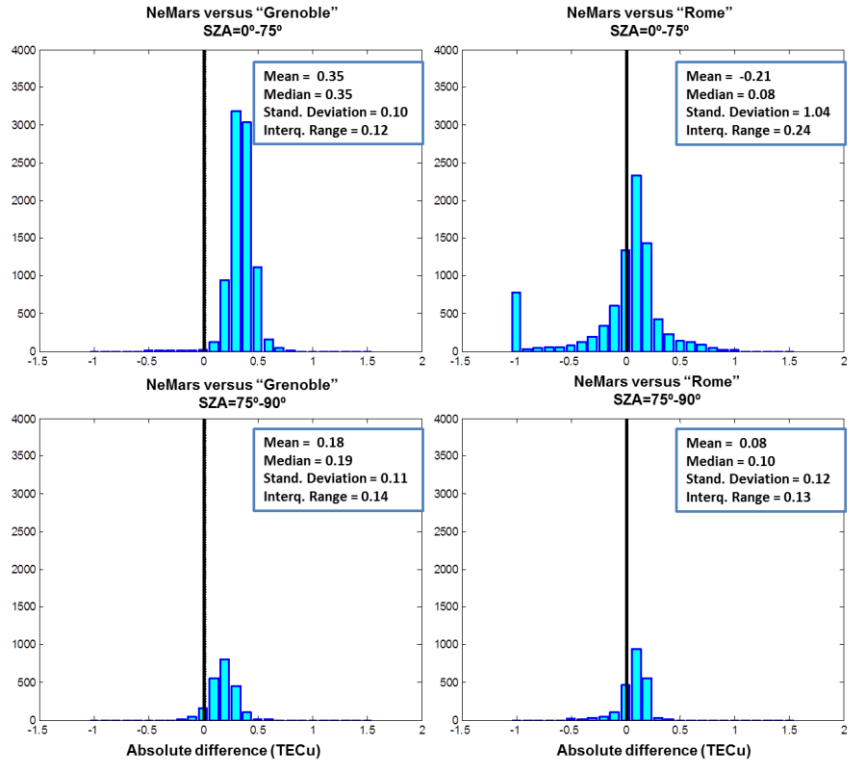

Figure 4.18: Comparison between TEC from NeMars model and "Grenoble" (left panel) / "Rome" (right panel) TEC data for two different solar zenith angle intervals: dayside (60º< χ<75º) (top panel) and dayside terminator (75º< χ<90º) (bottom panel). Nightside (χ>90º) is not compared since NeMars model only works for the dayside ionosphere. The vertical black line marks the null difference.

To complete this study, the deviation of subsurface data related to the topside TEC calculated with NeMars model has been analysed (Figure 4.19). Results confirm previous findings: the difference between "Grenoble" subsurface TEC and topside NeMars TEC is almost null (eight-hundredths of units of TEC for the mean and median relative differences), while "Rome" subsurface TEC versus topside TEC NeMars is an order of magnitude higher (less than 0.18 units of TEC).

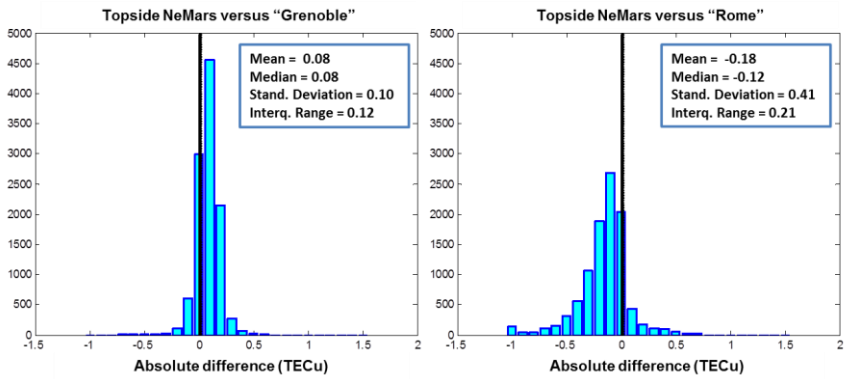

Figure 4.19: Comparison between TEC from topside NeMars model and "Grenoble" (left panel) / "Rome" (right panel) TEC. The statistic shows that "Grenoble" data is equivalent to the TEC obtaining only with the topside ionosphere. The vertical black line marks the null difference.

4.5 Discussion

As written at the beginning of the chapter, the Total Electron Content (TEC) is an useful physical quantity for describing the behaviour of the electron density in the ionosphere. As on Earth, the evolution of the electron content varies with time (diurnal, seasonal, 11 year solar variations…). This parameter, routinely measured by the Mars Express MARSIS radar, can be used to further test and validate the model developed in this doctoral thesis by comparing it with the TEC estimates obtained with NeMars model. However, the TEC values from both MARSIS modes of operation are currently difficult to reconcile, in particular on dayside.

Taking advantage of the large number of Mars Express orbits with ionospheric and subsurface data (including data from the MARSIS special campaign called "interleave orbits") and trying to understand the possible discrepancy in

MARSIS data, an objective statistical analysis has been carried out in this chapter for the first time. As a matter of fact, the discrepancy within the MARSIS data set has been pointed out many times, but never clearly quantified up to now. The comparisons have been performed with 21 Mars Express orbits belonging to the period 14-04-2007 to 23-06-2011. On one hand, MARSIS AIS (Active Ionospheric Sounding) data have been considered as the most adequate and trustable data to refer the comparisons based on a large sounding experience on Earth routinely, and therefore, based on a technique well known. The full procedure to obtain electron density profiles from these data, as well as, their uncertainty is explained in chapters 2 and 3 respectively. These data constitute a low limit in the comparisons since only represent the topside ionosphere. On the other hand, MARSIS SubS (SubSurface) data have been analysed carefully. There are several methods to retrieve TEC from the raw dataset of this operational mode. However, in this thesis, two techniques have been considered, identified as "Grenoble" and "Rome", due to the geographical localisation of the authors. The main problem is that both TEC values do not match, reaching a large difference in the dayside when the ionospheric dispersion and absorption of the electromagnetic signal is high.

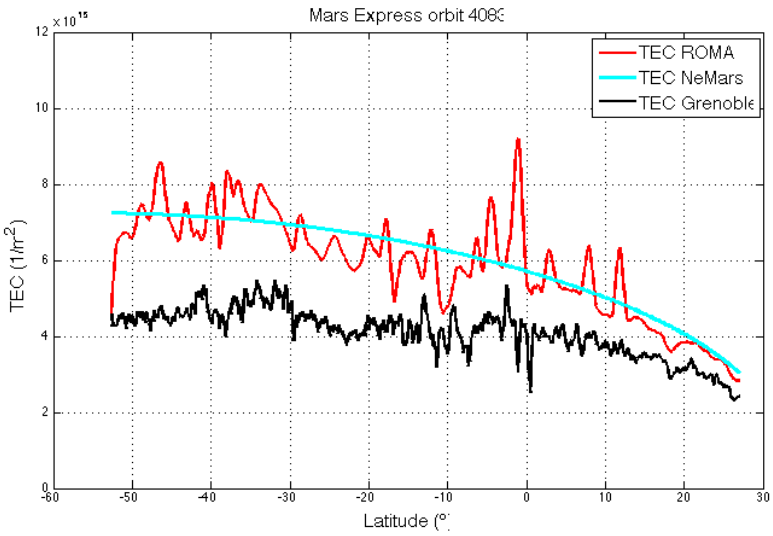

Figure 4.20: TEC-solar zenith angle variation for orbit 4083 (11-3-2007) characterised by a solar zenith angle interval: (75º>χ>90º, day terminator). The full ionosphere TEC derived from MARSIS subsurface mode (black from "Grenoble" method and red from "Rome" method) have been represented with the NeMars TEC for the dayside ionosphere (cyan). It can be perceived that "Rome" and NeMars TEC match quite well, while the difference with respect to "Grenoble" TEC is large, being higher for low solar zenith angle.

The most remarkable results are that at night (χ>90º), when the ionosphere is weak and its effect on radio-wave practically negligible, both MARSIS SubS procedures match satisfactorily (the mean and median absolute differences being almost zero). Close to the terminator (75º>χ>90º) the ionospheric effect on the dispersion of the electromagnetic signals starts to be appreciable (e.g. Figure 4.20). Here, small differences in the datasets can be seen. "Rome" matches quite well with the predicted values of NeMars model (absolute difference less than 0.1 TECu) while "Grenoble" underestimates a bit (absolute difference of less than 0.2 TECu). Moreover, in the dayside (60º>χ>75º), the difference between "Grenoble" and "Rome" datasets is considerably high. In this case, the NeMars model has been used to test how large is the difference between these datasets. Therefore, "Grenoble" results are clearly underestimating the martian ionospheric TEC (the mean and median of the absolute difference being 0.35 TECu) while "Rome" are more consistent with NeMars prediction although with a slight overestimation -predicted by Cartacci et al., 2013- (mean of the absolute difference -0.21 TECu, median 0.08 TECu and standard deviation of 1 TECu).

On the other hand, when direct topside MARSIS AIS data are compared with these both datasets for the exactly same positions (in latitude and solar zenith angle), as well as with the NeMars model for only the topside ionosphere, "Grenoble" methodology fits almost perfect with those (mean and median of the absolute difference 0.08 TECu).

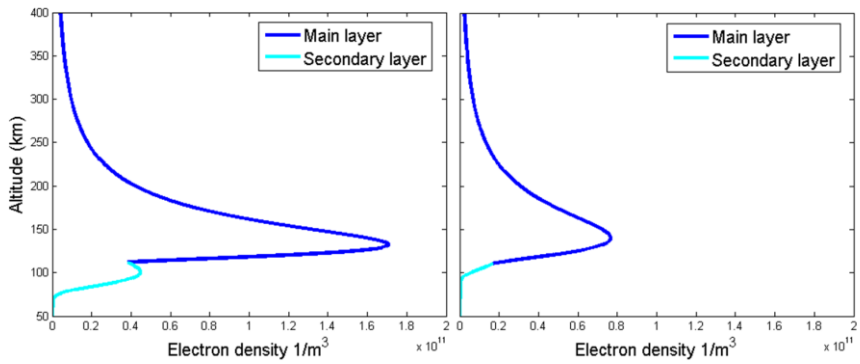

Figure 4.21: Comparison between two NeMars electron density profiles for solar zenith angle of 30º (left panel) and 80º (right panel). The rest of the characteristics, like heliocentric distance or solar activity, are the same. Close to the terminator, the ionization is reduced to the point that the secondary layer disappears almost completely.

These results are the confirmation that the "Grenoble" retrieval –the TEC archived in the ESA Planetary Science Archive-, although in principle physically and mathematically realistic, is almost equal to the TEC of the topside ionosphere. The "Rome" retrieval is more similar to the ionosphere predicted by NeMars model despite the observed overestimation of the result in daytime. As mentioned before, "Grenoble" data have been positively compared with the model Mendillo et al., (2011) at Mendillo et al., (2013a). Both MARSIS subsurface data processing have different assumptions on the ionosphere as a starting point. "Grenoble" assumes a Gaussian function to start the procedure, and then a Chapman shape to fit the profile by successive iterations, while "Rome" assumes an uniform ionosphere with a determined thickness "L".

Therefore, a possible explanation is that "Grenoble" method considers that all the atmospheric ionization can be represented reliably with one Chapman profile. Under this assumption, information about secondary layers below the main one is not taken into account and, in addition, part of the topside ionization information is missed because the basic Chapman theory used by "Grenoble" method does not consider a variable scale height for the topside (see chapter 3). However, close the terminator the method works well. Here, the ionosphere is critically controlled by the solar incidence and the secondary layer disappears as soon as the ionization of the main one decreases (Figure 4.21). Therefore, practically there is only one ionospheric layer, which fits properly with the hypothesis of the method.

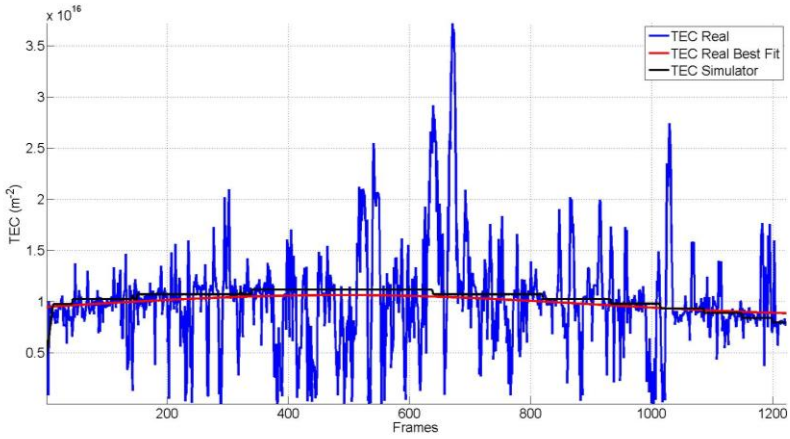

Figure 4.22: Preliminary result of the MARSIS SubS TEC simulation based on inputs from the NeMars model. Real TEC derive with the "Rome" procedure for the orbit 4207 have been plotted (blue). To facilitate comparisons, the red line represents the data best fit to polynomial. In black, simulated TEC from the phase shift calculated with NeMars model. A good agreement between both curves has been found.

An important remark is that the horizontal variation of both MARSIS SubS TEC data does not match either. For example, in Figure 4.20, one can clearly see how both TEC (obtained from the same raw data) have different variation behaviour along one orbit. Moreover, in "Rome" data is common to find some sharp spikes no related to the ionosphere structure for which with no interpretation has been proposed so far. Additionally, it should be noted that the NeMars model is designed to analyse the dayside. Although close the terminator the grazing incidence is considered (equation 1.13), the accuracy of some mathematical equations of the model should be contemplated when data at theses solar zenith angles are used.

In order to characterise in detail the inconsistencies among the results obtained with the available datasets and to propose a way to reconcile them, NeMars model is currently being used to simulate the results obtained with the MARSIS subsurface mode in the "Rome" retrieval by the MARSIS team. To test the "Rome" algorithm for the correction of ionospheric distortion, the computation of the synthetic phase (phase shift, equation 4.5 / 4.6) from NeMars model for all frequencies within the band of the signal is needed. Once the entire process is run, simulated TEC can be retrieved. A very first result is shown in Figure 4.22 where for the orbit 4207 the following data have been plotted: real "Rome" MARSIS SubS TEC, its best fitting to obtain an average TEC value of this orbit and the simulated TEC from the calculated NeMars phase shift. At this stage, the simulations seem to work properly giving similar results. In the near future, it is expected that MARSIS team can finish the simulations and the full validation of its technique.

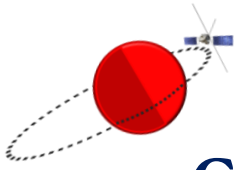

Chapter 5.

General discussion, summary, conclusions and future work

The upper atmosphere of Mars, which includes the ionosphere, is the first region of the martian system in direct contact with the solar wind because Mars does not have a global magnetosphere. Therefore, the ionosphere is strongly conditioned by the solar activity variations. It plays an important role in the volatile escape processes that have dehydrated the planet over solar system history. In this way, it strongly affects the evolution of the climate and the habitability of Mars over geological time. A good knowledge of the Mars' upper atmosphere and ionosphere is important, as key elements of the entire system.

The knowledge gained about this atmospheric layer, as well as the global picture of Mars, has undergone an exponential evolution in the last 5-10 years thanks to the massive Mars' exploration carried out primarily by NASA and ESA space agencies. A better understanding of the ionosphere-plasma system has emerged mainly thanks to almost 11 years of continuous measures of plasma properties by several instruments on board Mars Express: ASPERA, MaRS and MARSIS. Before, this knowledge was limited to a few time-intervals of data because no continuous measurements of the ionosphere had been performed for a long period. Consequently, for the first time in history, it is possible to analyse the martian ionosphere under a full solar cycle, something essential that can help the Mars' exploration. Hopefully, this comprehensive solar coverage will be enriched very soon with measurements taken simultaneously by the Mars Express and MAVEN (NASA mission Mars Atmosphere and Volatile EvolutioN) missions. Both spacecraft will make joint campaigns for a deeper analysis of the martian plasma characteristics, allowing exhaustive ionospheric studies by data comparison of each mission at the same time.

This doctoral work is under support of the Meiga-MetNet PRECURSOR project, which has formed a big group of martian studies at Universidad Complutense de Madrid. Among these studies stand out those devoted to analyse the boundary layer, charge particles in the atmosphere, ionosphere, Phobos eclipse predictions, and cloud computing. In particular, the ionospheric group had a previous experience on the development of empirical modelling for the Earth ionosphere. For many years, the Group of Ionospheric Studies and Global Navigation Satellite System (GNSS) has had a very close relationship with Professor Radicella from the Abdus Salam International Centre for Theoretical Physics (ICTP) in Trieste (Italy). Prof. Radicella is one of the two designers of the NeQuick model (Radicella and Letinger, 2001; Radicella, 2009),

which is largely used for describing the Earth ionosphere in a very quick and accurate way. This doctoral thesis is framed in this context.

With the objective to extrapolate the terrestrial ionospheric experience to Mars, a previous Master work was done about Mars Global Surveyor Radio Science experiment (Sánchez – Cano, 2010). The next step was to take advantage of the good coverage and accuracy of the Mars Express MARSIS radar instrument, which analysis has been the base of this work and which physics and retrieval procedure are similar to those uses by the Earth digisondes. This dataset had been largely unexploited in Europe, and allowed an original study about martian plasma.

The main purpose of this thesis has been to answer one of the key open questions: what is the behaviour of the martian ionosphere under different conditions (like solar incidence, solar activity, seasons, orbital distance to Sun…)? In this context and considering that the link among all chapters of this doctoral thesis is the data analysis and interpretation of the MARSIS AIS data set, the work has been articulated into the following studies:

- ☼ To study the general plasma physics theory, as well as, Earth and Mars ionospheric plasma theory.
- ☼ To learn the data analysis by using the MARSIS AIS data analysis tool.
- ☼ To perform the data analysis and comparison between topside sounder profiles and radio-science profiles with similar characteristics.
- ☼ To analyse a large data set to build an empirical model, as well as, the role that some parameters have in the ionosphere formation.
- ☼ To study the Total Electron Content (TEC).

The collaboration with the European Space Research and Technology Centre (ESTEC) of the European Space Agency and with the Abdus Salam International Center for Theoretical Physics (ICTP) led to the main definition of this work by using the MARSIS AIS dataset and the empirical model experience respectively.

- ☼ -

As already mentioned, the driver of this work has been the MARSIS AIS dataset analysis. Such data, represented by ionograms, are plots of the time delay of a frequency sweep. Although their access is free at the ESA Planetary Science Archive, there is no public software available for the data processing. A software, called MAISDAT tool, developed at ESTEC, has been used to analyse

the data. In order to derive a vertical electron density profile, it is necessary to scale manually each individual ionogram, following a routine explained at Chapter 2. Since the amount of data is large, ionograms with the best visual characteristic (clear trace, presence of harmonics…) have been selected to ensure the best quality of information.

A comparison with electron density profiles derived from Mars Express radio-occultation data was done to analyse how close are both kind of profiles, and therefore, to check that both the technique and the procedure used to derive the profile of electron density were correct. Radio-occultation technique is well known in the study of the Earth and planetary ionospheres and can be considered as a reliable reference, although its accuracy is one order of magnitude less than the topside sounder (see Paetzold et al., 2005 and Gurnett et al., 2008). After comparing different profiles acquired from both experiments under similar conditions, it was possible to remark that equivalent results were obtained, in particular in the region of maximum ionization. The differences at high altitudes could be due to differences in accuracy, clearly a point for future investigations.

This detailed analysis, which is explained in Chapter 2 of this manuscript, led to the publication of an article in the *open access* journal *Geoscientific Instrumentation, Methods and Data Systems (GI)*, devoted to geophysical instrumentation under the title "Retrieval of ionospheric profiles from the Mars Express MARSIS experiment data and comparison with radio-occultation data".

- ☼ -

This data processing has been the backbone of this work, allowing the construction of an empirical model for the martian dayside ionosphere, called NeMars. It is remarkable that, although in every moment the model is called "empirical" for simplicity, in reality it should be called "semi-empirical" because it is not only based on the best-fitting data, it also follows general principles of ionospheric plasma physics. This model resembles the terrestrial ionosphere model NeQuick (Radicella and Letinger, 2001; Radicella, 2009) which was developed at ICTP in Italy in collaboration with the Univerisity of Graz (Austria) during the nineties of the last century. This model has been used by the European Space Agency in their Global Navigation Satellite System (GNSS), in particular by the GALILEO single frequency operations to compute ionospheric corrections.

NeMars model is mainly based on data from the low frequency radar MARSIS. Particularly, the behaviour of the main global ionospheric layer was based on AIS data (AIS electron density profiles only gives information of the

ionospheric topside), and the secondary global layer was characterized with radio-occultation data from the NASA Mars Global Surveyor mission. The model predicts pretty well the main characteristics of both ionospheric regions (electron density and peak altitudes, scale heights, shape of the profiles and TEC of the entire ionosphere) in a simple and quick way from the following inputs: solar zenith angle, solar flux F10.7 as a proxy of the solar activity, and heliocentric distance.

The ionograms and radio-occultation profiles were carefully chosen one by one. It is important to remark that the measurements taken by the radio science experiment on board Mars Global Surveyor are restricted in solar zenith angle (70º-90º) and latitude (60º-85º North or South) due essentially to the observing geometry limitations between Mars and Earth orbits (Withers and Mendillo, 2005). This disadvantage was partially solved with the theoretical study of the solar zenith angle described in the Chapter 3. Further improvements of the empirical equations will be held as soon as new data are available with greater variation of this parameter. Moreover, as the secondary peak in a radio-occultation profile is not always visible because is embedded in the main one, this layer has been examined in the most prominent case, when the secondary peak was clearly visible. The criterion was to know the peak behaviour in the visible cases and then, mathematically extrapolate to the rest (see Appendix I). Therefore, possible overestimation errors could be introduced although NeMars equations can describe the behaviour of this layer also when is embedded in the main one. As soon as new data with larger variability become available, the equations could be improved.

The whole model is based on the consideration that the martian ionosphere is in photochemical equilibrium and the two main layers can be represented by the α-Chapman theory. However, to give a more realistic description, other input parameters like solar activity or heliocentric distance have been included. Regarding the **main layer**, the electron density peak is calculated with high accuracy from the inputs solar zenith angle, solar flux index $F_{10.7}$ and heliocentric distance. However, the altitude of the main peak cannot be calculated from the same inputs as the large height variation of the AIS data and their slight variation with the solar activity hide the possible variation of the height peak with the $F_{10.7}$ index. Nevertheless, there is a significant dependence with the solar zenith angle and the statistics shows that with this unique dependence, the model adjusts reasonably well. Regarding the scale height, the MARSIS AIS data profile is better reproduced when a linearly variable scale height with altitude and solar zenith angle is considered, being the median relative differences (%) between the real and the model profiles lower than 6% even at altitudes about 60 km over the maximum peak. This scale height

hypothesis has been compared with previous works as Němec et al., (2011) where a constant scale height is used, showing that this approach works better even at high altitudes. In relation to the **secondary layer**, the shape of the electron density peak equations is similar to the main one with the foremost difference in that a constant scale height of 12 km has been considered.

In general, NeMars is a powerful tool to accurately and quickly describe the "normal and undisturbed" ionosphere of Mars at any location and time. However, given the selected data sample, the model does not address ionospheric disturbances. As a test, the model was compared with some electron profiles recorded during extreme conditions of magnetic field (from solar wind and from magnetic surface anomalies) and with profiles where a third layer at very low altitudes appears. In these cases, despite of the irregularities in the profiles, the modelled results were not far from reality. To deepen in this trend of research, the model will be improved in the next future to consider the magnetic field input from the solar wind and form the planet itself.

This detailed work, which is shown in Chapter 3 of this doctoral thesis, led to the publication of an article in the journal *Icarus*, under the title "An empirical model of the martian dayside ionosphere based on Mars Express MARSIS data". Analogously, this work has been presented at numerous national and international conferences, which are listed in the Appendix III of the manuscript. Recently, the most recent efforts of the scientific community are directed towards creating an International Reference Model for Mars ionosphere -called MIRI- taking advantage of the large available amount of Mars' ionosphere data and of the large scientific experience with the International Reference Model (IRI) for the Earth ionosphere (Mendillo et al., 2013b). This reference model is an international project sponsored by the Committee on Space Research (COSPAR) and the International Union of Radio Science (URSI). The work carried out in this thesis will most likely contribute to this model by providing processed MARSIS AIS data, outputs of the NeMars model, by sharing the experience in analysing different datasets and comparing them (MARSIS with radio-occultation, MARSIS AIS with MARSIS SubS…), and finally by sharing the critical analysis of the total electron content data sets.

- ☼ -

Once the model is run, several by-products can be obtained, in particular the total electron content (TEC). This parameter can be used to validate the model by comparing the observational TEC values given by MARSIS with the estimates obtained with NeMars. Therefore, the NeMars TEC was compared with the TEC measurements deduced from MARSIS subsurface mode

(Mouginot et al., 2008 –called also in this work "Grenoble" group- and Cartacci et al., 2013 –called also in this work "Rome" group-). The most intriguing result was that the TEC derived from MARSIS instrument, subsurface mode and ionosphere topside electron density integrated mode, are not consistent. Both modes practically give the same value, which is difficult to understand given the fact that the "subsurface" TEC corresponds to the entire ionosphere, while the "AIS" TEC corresponds only to the ionosphere above the main peak. Since the TEC values are currently difficult to reconcile, it was decided to carry out an objective and unbiased comparison between both techniques taking advantage of the large number of Mars Express orbits with ionospheric and subsurface data (including data from the MARSIS special campaign called "interleaved mode orbits") to characterise in detail the inconsistencies among the results obtained with the available datasets and to propose a way to reconcile them. This discrepancy within the MARSIS data set has been pointed out many times, but never clearly quantified up to now.

The comparisons were performed with 21 Mars Express orbits belonging to the period 14-04-2007 to 23-06-2011. The most remarkable results are that at night (χ>90º), when the ionosphere is weak and its effect on radio-wave practically negligible, both MARSIS SubS procedures ("Grenoble" and "Rome" retrievals) match satisfactorily. Close to the terminator (75º>χ>90º) the ionospheric effect on the dispersion of the electromagnetic signals starts to be appreciable and small differences in the datasets can be spotted. "Rome" matches quite well with the predictable values of NeMars model while "Grenoble" underestimates slightly. Furthermore, in the full dayside (60º>χ>75º), the difference between "Grenoble" and "Rome" datasets is high. In this case, the NeMars model has been used to test how large is the difference between these datasets, showing that the "Grenoble" values are clearly underestimated, while the "Rome" results are more consistent although with a slight overestimation -predicted in fact by Cartacci et al., 2013-.

The main conclusion is that "Grenoble" retrieval –the TEC archived in the ESA Planetary Science Archive-, although in principle physically and mathematically realistic, is almost equal to the TEC of the topside ionosphere; whilst the "Rome" retrieval is more similar to the ionosphere predicted by NeMars model despite the already mentioned overestimation of the result in the daytime. One remark is that "Grenoble" data have been positively compared with the model Mendillo et al., (2011) at Mendillo et al., (2013a). Arguably, at least these results are not consistent with those obtained with the MARSIS radar sounder in the ionospheric mode.

Both MARSIS subsurface data processing have different assumptions on the ionosphere as a starting point. "Grenoble" assumes a Gaussian function to start the procedure, and then a Chapman shape to fit the profile by successive iterations, while "Rome" assumes a uniform ionosphere with a determined thickness "L". Therefore, a possible explanation is that "Grenoble" method considers that all the atmospheric ionization can be represented reliably with one Chapman profile. Under this assumption, information about secondary layers below the main one are not considered and also, part of the topside ionization information is lost because of Chapman theory does not considered a variable scale height for the topside. However, close the terminator the method works well. Here, the ionosphere is critically controlled by the solar incidence and practically there is only one ionospheric layer, which fits properly with the hypothesis of the method.

This exhaustive analysis is shown in Chapter 4 of this doctoral thesis, and part of this was published in the journal *Icarus*, under the title "An empirical model of the martian dayside ionosphere based on Mars Express MARSIS data". The rest of the work is currently under review at *Icarus* with the title "Study of the Total Electron Content in the martian atmosphere: a critical assessment of the Mars Express MARSIS dataset". Also, this work has been presented at numerous conferences on national and international level, which appear listed in the Appendix III. In passing, it is interesting to mention that this work allowed identifying an error in the MARSIS AIS data in the Planetary Science Archive of the European Space Agency (see Appendix II for more information). These data were published for the scientific community for more than 8 years with the planetary longitude given in westward direction although in the archive and in the technical notes (e.g. EAICD section 3.2.3) were written: "Longitude is given in positive-East coordinates in the range 0º-360º".

- ☼ -

Besides the main line of research that has been described along this book, this thesis has led to other collateral research works that currently are on-going. In the same vein as analysing a large sample of MARSIS data, the altitude variations of the main ionospheric peak related to topographic causes, is being studied. In other words, the potential coupling between ionosphere and topography on Mars is receiving more attention. The objective was to check results of some previous works as Keating et al., (1998) or Wang and Nielsen, (2004) where this effect could be understood as a modulation of the near-surface atmospheric pressure by topography. If the ionosphere was spherically uniform, no differences in the altitude measurement among different topographic edifices would be expected in a first approximation and taking into

account the reference system of the instrument. Nevertheless, the altitude of the main ionospheric peak shows some regional variations, which are not directly above any prominent topographic features. Currently, using the entire MARSIS dataset, the effect of the topography is not confirmed, although large variations in the peak height have been found, most likely due to gravity waves.

Another collateral studies, which are currently on-going in collaboration with other members of the Meiga-MetNet Precursor Project (which mainly has supported this PhD), are related to the analysis of the magnetic field environment from the surface to the upper atmosphere of Mars. These studies have been caused by the development of a triaxial magnetometer, called MOURA, specially developed for space exploration at INTA (Instituto Nacional de Técnica Aeroespacial). Inside this spatial-atmosphere, different studies for calibration of MOURA magnetometer are being carried out, as well as, an empirical analysis of the magnetic field at the upper atmosphere level by using the absolute value at the spacecraft altitude, registered in the ionograms from the Mars Express MARSIS AIS dataset (see main characteristics of the ionograms in chapters 2 and 3).

- ☼ -

This doctoral thesis has attempted to answer the question of what is the empirical behaviour of the Mars' ionosphere under different situations like solar activity, solar incidence or orbital characteristics. Nonetheless, currently there are still many important open questions such as: the importance of atmospheric escape for the evolution of the planet's climate; how solar forcing determines ionospheric properties… therefore, there are still many possibilities to further our understanding of the plasma environment, and this thesis is a small contribution to this big picture.

As mentioned at the beginning of this chapter, one of these open questions is to understand the Mars' ionosphere behaviour over a whole solar cycle, since the ionosphere is strongly depending on solar activity. Accordingly, the ionospheric behaviour between low, medium and high solar activity is different and it is necessary to model it accurately since the entire planet system can be affected (e.g. climate, temperature, radiative balance, dispersion of electromagnetic signals…). One of the most interesting plans to continue this work is to improve our knowledge of the martian ionosphere, carrying out a more thorough analysis of the latest years of solar activity. This is possible for first time in history thanks to the successful eleven years of Mars Express in orbit. Moreover, this knowledge will be enriched with the analysis of measurements taken simultaneously by Mars Express and MAVEN. Both spacecraft will make joint campaigns for a deeper analysis of the martian plasma characteristics,

allowing exhaustive ionospheric studies by data comparison of every mission at the same time.

Plasma modelling with solar activity is a key element because once the model is validated with experimental observations, the ionosphere can be simulated in any circumstance. Currently, the empirical model NeMars reproduces the shape of the ionosphere and its variation with the solar activity and the heliocentric distance, in a very quick way and with high precision up to the diffusion-controlled region (about 200 km over the surface). However, the plasma transport in this region is not well described and the model assumptions need to be revisited. In addition, it is necessary to consider possible variations in the behaviour of the electron density in the period of low activity 2007-2009 as it happened on the Earth ionosphere. This shortcoming could be significant because the effect of this low activity period on Earth was unpredictable by solar models and caused many mismatches to the terrestrial ionospheric models (e.g. Klenzing et al., 2012) and therefore, to communications. Therefore, a future step to improve the model could be to take into account and complement it with other models, which consider more additional phenomena. An example could be the fluid-numerical model TRANSMARS, based on the physical processes acting in the ionosphere and developed at ESTEC and IRAP (Toulouse, CNRS), that take into account the transport in the ionosphere, as well as the magnetic field coming from the solar wind, and which code has been extensively and successfully used to describe the Earth ionosphere. The combination NeMars-TRANSMARS and their validation with data analysis would provide an important improvement for both models, giving a broader control of the solar activity effects and the phenomena that play an important role in the formation and variability of the martian ionosphere. Furthermore, other issues as the chemistry and the temperature of the martian upper atmosphere (Forget et al., 2009), the dependence of the height on the neutral atmospheric density (Bougher et al., 2001 and Zou et al., 2011) and the ionospheric effect of the crustal magnetic field on the Southern hemisphere (Nielsen et al., 2007) could be considered to improve the model.

Another important application of the empirical model develop in this doctoral thesis is to simulate the MARSIS experiment (in subsurface mode). These simulations could solve the current discrepancy in the TEC measurements commented above. Currently, the NeMars model outputs are being used to simulate the radio-wave propagation obtained with the MARSIS subsurface mode in the "Rome" retrieval by the MARSIS team to study the TEC retrieving techniques constrains and limits. To test the "Rome" algorithm for the correction of ionospheric distortion, NeMars model is being used to calculate the synthetic phase from all frequencies and bands of the signal. Once the entire

process is run, simulated TEC can be retrieved. At this stage, the simulations seem to work properly giving similar results. In the near future, it is expected that MARSIS team can finish the simulations and the full validation of its technique. This way of using models to analyse data is something new and, in the frame of the on-going collaboration with the Mars Express MARSIS team, has been recently proven to be very fruitful.

- ☼ -

Looking at the future of Mars' research, and in particular about its ionosphere, a largely unexplored field is the lower ionosphere. This PhD has been a great opportunity to gain a unique experience on data analysis from the topside sounder MARSIS. This expertise could be useful in case future surface assets would embark an ionosonde. This would allow new studies of the lower layers of the ionosphere to be performed, in particular to detect lower layers, which have only been postulated theoretically. Also, such studies would permit the effect of dust storms on the electrification of the lower atmosphere.

Another interesting future line for the martian exploration would be the study of the Mars' interior through the analysis of the possible lithosphere-ionosphere coupling and the propagation of seismic-induced waves through the ionosphere (Pulinets and Ouzounov, 2011). As several research groups studied on Earth, the ionosphere is an excellent wave-propagator medium which can allow monitoring seismic activity on the planet (Lognonné et al., 2006). Taking advantage of the next NASA mission to Mars InSight (Interior Exploration using Seismic Investigations, Geodesy and Heat Transport), it should be possible to monitor the possible martian seismicity by using , by using Mars Express and MAVEN plasma instruments. InSight mission is an unmanned Mars lander mission due to launch in March 2016 with the objective of placing a stationary lander equipped with a seismometer and heat flow probe on the surface of Mars to study its early geological evolution. Therefore, it will allow having more information about the internal structure of Mars.

Step by step, the knowledge of the red planet grows and with it, our cultural richness progresses. Nobody should ever forget that tomorrow is another day.

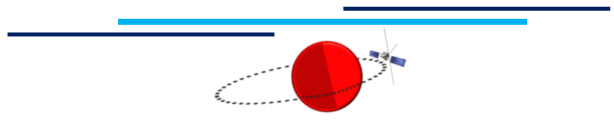

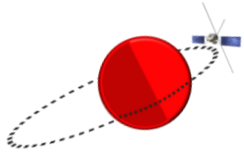

References

☼ Acuña, M.H., Connerney, J.E.P., Wasilewski, P., Lin, R.P., Anderson, K.A., Carlson, C.W., McFadden, J., Curtis, D.W., Mitchell, D., Rème, H., Mazelle, C., Sauvaud, J.A., d'Uston, C., Cros, A., Medale, J.L., Bauer, S.J., Cloutier, P., Mayhew, M., Winterhalter, D., Ness, N.F., 1998. Magnetic field and plasma observations at Mars: Initial results of the Mars Global Surveyor mission. Science. 279, 1676. doi:10.1126/science.279.5357.1676.

☼ Acuña, M.H., Connerney, J.E.P., Ness, N.F., Lin, R.P., Mitchell, D., Carlson, C.W., McFadden, J., Anderson, K.A., Rème, H., Mazelle, C., Vignes, D., Wasilewski, P., Cloutier, P., 1999. Global Distribution of Crustal Magnetization Discovered by the Mars Global Surveyor MAG/ER Experiment. *Scienc.* 284, 5415, 790-793. doi: 10.1126/science.284.5415.790.

☼ Andrews, D.J., André, M., Opgenoorth, H.J., Edberg, N.J.T., Diéval, C., Duru, F., Gurnett, D.A., Morgan, D., Witasse, O., 2014. Oblique reflections in the Mars Express MARSIS data set: Stable density structures in the Martian ionosphere. Submitted to Journal of Geophysical Research.

☼ Arkani-Hamed, J., 2004. Timing of the Martian core dynamo, J. Geophys. Res., 109, E03006, doi:10.1029/2003JE002195.

☼ Barabash, S., Lundin, R., Andersson, H., Gimholt, J., Holmström, M., Norberg, O., Yamauchi, M., Asamura, K., Coates, A. J., Linder, D. R., Kataria, D. O., Curtis, C. C., Hsieh, K. C., Sandel, B. R., Fedorov, A., Grigoriev, A., Budnik, E., Grande, M., Carter, M., Reading, D. H., Koskinen, H., Kallio, E., Riihela, P., Säles, T., Kozyra, J., Krupp, N., Livi, S., Woch, J., Luhmann, J., McKenna-Lawlor, S., Orsini, S., Cerulli-Irelli, R., Maggi, M., Morbidini, A.; Mura, A., Milillo, A., Roelof, E., Williams, D., Sauvaud, J.-A., Thocaven, J.-J., Moreau, T., Winningham, D., Frahm, R., Scherrer, J., Sharber, J., Wurz, P., Bochsler, P., 2004. ASPERA-3: analyser of space plasmas and energetic ions for Mars Express. In: Mars Express: the scientific payload. Ed. by Andrew Wilson, scientific coordination: Agustin Chicarro. ESA SP-1240, Noordwijk, Netherlands: ESA Publications Division, ISBN 92-9092-556-6, 2004, p. 121 – 139.

☼ Barabash, S; Fedorov, A., Lundin, R., Sauvaud, J.-A., 2007. Martian Atmospheric Erosion Rates. Science, Volume 315, Issue 5811, pp. 501- 503. *DOI:* 10.1126/science.1134358.

☼ Bertaux, J.L., Leblanc, F., Perrier, S., Quemerais, E., Korablev, O., Dimarellis, E., Reberac, A., Forget, F., Simon, P.C., Stern, S.A., Sandel, B., the SPICAM team., 2005. Nightglow in the Upper Atmosphere of Mars and Implications for Atmospheric Transport. Science. Vol. 307 no. 5709 pp. 566-569. *DOI:* 10.1126/science.1106957

☼ Bauer, J., 2008. Analysis of ionospheric sounding data from Mars Express. Master's thesis. Kiruna University, Kiruna, Sweden.

☼ Bougher, S.W., Engel, S., Hinson, D.P., Forbes, J.M., 2001. Mars Global Surveyor Radio Science Electron Density Profiles: Neutral Atmosphere Implications. Geophysical Research Letters. 28, 3091–3094.

☼ Budden, K.G., 1985. The Propagation of Radio Waves. Cambridge University Press. Cambridge.

☼ Campbell, B.A., Putzig, N.E., Carter, L.M., Phillips, R.J., 2011. Autofocus correction of phase distortion effects on SHARAD echoes. IEEE geoscience and remote sensing letters, vol. 8, no. 5.

☼ Campbell, B.A., Putzig, N.E., Foss, F.J., Phillips. R.J., 2013. SHARAD signal attenuation and delay offsets due to the Martian ionosphere. Accepted at IEEE geoscience and remote sensing letters.

☼ Cartacci, M., Amata, E., Cicchetti, A., Noschese, R., Giuppi, S., Langlais, B., Frigeri, A., Orosei, R., Picardi, G., 2013. Mars ionosphere total electron content analysis from MARSIS subsurface data. Icarus, Volume 223, Issue 1, p. 423-437. doi: 10.1016/j.icarus.2012.12.011.

☼ Chapman, S., 1931a. Absorption and dissociative or ionizing effects of monochromatic radiation in an atmosphere on a rotating earth. Proc. Phys. Soc.. London 43, 26-45.

☼ Chapman, S., 1931b. Absorption and dissociative or ionizing effect of monochromatic radiation in an atmosphere on a rotating earth part II. Grazing incidence. Proc. Phys. Soc.. London 43, 483-501.

☼ Chapman, S., Bartels, J., 1940. Geomagnetism. Oxford University Press. Oxford.

☼ Chicarro, A., Martin, P., and Traunter, R., 2004. Mars Express: A European mission to the red planet. European Space Agency Publication Division. SP-1240,pp. 3-16, Noordwijk, Netherlands.

☼ Chen, R. H., Cravens, T.E., Nagy. A.F., 1978. The Martian ionosphere in light of the Viking observations, J. Geophys. Res., 83, 3871–3876.

☼ Cravens, T. E., 1997. Comet Hyakutake X-ray source: Charge transfer of solar wind heavy ions. Geophys. Res. Lett., 24, 105-108.

☼ Duru, F., Gurnett, D.A., Averkamp, T.F., Kirchner, D.L., Huff, R.L., Persoon, A.M., Plaut, J.J., Picardi, G., 2006. Magnetically controlled structures in the ionosphere of Mars. Journal of Geophysical Research 111. doi: 10.1029/2006JA011975. issn: 0148-0227.

☼ Duru, F., Gurnett, D.A., Morgan, D.D., Modolo, R., Nagy, A.F., Najib, D., 2008. Electron densities in the upper ionosphere of Mars from the excitation of electron plasma oscillations. J. Geophys. Res., 113, A07302, doi:10.1029/2008JA013073.

☼ Duru, F., Gurnett, D.A., Frahm, R.A., Winningham, J.D., Morgan, D.D., Howes, G.G., 2009. Steep, transient density gradients in the Martian ionosphere similar to the ionopause at Venus. J. Geophys. Res., 114, A12310, doi:10.1029/2009JA014711.

☼ Forget, F., Montmessin, F., Bertaux, J.-L., González-Galindo, F., Lebonnois, S., Quémerais, E., Reberac, A., Dimarellis, E., López-Valverde, M.A., 2009. Density and

Temperatures of the Upper Martian Atmosphere Measured by Stellar Occultations with Mars Express SPICAM. Journal of Geophysical Research. 114, E1, E01004, 114, doi:10.1029/2008JE003086.

☼ Fox, J. L., 2009. Morphology of the Dayside Ionosphere of Mars: Implications for Ion Outflows. Journal of Geophysical Research. 114, E12005, doi:10.1029/2009JE003432.

☼ Gronoff, G., Lilensten, J., Simon, C., Barthélemy, M., Leblanc, F., Dutuit, O., 2008. Modelling the Venusian airglow. Astronomy and Astrophysics, Volume 482, Issue 3, 2008, pp.1015-1029. Doi: 10.1051/0004-6361:20077503.

☼ Gronoff, G., Lilensten, J., Desorgher, L.; Flückiger, E., 2009a. Ionization processes in the atmosphere of Titan. I. Ionization in the whole atmosphere. Astronomy and Astrophysics, Volume 506, Issue 2, 2009, pp.955-964. Doi: 10.1051/0004-6361/200912371.

☼ Gronoff, G., Lilensten, J., Modolo, R., 2009b. Ionization processes in the atmosphere of Titan. II. Electron precipitation along magnetic field lines. Astronomy and Astrophysics, Volume 506, Issue 2, 2009, pp.965-970. Doi: 2009A&A...506..965G.

☼ Gurnett, D.A., Kirchner, D.L., Huff, R.L., Morgan, D.D., Persoon, A.M., Averkamp, T.F., Duru, F., Nielsen, E., Safaeinili, A., Plaut, J.J., Picardi, G., 2005. Radar soundings of the ionosphere of Mars. Science. 310, 1999-1933.

☼ Gurnett,D.A., R.L. Huff., D.D. Morgan., A.M. Persoon., T.F. Averkamp., D.L. Kirchner., F. Duru., F. Akalin., A.J. Kopf., E. Nielsen., A. Safaeinili., J.J. Plaut., G. Picardi., 2008. An overview of radar soundings of the Martian ionosphere from the Mars Express spacecraft. Adv. Space Research. 41, 1335-1346.

☼ Hargreaves, J. K., 1992. The Solar-Terrestrial environment. Cambridge University Press. p 218.

☼ Hanson, W. B., Sanatani, S., Zuccaro, D.R., 1977. The Martian ionosphere as observed by the Viking retarding potential analyzers. J. Geophys. Res.. 82(28), 4351–4363.

☼ Hanson, W. B., Mantas, G.P., 1988. Viking electron temperature measurements: Evidence for a magnetic field in the Martian ionosphere. J. Geophys. Res.. 93(A7), 7538–7544.

☼ Hantsch, M.H., Bauer, S.J., 1990. Solar control of the Mars ionosphere. Planet. Space Sci. 38, 539–542, doi:10.1016/0032-0633(90)90146-H.

☼ Huestis, D. L., Slanger, T. G., Sharpee, B. D., Fox, J. L., 2010. Chemical Origins of the Mars Ultraviolet Dayglow. *Faraday Discussions, 147*, 307-322.

☼ Ilyushin, Ya.A., Kunitsyn, V.E., 2004. Methods for correcting ionosphere distortions

of orbital ground-penetrating radar signals. J. Commun. Technol. Electron. 49, 154-165.

☼ Kopf, A.J., Gurnett, D.A., Morgan, D.D., Kirchner, D.L., 2008. Transient layers in the topside ionosphere of Mars. Geophys. Res. Lett. 35, L17102. doi:10.1029/2008GL034948.

☼ Klenzing, J., Simoes, F., Ivanov, S., Bilitza, D., Heelis, R.A., Rowland, D., 2012. Performance of the IRI-2007 model for equatorial topside ion density in the African sector for low and extremely low solar activity. NASA Technical Reports Server (NTRS). Report/Patent Number: GSFC.JA.00372.2012. NASA Goddard Space Flight Center; Greenbelt, MD, United States.

☼ Klobuchar and Aarons, 1973. Importance of the Total Electron Content parameter. In: Total Electron Content studies of the ionosphere. Air Force Survey in geophysics, no. 257, Bedford, Massachusetts.

☼ Krymskii, A.M., Breus, T.K., Ness, N.F., Hanson, D.P., Bojkov, D.I., 2003. Effect of crustal magnetic fields on the near terminator ionosphere of Mars: Comparison of in situ magnetic field measurements with the data of radio science experiments on board Mars Global Surveyor. J. Geophys. Res. 108, 1431. doi:10.1029/2002JA009662.

☼ Kutiev, I.S., Marinov, P.G., Watanabe, S., 2006. Model of topside ionosphere scale height based on topside sounder data. Adv. Space Res.. 37, 943-950.

☼ Langlais, B., Purucker, *M.E.,* Mandea, M., 2004. Crustal magnetic field of Mars, J. Geophys. Res., 109, *E02008,* doi:10.1029/2003JE002048.

☼ Leblanc, F., Witasse, O., Winningham, J., Brain, D., Lilensten, J., Blelly, P.-L., Frahm, R.A., Halekas, J.S., Bertaux, J.L., 2006. Origins of the Martian aurora observed by Spectroscopy for Investigation of Characteristics of the Atmosphere of Mars (SPICAM) on board Mars Express. J. Geophys. Res., 111, A09313, doi:10.1029/2006JA011763.

☼ Lillis, R. J., Fillingim, M.O., Peticolas, L.M., Brain, D.A., Lin, R.P., Bougher, S.W., 2009. Nightside ionosphere of Mars: Modeling the effects of crustal magnetic fields and electron pitch angle distributions on electron impact ionization. J. Geophys. Res. 114, E11009,doi:10.1029/2009JE003379.

☼ Lillis, R.J., Brain, D.A., England, S.L., Withers, P., Fillingim,M.O., and Safaeinili, A., 2010. Total electron content in the Mars ionosphere: Temporal studies and dependence on solar EUV flux. J. Geophys. Res.. 115, A11314.

☼ Liu, L., Le, H., Wan, W., Sulzer, M.P., Lei, J., Zhang, M.L., 2007. An analysis of the scale heights in the lower topside ionosphere based on the Arecibo incoherent radar measurements. J. Geophys. Res.. 112, A06307, doi: 10.1029/2007JA012250.

☼ Lognonné, P., Artru, J., Garcia, R., Crespon, F., 2006. Ground-based GPS imaging of ionospheric post-seismic signal. Planetary and Space Science, 54, 528-540.

☼ Lundin, R., Barabash, S., Holmström, M., Andersson, H., Yamauchi, M., Nilsson, H., Winningham, D., Frahm, R., Sharber, JR., Sauvaud, J-A., Fedorov, A., Budnik, E., Thocaven, J-J., Asamura, K., Hayakawa, H., Coates, AJ., Soobiah, Y., Linder, DR., Kataria, DO., Curtis, C., Hsieh, KC., Sandel, BR., Grande, M., Carter, M., Reading, DH., Koskinen, H., Kallio, E., Riihela, P., Sales, T., Kozyra, J., Krupp, N., Woch, J., Fraenz, M., Luhmann, J., Brain, D., McKenna-Lawler, S., Cerulli-Irelli, R., Orsini, S., Maggi, M., Milillo, A., Roelof, E., Livi, S., Brandt, P., Wurz, P., Bochsler, P., Galli, A., Grigorev, A., 2009. Aspera-3: Analyser of space plasmas and energetic neutral atoms. European Space Agency, (Special Publication) ESA-SP, 1291, Vol.2, 199 - 215.

☼ Ma, Y., Nagy, A.F., Hansen, K.C., DeZeeuw, D.L., Gombosi, T.I., Powell, K.G., 2002. Three-dimensional multispecies MHD studies of the solar wind interaction with Mars in the presence of crustal fields. *JGR-Space Physics.* 107, A10, 1282, doi:10.1029/2002JA009293.

☼ Menager, H., Barthélemy, M., Koskinen, T., Lilensten, J., Ehrenreich, D., Parkinson, C. D., 2013. Calculation of the H Lyman α emission of the hot Jupiters HD 209458b and HD 189733b. Icarus, Volume 226, Issue 2, p. 1709-1718. Doi: 2013Icar..226.1709M.

☼ Mendillo, M., Lollo, A., Withers, P., Matta, M., Pätzold, M., Tellmann, S., 2011. Modeling Mars' ionosphere with constraints from same-day observations by Mars Global Surveyor and Mars Express. J. Geophys. Res.. 116, A11303, doi:10.1029/2011JA016865.

☼ Mendillo, M., Narvaez, C., Withers, P., Matta, M., Kofman, W., Mouginot, J., 2013a. Variability in ionospheric total electron content at Mars. Planetary and Space Science, 86, 117-129. http://dx.doi.org/10.1016/j.pss.2013.08.010.

☼ Mendillo, M., Marusiak, A.G., Withers, P., Morgan, D.D., Gurnett, D., 2013a. A new semiempirical model of the peak electron density of the Martian ionosphere. Geophysical Research Letters. Vol. 40, Issue 20, pages 5361–5365.

☼ Molina-Cuberos, G.J., Witasse, O., Lebreton, J.-P., Rodrigo, R., López-Moreno, J.J., 2003. Meteoric ions in the atmosphere of Mars. Planetary and Space Science. 51, 3, 239-249, doi:10.1016/S0032-0633(02)00197-6.

☼ Morel, L., Witasse, O., Warnant, R., Cerisier, J.-C., Blelly, P.-L., Lilensten, J., 2004. Diagnostic of the dayside ionosphere of Mars using the Total Electron Content measurement by the NEIGE/Netlander experiment: An assessment study. Planetary and Space Science, 52, 7, p. 603-611, doi:10.1016/j.pss.2003.12.007.

☼ Morgan, D.D., Gurnett, D.A., Kirchner, D.L., Fox, J.L., Nielsen, E., Plaut, J.J., 2008. Variation of the Martian ionospheric electron density from Mars Express radar soundings. J. Geophys. Res.. 113, A09303, doi:10.1029/2008JA013313.

☼ Morgan, D.D., 2013a. Total Electron Content from MARSIS Active Ionospheric Sounding Electron Density Profiles and Surface Reflections. Mars Upper Atmosphere Network (MUAN) meeting, Boston, United States of America. Private communication.

☼ Morgan, D.D., Witasse, O., Nielsen, E., Gurnett, D.A., Duru, F., Kirchner, D.L., 2013b. The processing of electron density profiles from the Mars Express MARSIS topside sounder. Radio Science, Vol. 48, Nº 3, 197-207.

☼ Mouginot, J., Kofman, W., Safaeinili, A., Herique, A., 2008. Correction of the ionospheric distortion on the MARSIS surface sounding echoes. Planetary and Space Science. 56, 917-926, doi:10.1016/j.pss.2008.01.010.

☼ Němec, F., Morgan, D.D., Gurnett, D.A., Duru, F., 2010. Nightside ionosphere of Mars: Radar soundings by the Mars Express spacecraft. J. Geophys. Res., 115, E12009. doi:10.1029/2010JE003663

☼ Němec, F., Morgan, D.D., Gurnett, D.A., Duru, F., Truhlík, V., 2011. Dayside ionosphere of Mars: Empirical model based on data from the MARSIS instrument. J. Geophys. Res.. 116, E07003, doi:10.1029/2010JE003789.

☼ Nicholson, W.P., Gronoff, G., Lilensten, J., Aylward, A.D., Simon, C., 2009. A fast computation of the secondary ion production in the ionosphere of Mars. Mons. Not. R. Astron., 400, 369–382. doi:10.1111/j.1365-2966.2009.15463.x.

☼ Nielsen, E., Fraenz, M., Zou, H., Wang, J.-S., Gurnett, D.A., Kirchner, D.L., Morgan, D.D., Huff, R., Safaeinili, A., Plaut, J.J., Picardi, G., Winningham, J.D., Frahm, R.A., Lundin, R., 2007. Local plasma processes and enhanced electron densities in the lower ionosphere in magnetic cusp regions on Mars. Planetary and Space Science. 55, 2164-2172.

☼ Paetzold, M., Tellmann, S., Häusler, B., Hinson, D., Schaa, R., Tyler, G.L., 2005. A sporadic third layer in the ionosphere of Mars. Science 310. 837–839.

☼ Peter, K., Molina-Cuberos, G., Witasse, O., Pätzold., M., 2012. The ionosphere of Mars: modeling the photochemical dominated region and subjacent meteor layers. European Planetary Science Congress. Private communication.

☼ Peter, K., Withers, P., Pätzold, M., Birda, M.K., Molina-Cuberos, G., Häusler, B., Hinsong, D.P., Witasse, O., Tellmann, S., González-Galindo, F., Tyler, G.L., 2014. The dayside ionospheres of Mars and Venus: Comparing a one-dimensional photochemical model with MaRS (Mars Express) and VeRa (Venus Express) observations. Icarus 233 (2014) 66–82. http://dx.doi.org/10.1016/j.icarus.2014.01.028.

☼ Pi, X., Edwards, C.D., Hajj, G.A., Ao, C., Romans, L.J., Callas, J.L., Mannucci, A.J., Asmar, A.W., Kahan, D.S., 2008. A Chapman-Layers ionospheric model for Mars. JPL publication, 08-24.

☼ Picardi, G., Sorge, S., 2000. Adaptive compensation of ionosphere dispersion to improve subsurface detection capabilities in low-frequency radar systems. In: Proc.

SPIE. Eighth International Conference on Ground Penetrating Radar, vol.4084, pp. 624–629.

☼ Picardi, G., Biccari, D., Seu, R., Plaut, J., Johnson, W. T. K., Jordan, R. L., Safaeinili, A., Gurnett, D. A., Huff, R., Orosei, R., Bombaci, O., Calabrese, D., and Zampolini, E., 2004. Mars Express: A European mission to the red planet, MARSIS: Mars Advanced Radar for Subsurface and Ionosphere Sounding. European Space Agency Publication Division. SP-1240, pp.51- 70, Noordwijk, Netherlands.

☼ Picardi, G., Plaut, J.J., Biccari, D., Bombaci, O., Calabrese, D., Cartacci, M., Cicchetti, A., Clifford, S.M., Edenhofer, P., Farrell, W.M., Federico, C., Frigeri, A., Gurnett, D.A., Hagfors, t., Heggy, E., Herique, A., Huff, R.L., Ivanov, A.B., Johnson, W.T.K., Jordan, R.L., Kirchner, D.L., Kofman, W., Leuschen, C.J., Nielsen, E., Orosei, R., Pettinelli, E., Phillips, R.J., Plettemeier, D., Safaeinili, A., Seu, R., Stofan, E.R., Vannaroni, G., Watters, T.R., Zampolini, E., 2005. Radar soundings of the subsurface of Mars. Science. 310, 1925-1928.

☼ Picardi, G., Cartacci, M., Cicchetti, A., Cutign, M., Iorio,M., Masdea, A., Seu, R., Plaue, J.J., Johnson, W.T.K., Jordan, R.L., Safaeinili, A., Bombace, O., Calabrese, D., Zampoline, E., Gumett , D.A., Nielsen, E., 2008. Mars ionosphere data inversion by MARSIS Surface and Subsurface Signals analysis. IEEE RADAR CONFERENCE, VOLS. 1-4 Colection: IEEE Radar Conference, pages: 1278-1282.

☼ Pulinet, S., Ouzounov, D., 2011. Lithosphere-Atmosphere-Ionosphere Coupling (LAIC) model – An unified concept for earthquake precursors validation. Journal of Asian Earth Sciences, 41, 371-382, doi: 10.1016/j.jseaes.2010.03.005.

☼ Radicella, S.M., Letinger, R., 2001. The evolution of the DGR approach to model electron density profiles, *Adv. Space. Res.* 27, 35-40.

☼ Radicella, S.M., 2009. The NeQuick model, genesis, uses and evolution, Annals of Geophysics, 52, p. 417-422.

☼ Rawer, K., 1993. Wave propagation in the ionosphere. Kluwer academic publishers, Dordrecht, The Netherlands. ISBN: 0-7923-0775-5.

☼ Safaeinili, A., Kofman, W., Nouvel, J.-F., Herique, A., Jordan, R.L., 2003. Impact of Mars ionosphere on orbital radar sounder operation and data processing. Planet. Space Sci.. 51, 505 – 515, doi:10.1016/S0032-0633(03)00048-5.

☼ Safaeinili, A., Kofman, W., Mouginot, J., Gim, Y., Herique, A., Ivanov, A. B., Plaut, J. J., Picardi, G., 2007. Estimation of the total electron content of the Martian ionosphere using radar sounder surface echoes. Geophys. Res. Lett.. 34, L23204, doi:10.1029/2007GL032154.

☼ Sánchez - Cano, B., 2010. Estudios preliminares para un modelado empírico de la densidad electrónica en la ionosfera de Marte. Master thesis, Dpto. Física de la Tierra, Astronomía y Astrofísica I (Geofísica y Meteorología), Universidad Complutense de Madrid, Madrid, Spain.

☼ Sánchez-Cano, B., Herraiz, M., Rodriguez-Caderot, G., Radicella, S.M., 2010. A study of the ionosphere of Mars: Applications and limitations of the Chapman layer model. Highlights of Spanish Astrophysics VI, Proceedings of the IX Scientific Meeting of the Spanish Astronomical Society (Eds).

☼ Sánchez-Cano, B., Witasse, O., Herraiz, M., Radicella, S. M., Bauer, J., Blelly, P.-L., and Rodríguez-Caderot, G., 2012. Retrieval of ionospheric profiles from the Mars Express MARSIS experiment data and comparison with radio-occultation data, Geosci. Instrum. Method. Data Syst., 1, 77-84, doi:10.5194/gi-1-77-2012.

☼ Sánchez – Cano, B., Radicella, S.M., Herraiz, M., Witasse, O., Rodríguez – Caderot, G., 2013. NeMars: An empirical model of the Martian dayside ionosphere based on Mars Express MARSIS data, Icarus, 225, 236-247.
doi: http://dx.doi.org/10.1016/j.icarus.2013.03.021

☼ Sánchez-Cano, B., Morgan, D.D., Witasse, O., Radicella, S.M., Herraiz, M., Orosei, R., Cartacci, M., Cicchetti, A., Kofman, W., Grima, Mouginot, J., Gurnett, D.A., Blelly, P.-L., Opgenoorth, H., Study of the Total Electron Content in the martian atmosphere: a critical assessment of the Mars Express MARSIS dataset. Submitted to Icarus.

☼ Schunk, R., Nagy, A.F., 2009. Ionospheres: Physics, Plasma Physics, and Chemistry. Cambridge University Press. ISBN 978-0-521-87706-0.

☼ Smith, D.E., Zuber, M.T., Frey, H.V., Garvin, J.B., Head, J.W., Muhleman, D.O., Pettengill, G.H., Phillips, R.J., Solomon, S.C., Zwally, H.J., Banerdt, W.B., Duxbury, T.C., Golombek, M.P., Lemome, F.G., Neumann, G.A., Rowlands, D.D., Aharonson, O., Ford, P.G., Ivanov, A.B., McGovern, P.J., Abshire, J.B., Afzal, R.S., Sun, X., 2001. Mars Orbiter Laser Altimeter (MOLA): experiment summary after the first year of global mapping of Mars. J. Geophys. Res., 106, 23689–23722.

☼ Stankov, S.M., Jakowski, N., 2006. Topside plasma scale height retrieved from radio occultation measurements. Adv. Space Res., 37, 958-962.

☼ Technical note: Mars Express – MARSIS to planetary science archive interface control document (INFOCOM TR 024.005.2003), May 28, 2008.

☼ Wang, J.-S., Nielsen, E., 2004. Evidence for topographic effects on the Martian ionosphere. Planetary and Space Science, 52, 9, 881-886.

☼ Whitten, R.C., Colin, L., 1974. The ionospheres of Mars and Venus. Reviews of geophysics and space physics. Vol.12, NO.2, 155-192.

☼ Witasse, O., 2000. Modélisation des Ionosphères planétaires et de leur Rayonnement: la Terre et Mars. PhD thesis, Laboratoire de Planétologie, Université Joseph Fourier, Grenoble, France.

☼ Witasse, O., Dutuit, O., Lilensten, J., Thissen, R., Zabka, J., Alcaraz, C., Blelly, P.-L., Bougher, S. W., Engel, S., Andersen, L. H., Seiersen, K., 2002. Prediction of a CO_2^{2+} layer in the atmosphere of Mars. Geophysical Research Letters, 29, 8, pp. 104-1, 1263, doi:10.1029/2002GL014781.

☼ Witasse, O., Cravens, T., Mendillo, M., Moses, J., Kliore, A., Nagy, A.F., Breus, T., 2008. Solar System Ionospheres. Space Sci Rev. 139: 235–265, doi 10.1007/s11214-008-9395-3.

☼ Withers, P., Mendillo, M., 2005. Response of peak electron densities in the Martian ionosphere to day to-day changes in solar flux due to solar rotation. Planet. Space Sci. 53, 1401–1418, doi:10.1016/j.pss.2005.07.010.

☼ Withers, P., 2009. A review of observed variability in the dayside ionosphere of Mars. Advances in Space Research. 44, 277-307.

☼ Withers, P., and 42 colleagues, 2009. The ionosphere of Mars and its importance for climate evolution, white paper submitted to Planetary Science Decadal Survey.

☼ Withers, P., Fallows, K., Girazian, Z., Matta, M., Häusler, B., Hinson, D., Tyler, L., Morgan, D., Pätzold, M., Peter, K., Tellmann, S., Peralta, J., Witasse, O., 2012a. A clear view of the multifaceted dayside ionosphere of Mars. Geophysical Research Letters, Vol. 39, L18202. doi:10.1029/2012GL053193.

☼ Withers, P., Fillingim, M.O., Lillis, R.J., Häusler, B., Hinson, D.P., Tyler, G.L., Pätzold, M., Peter, K., Tellmann, S., Witasse, O., 2012b. Observations of the nightside ionosphere of Mars by the Mars Express Radio Science Experiment (MaRS). J. Geophys. Res., 117 , A12307. doi:10.1029/2012JA018185.

☼ Zhang, Z., Nielsen, E., Plaut, J.J., Orosei, R., Picardi, G., 2009. Ionospheric corrections of MARSIS subsurface sounding signals with filters including collision frequency. Planetary and Space Science 57, ,393–403. doi:10.1016/j.pss.2008.11.016.

☼ Zou, H., Lillis, R.J., Wang, J.S., Nielsen, E., 2011. Determination of Seasonal Variations in the Martian Neutral Atmosphere from Observations of Ionospheric Peak Height. Journal of Geophysical Research. 116. doi:201110.1029/2011JE003833.

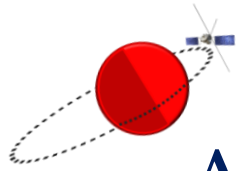

Appendix I.

Additional material

The objective of this appendix is to add complementary information and figures related to the essential sections of this manuscript that can help to understand this work.

Additional material from Chapter 3

Complementary information for Figure 3.5:

Peak electron density fitted with their corresponding $F_{10.7}$ for small solar zenith angle intervals. A larger sample of figures is presented. Because of spatial coherence of this manuscript, not all the figures obtained are shown, although all results are similar to those presented here. The complete material is available upon request.

For the *main layer*:

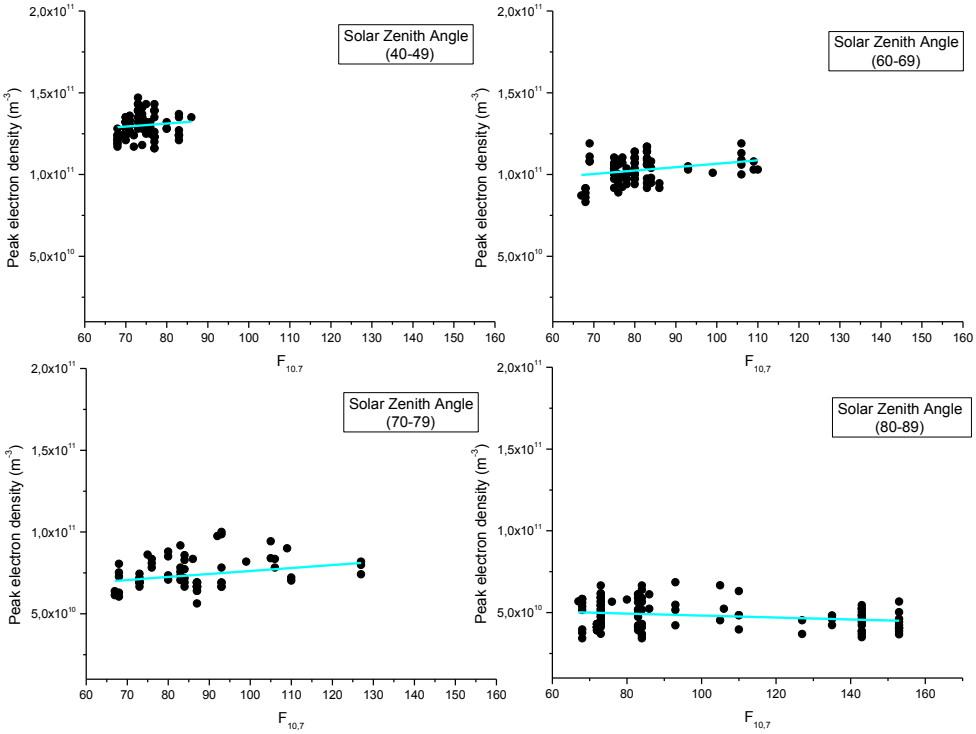

For the *secondary layer*: Due to the small variation of these data with the solar zenith angle, they were split in intervals of this angle much smaller than for the main layer.

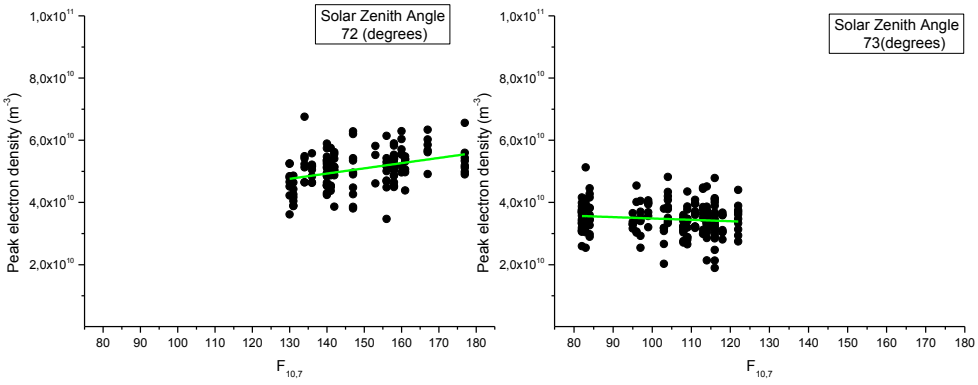

And from these data, synthetic data were re-created following the general Chapman theory as it is explained in Chapter 3:

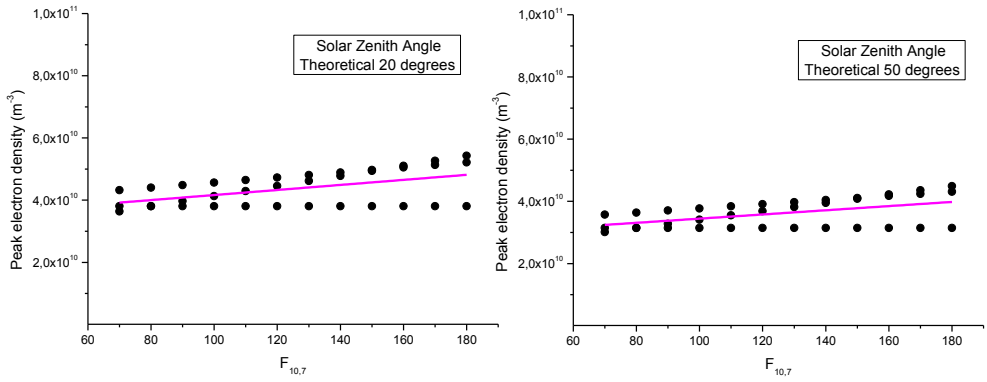

Complementary information for Figure 3.6:

Electron density of the main peak versus solar zenith angle for different values of solar flux. The main layer plot is shown in the manuscript, here it is added the figure for secondary layer:

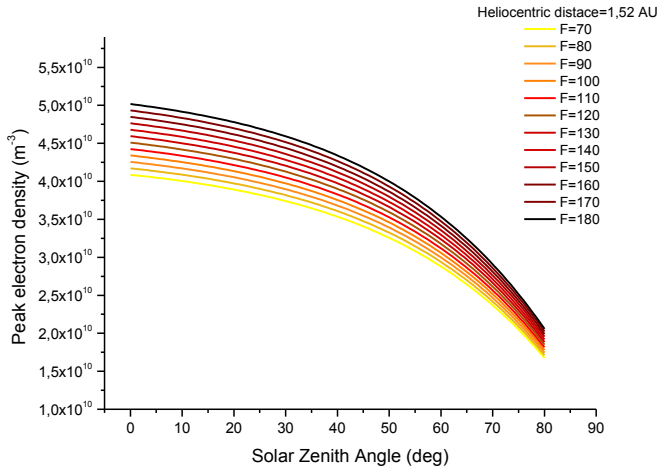

Complementary information for the data coverage:

Histograms of the data coverage of the Mars Express MARSIS AIS data used to develop the empirical model.

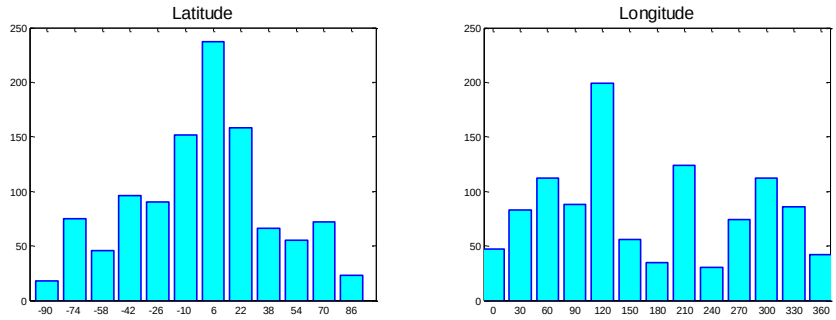

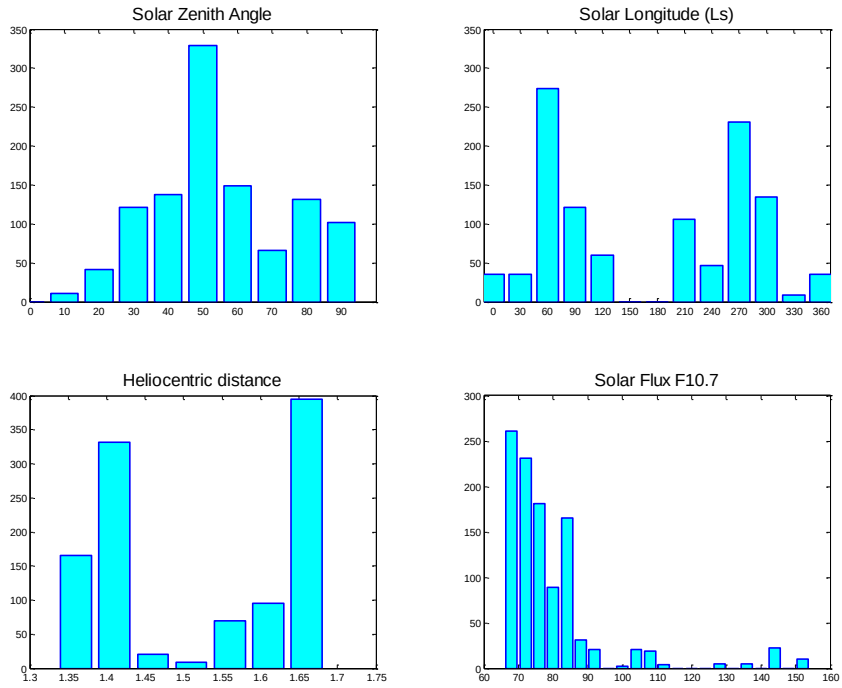

Complementary information for the validation section:

In the manuscript, data from a wide range of solar zenith angle, solar activity and heliocentric distance were compared in a table since should be more explicative. However, just to clarify, here some comparisons are shown:

For the *main peak*:

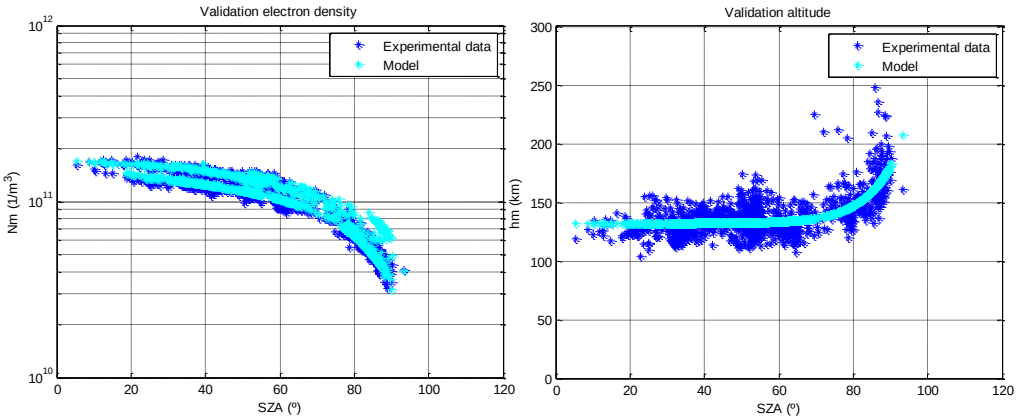

For the *secondary peak*:

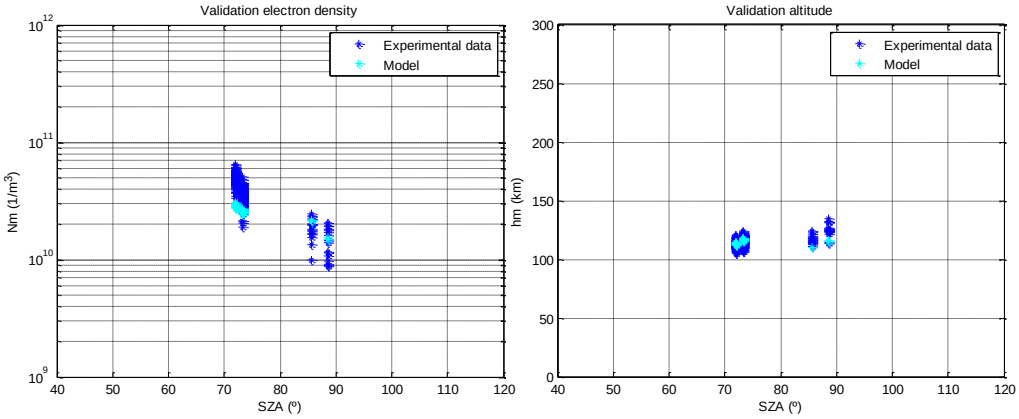

Complementary information for the secondary peak when is embedded in the main layer:

Here an example of a MGS profile which secondary peak is embedded in the main layer is shown (left-panel). The second plot (right-panel) shows the corresponded NeMars profile for the same conditions where it is possible to see that NeMars can reproduce the secondary peak also when is embedded in the main one.

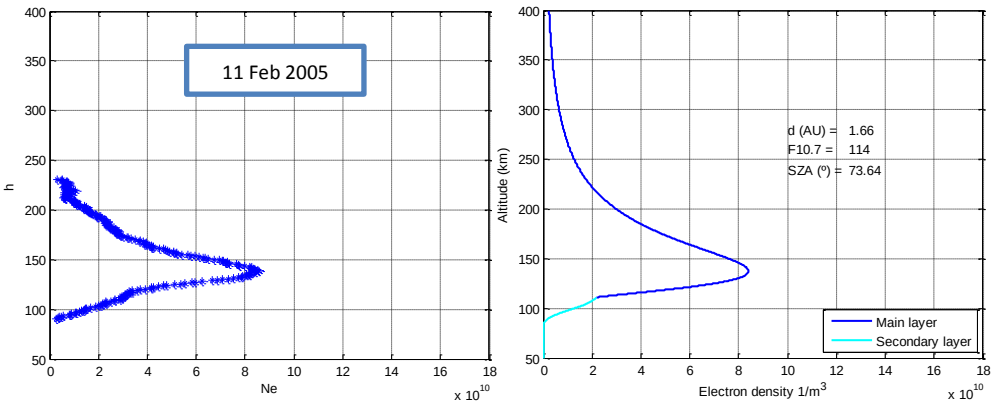

Additional material from Chapter 4

Complementary information for Figures 4.11 and 4.16:

TEC-solar zenith angle variation and TEC-latitude for the same orbits. The full TEC derived from MARSIS subsurface mode (black from "Grenoble" method and red from "Rome" method) has been represented with the real topside integral MARSIS ionogram TEC (blue). The two first figures show also the best-fitting used in this work for "Grenoble" (in grey) and "Rome" (in pink) methods, and the two second figures show also the NeMars TEC for the dayside ionosphere (cyan).

Because of spatial coherence of this manuscript, only figures from two orbits are shown, although all results are similar to those presented here. The complete material is available upon request.

Orbit 9528, best-fitting of TEC with Latitude and TEC with Solar Zenith Angle respectively:

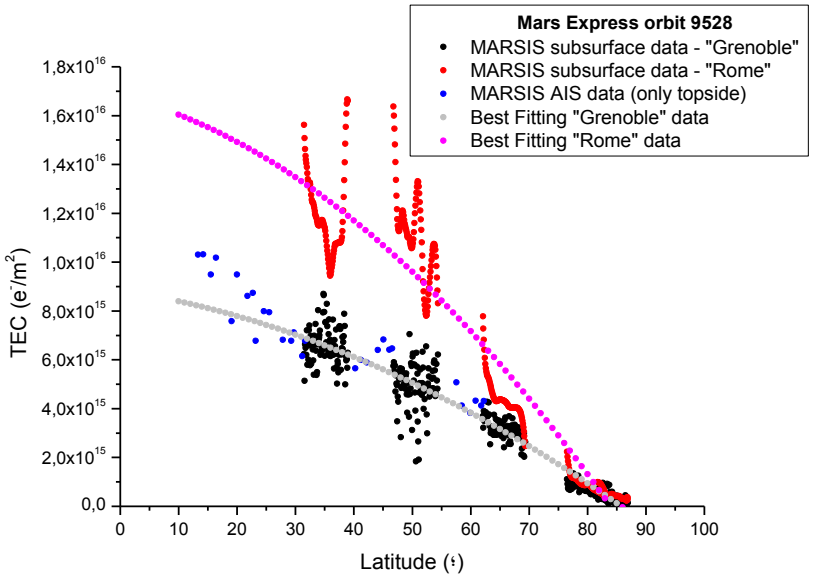

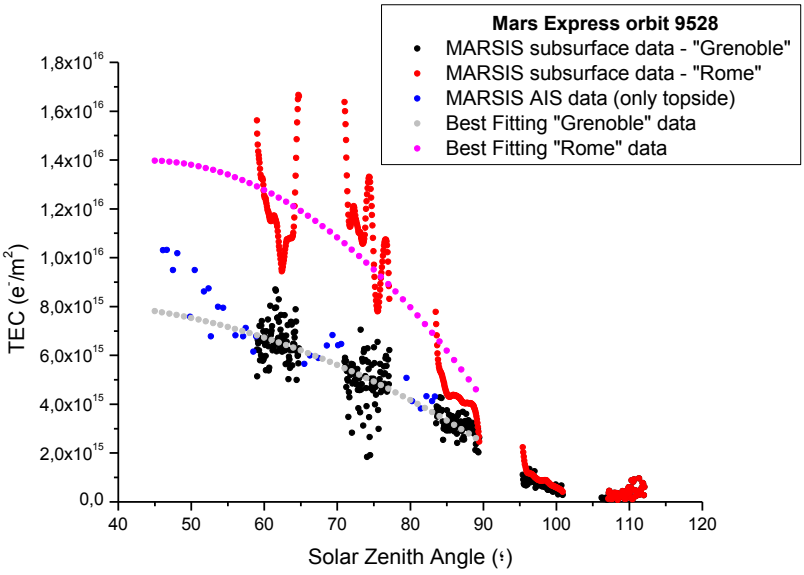

Orbit 9528, TEC with NeMars TEC:

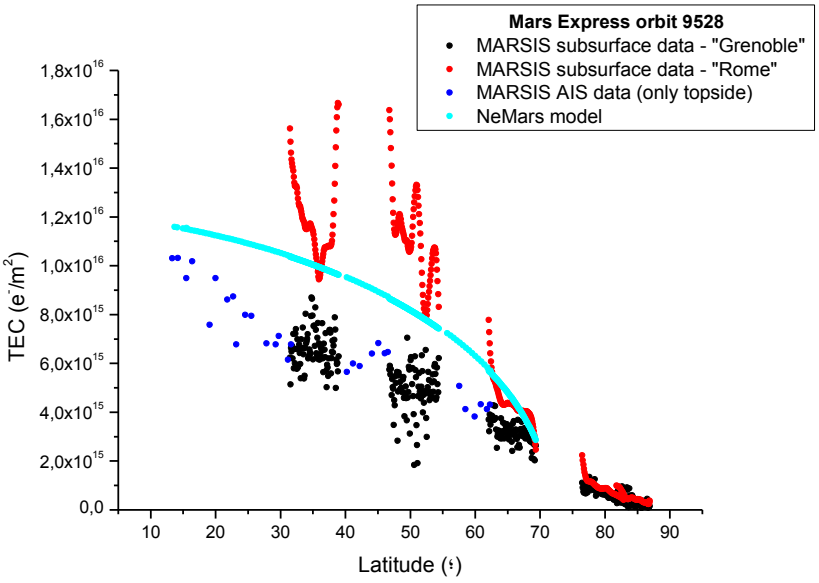

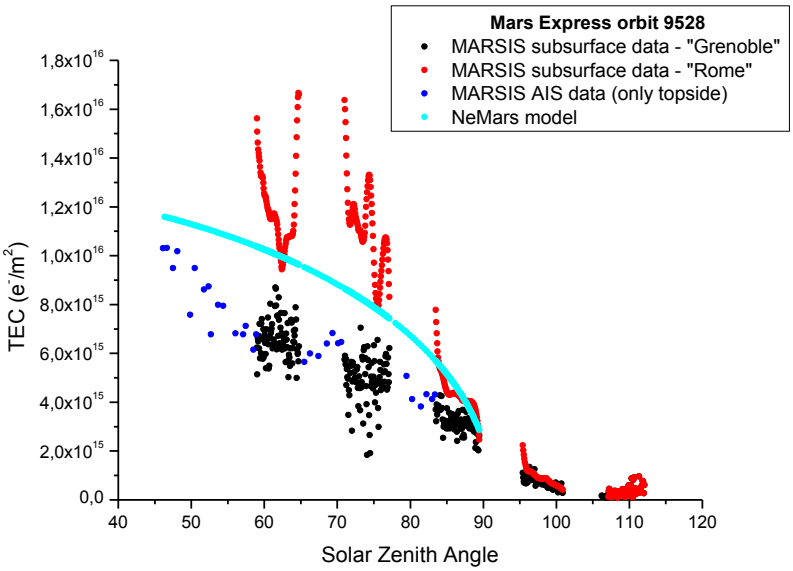

Orbit 4223, best-fitting of TEC with Latitude and TEC with Solar Zenith Angle respectively:

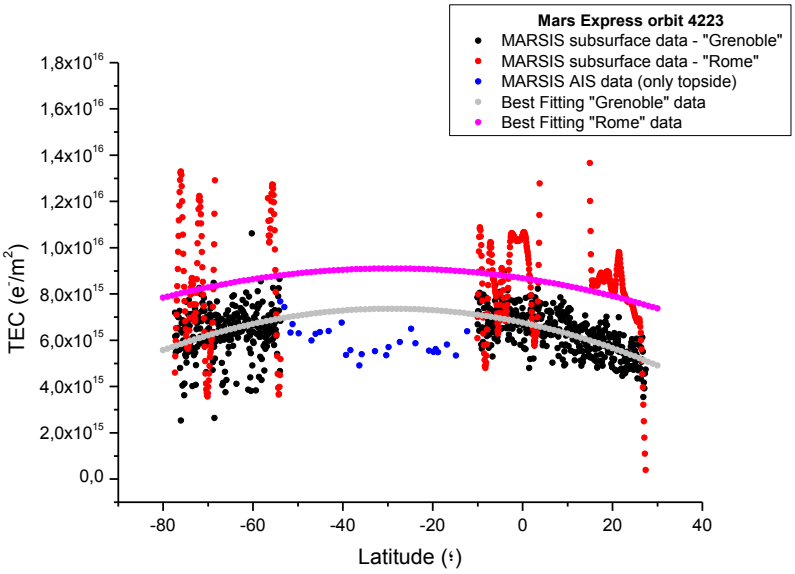

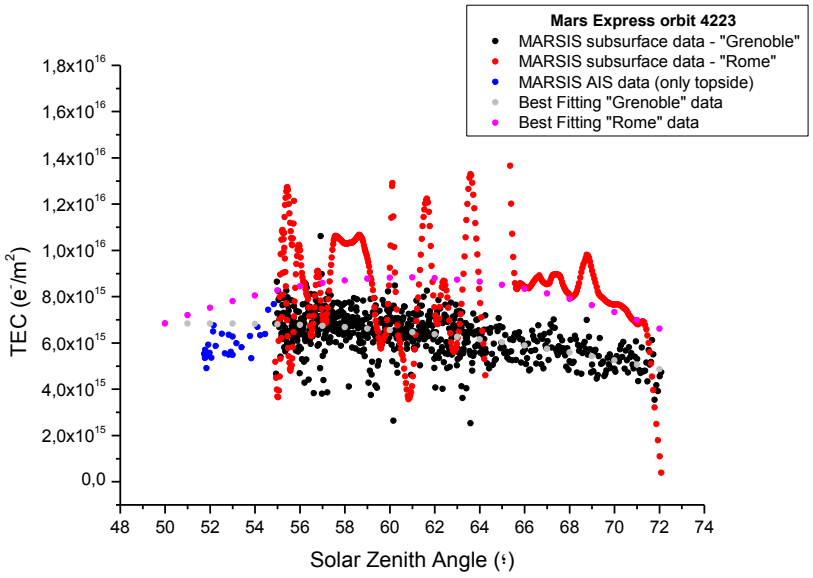

Orbit 4223, TEC with NeMars TEC:

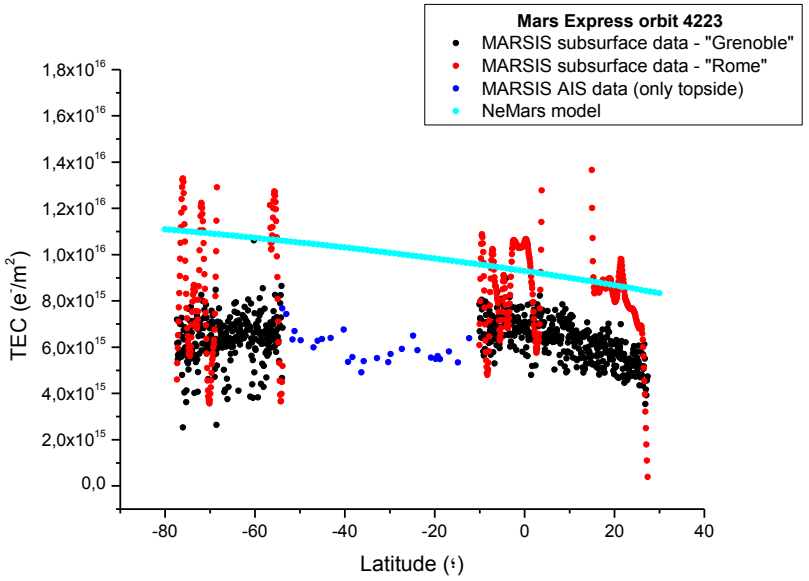

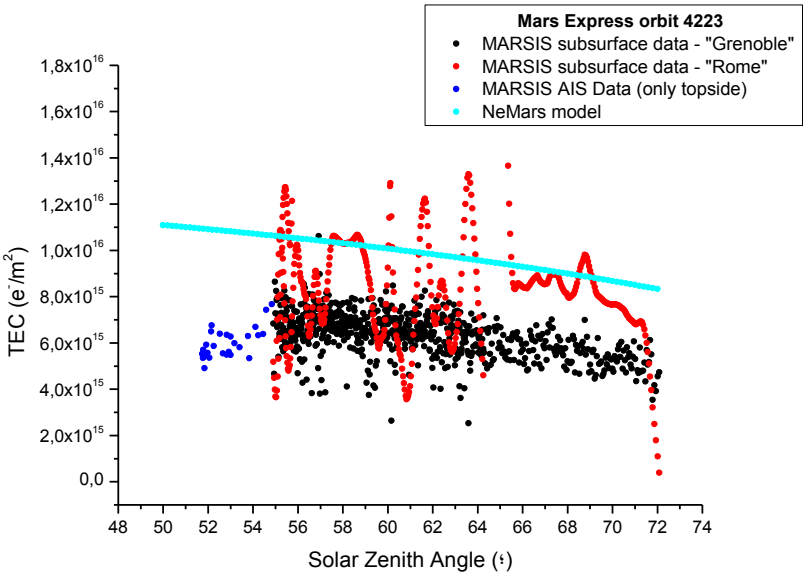
Mars Express orbit 4223
MARSIS subsurface data - "Grenoble"
MARSIS subsurface data - "Rome"
MARSIS AIS Data (only topside)
NeMars model
TEC (e⁻/m²)
1,8x10¹⁶
1,6x10¹⁶
1,4x10¹⁶
1,2x10¹⁶
1,0x10¹⁶
8,0x10¹⁵
6,0x10¹⁵
4,0x10¹⁵
2,0x10¹⁵
0,0
48 50 52 54 56 58 60 62 64 66 68 70 72 74
Solar Zenith Angle (°)

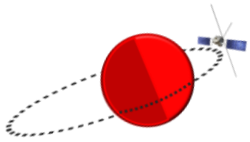

Appendix II.

MARSIS AIS longitude error

A by-product of this doctoral thesis was the identification of a mistake in the Mars Express MARSIS Active Ionospheric Sounding (AIS) data in the Planetary Science Archive of the European Space Agency (http://www.rssd.esa.int/index.php?project =PSA).

In the *interface control document* of the instrument (technical note EAICD section 3.2.3) was described that the kind of coordinates used by MARSIS AIS are the Planetocentric coordinates, while the real coordinates used are the Planetographic one. Consequently, the most affected parameter was the planetary longitude, which was considered positive to east rather than positive to west.

These data were published in the European Space Agency archive for the scientific community for more than 8 years, and thanks to this work, a rectification was done.

The following attached documents correspond to:

- Document sent to the European Space Agency where the error identification is explained.

- Errata.txt document where the MARSIS team rectifies the coordinates. This text can be found in every folder of the MARSIS AIS data in the ESA archive. For example at: ftp://psa.esac.esa.int/pub/mirror/MARS-EXPRESS/MARSIS/MEX-M-MARSIS-3-RDR-AIS-EXT1-V1.0/

IDENTIFICATION DOCUMENT:

UNIVERSIDAD COMPLUTENSE MADRID

FACULTAD DE CIENCIAS FÍSICAS
Departamento de Física de la Tierra, Astronomía y Astrofísica I
Ciudad Universitaria s/n. 28040 Madrid

Teléfono 91 394 4390 Fax: 91 394 43 98

Short technical note about AIS data longitude values

The ionosphere of Mars is being mapped since June 2005 by the MARSIS instrument (Mars Advanced Radar for Subsurface and Ionosphere Sounding) on board Mars Express mission. This instrument has two different operation modes which operate not simultaneously: Active Ionospheric Sounding (AIS) and Subsurface. The first one is specially designed to sound the ionosphere by doing a frequency-sweep and the second one, although originally designed for finding buried materials and interfaces in the Martian subsurface, allows knowing the total electron content (TEC) of the Martian ionosphere as a by-product. Both kinds of data are available in the ESA Planetary Science Archive. When data are analyzed, it is common to find, for the same orbit, ionospheric and subsurface consecutive measurements, i.e. AIS for 10 minutes, then subsurface mode for 20 minutes and then AIS again for 10 minutes. This fact gives the opportunity to analyze the TEC parameter from both modes.

When, in the frame of our research we were analyzing the orbit 4210 of Mars Express, we realized that the longitude coordinates were different for each case what seems to be an inconsistency. The figures of this document show this statement: The first one corresponds to an image of the spectrogram from the AIS mode and the second one to an image of the subsurface file. Both were downloaded from the ESA archive and correspond to the orbit 4210. Similar discrepancies have been found in many other orbits.

After checking with other instruments on board Mars Express, the longitude of the subsurface mode seems to be right and the longitude of the ionospheric mode seems to be wrong. In particular, it looks as if the AIS longitude values were given in westward direction although in the archive and in the technical notes (e.g. EAICD section 3.2.3) is written: "Longitude is given in positive-East coordinates in the range 0°-360°". However this error seems to occur only in the RDR-AIS folders of the archive, because the longitude information in the EDR (AIS) folders is correct, at least in the sub-folders CALIB and DATA (in the Footprint Point Longitude).

In summary, and in the spirit of helping to solve the possible misunderstanding with data, we consider that the longitude given in the AIS BROWSE, AIS DATA and AIS GEO_MARS index table is wrong, whereas that in the AIS EDR folders is correct. We trust that this information can be helpful to identify any kind of data mistake.

Beatriz Sánchez – Cano Miguel Herraiz

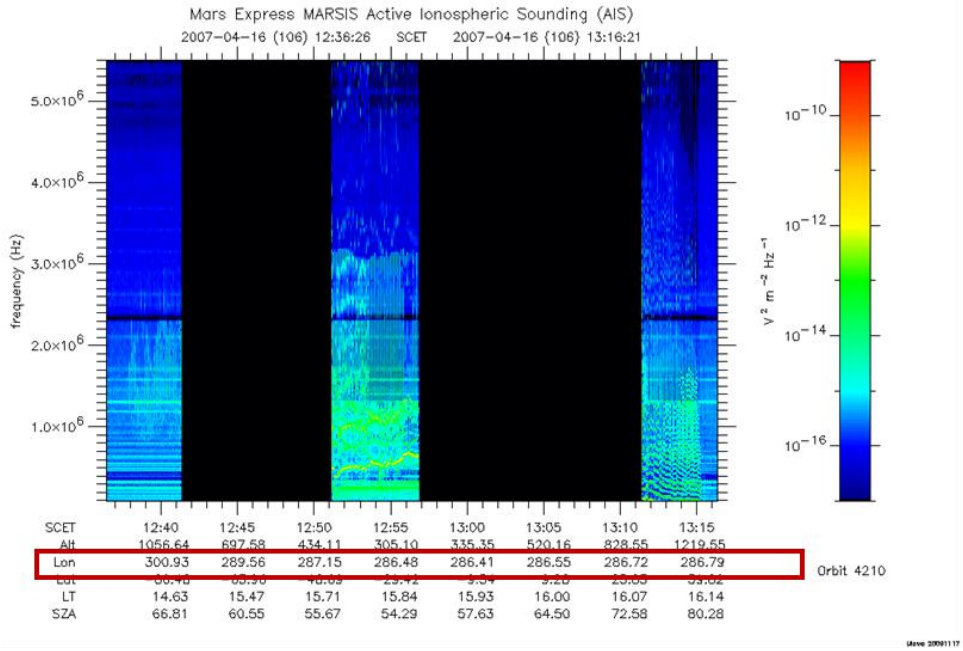

Figure 1: Spectrogram of AIS data for the orbit 4210. The longitude values are marked with the red square.

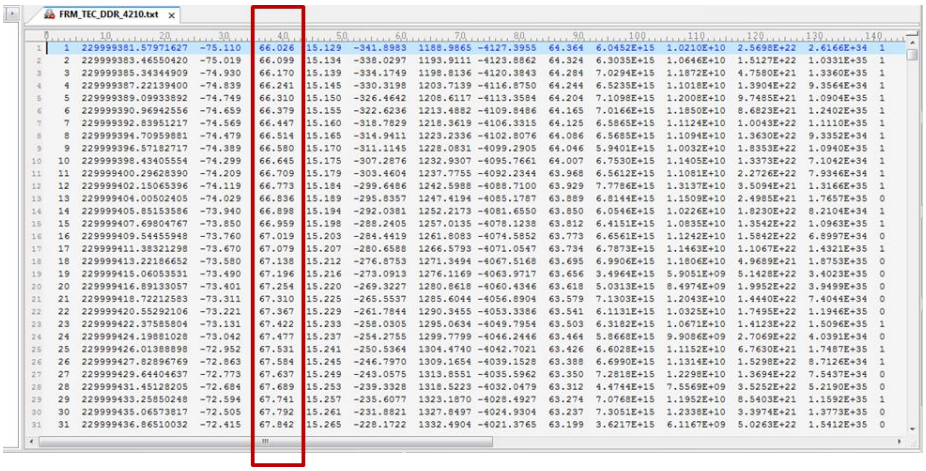

1	1	229999381.57971627	-75.110	66.026	15.129	-341.8983	1188.9865	-4127.3955	64.364	6.0452E+15	1.0210E+10	2.5698E+22	2.6166E+34	1
2	2	229999383.46550420	-75.019	66.099	15.134	-338.0297	1193.9111	-4123.8862	64.324	6.3035E+15	1.0646E+10	1.5127E+22	1.0331E+35	1
3	3	229999385.34344909	-74.930	66.170	15.139	-334.1749	1198.8136	-4120.3843	64.284	7.0294E+15	1.1872E+10	4.7580E+21	1.3360E+35	1
4	4	229999387.22139400	-74.839	66.241	15.145	-330.3198	1203.7139	-4116.8750	64.244	6.5235E+15	1.1018E+10	1.3904E+22	9.3564E+34	1
5	5	229999389.09933892	-74.749	66.310	15.150	-326.4642	1208.6117	-4113.3584	64.204	7.1098E+15	1.2008E+10	9.7485E+21	1.0904E+35	1
6	6	229999390.96942556	-74.659	66.379	15.155	-322.6236	1213.4882	-4109.8486	64.165	7.0166E+15	1.1850E+10	8.6823E+21	1.2402E+35	1
7	7	229999392.83951217	-74.569	66.447	15.160	-318.7829	1218.3619	-4106.3315	64.125	6.5865E+15	1.1124E+10	1.0043E+22	1.1110E+35	1
8	8	229999394.70959881	-74.479	66.514	15.165	-314.9411	1223.2336	-4102.8076	64.086	6.5685E+15	1.1094E+10	1.3630E+22	9.3352E+34	1
9	9	229999396.57182717	-74.389	66.580	15.170	-311.1145	1228.0831	-4099.2905	64.046	5.9401E+15	1.0032E+10	1.8353E+22	1.0940E+35	1
10	10	229999398.43405554	-74.299	66.645	15.175	-307.2876	1232.9307	-4095.7661	64.007	6.7530E+15	1.1405E+10	1.3373E+22	7.1042E+34	1
11	11	229999400.29628390	-74.209	66.709	15.179	-303.4604	1237.7755	-4092.2344	63.968	6.5612E+15	1.1081E+10	2.2726E+22	7.9366E+34	1
12	12	229999402.15065396	-74.119	66.773	15.184	-299.6686	1242.5988	-4088.7100	63.929	7.7786E+15	1.3137E+10	3.5094E+21	1.3166E+35	1
13	13	229999404.00502405	-74.029	66.836	15.189	-295.8357	1247.4194	-4085.1787	63.889	6.8144E+15	1.1509E+10	2.4985E+21	1.7657E+35	0
14	14	229999405.85153586	-73.940	66.898	15.194	-292.0381	1252.2173	-4081.6550	63.850	6.0546E+15	1.0226E+10	1.8230E+22	8.2104E+34	1
15	15	229999407.69804767	-73.850	66.959	15.198	-288.2405	1257.0135	-4078.1238	63.812	6.4151E+15	1.0835E+10	1.3542E+22	1.0963E+35	1
16	16	229999409.54455948	-73.760	67.019	15.203	-284.4419	1261.8083	-4074.5852	63.773	6.6561E+15	1.1242E+10	1.5842E+22	6.8997E+34	0
17	17	229999411.38321298	-73.670	67.079	15.207	-280.6588	1266.5793	-4071.0547	63.734	6.7873E+15	1.1463E+10	1.1067E+22	1.4321E+35	1
18	18	229999413.22186652	-73.580	67.138	15.212	-276.8753	1271.3494	-4067.5168	63.695	6.9906E+15	1.1806E+10	4.9689E+21	1.8753E+35	0
19	19	229999415.06053531	-73.490	67.196	15.216	-273.0913	1276.1169	-4063.9717	63.656	3.4964E+15	5.9051E+09	5.1428E+22	3.4023E+35	0
20	20	229999416.89133057	-73.401	67.254	15.220	-269.3227	1280.8618	-4060.4346	63.618	5.0313E+15	8.4974E+09	1.9952E+22	3.9499E+35	0
21	21	229999418.72212583	-73.311	67.310	15.225	-265.5537	1285.6044	-4056.8904	63.579	7.1303E+15	1.2043E+10	1.4440E+22	7.4044E+34	0
22	22	229999420.55292106	-73.221	67.367	15.229	-261.7844	1290.3455	-4053.3386	63.541	6.1131E+15	1.0325E+10	1.7495E+22	1.1946E+35	0
23	23	229999422.37585804	-73.131	67.422	15.233	-258.0305	1295.0634	-4049.7954	63.503	6.3182E+15	1.0671E+10	1.4123E+22	1.5096E+35	1
24	24	229999424.19881028	-73.042	67.477	15.237	-254.2755	1299.7799	-4046.2446	63.464	5.8668E+15	9.9086E+09	2.7069E+22	4.0391E+34	0
25	25	229999426.01388898	-72.952	67.531	15.241	-250.5364	1304.4740	-4042.7021	63.426	6.6028E+15	1.1152E+10	6.7630E+21	1.7487E+35	1
26	26	229999427.82896769	-72.863	67.584	15.245	-246.7970	1309.1654	-4039.1528	63.388	6.6990E+15	1.1314E+10	1.5298E+22	8.7126E+34	1
27	27	229999429.64404637	-72.773	67.637	15.249	-243.0575	1313.8551	-4035.5962	63.350	7.2818E+15	1.2298E+10	1.3694E+22	7.5457E+34	0
28	28	229999431.45128205	-72.684	67.689	15.253	-239.3328	1318.5223	-4032.0479	63.312	4.4744E+15	7.5569E+09	3.5252E+22	5.2190E+35	0
29	29	229999433.25850248	-72.594	67.741	15.257	-235.6077	1323.1870	-4028.4927	63.274	7.0768E+15	1.1952E+10	8.5403E+21	1.1592E+35	1
30	30	229999435.06573817	-72.505	67.792	15.261	-231.8821	1327.8497	-4024.9304	63.237	7.3051E+15	1.2338E+10	3.3974E+21	1.3773E+35	0
31	31	229999436.86510032	-72.415	67.842	15.265	-228.1722	1332.4904	-4021.3765	63.199	3.6217E+15	6.1167E+09	5.0263E+22	1.5412E+35	0

Figure 2: Close-up of the subsurface TEC file for the orbit 4210. The longitude values are marked with the red square.

ERRATA.TXT:

END_OBJECT = TEXT
END

Users are encouraged to provide comments back to the MARSIS AIS team if errors or omissions are found either in data or in documentation. Please send comments by e-mail or U.S. mail to

David Morgan, david-morgan@uiowa.edu
Department of Physics and Astronomy
The University of Iowa
Iowa City, IA 52242-1479 USA

General disclaimer
==========

All trademarks are acknowledged as the property of their respective owners. The producers and publishers of this archive do not endorse any commercial entities which may be mentioned for clarity.

Variances applying to this archive
==========

A web link to http://validator.w3.org/check/referer is associated with the "Valid HTML 3.2" image at the bottom of html documents. This link provides a mechanism for checking conformance of the document to html standards, but will only work if the document is being viewed via a web-accessible (e.g. http:) URL. If the file is accessed as a local file system reference (e.g. file:) URL, then, of course, the remote validation service will not be able to access the file in order to check it.

The following erratum in all mission phases of MARSIS AIS archived data has been noted:

All planet-based coordinates have been archived in planetographic rather than planetocentric coordinates. This discrepancy entails

(1) Longitude is given in west rather than east longitude.
To convert archived west longitude WL to east longitude EL, subtract from 360; i. e.,

EL = 360 - WL

(2) Latitude is based on normal to a representative ellipsoid surface rather than the radius vector from the center of the planet.

(3) Altitude is taken along the normal to the ellipsoid surface, from the spacecraft to the ellipsoid surface, rather than along the radius vector from the spacecraft to the center of the planet, down to the nominal planetary radius of 3396.2 km.

Note regarding derived products
==========

This data set does not contain derived electron densities, density profiles, etc. For documents relating to the derivation of these parameters refer to the files included in the DOCUMENTS directory.

Update history:
==========

Date	Change
2013-05-13	Errata updated to describe use of planetographic coordinates

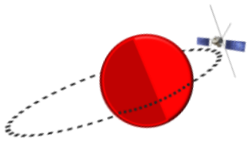

Appendix III.

Scientific activities originated by this PhD

The development of this doctoral thesis has allowed the realization of the following scientific activities:

REFEREED PUBLICATIONS

Sanchez-Cano, B., Morgan, D.D., Witasse, O., Radicella, S.M., Herraiz, M., Orosei, R., Cartacci, M., Cicchetti, A., Kofman, W., Grima, C., Mouginot, J., Gurnett, D.A., Blelly, P.-L., Opgenoorth, H., Study of the Total Electron Content in the martian atmosphere: a critical assessment of the Mars Express MARSIS dataset. Submitted to Icarus.

Sánchez – Cano, B., Radicella, S.M., Herraiz, M., Witasse, O., Rodríguez – Caderot, G., 2013. NeMars: An empirical model of the Martian dayside ionosphere based on Mars Express MARSIS data, Icarus, 225, 236-247.
doi: http://dx.doi.org/10.1016/j.icarus.2013.03.021
(http://adsabs.harvard.edu/abs/2013Icar..225..236S)

Sánchez-Cano, B., Witasse, O., Herraiz, M., Radicella, S. M., Bauer, J., Blelly, P.-L., Rodríguez-Caderot, G., 2012. Retrieval of ionospheric profiles from the Mars Express MARSIS experiment data and comparison with radio-occultation data, Geosci. Instrum. Method. Data Syst., 1, 77-84. doi:10.5194/gi-1-77-2012.
(http://adsabs.harvard.edu/abs/2012GID.....2...87S)

PROCEEDINGS

Sánchez - Cano, B., Herraiz, M., Rodríguez – Caderot, G., Radicella, S.M., 2010. Study of the ionosphere of Mars: application and limitations of the Chapman-layer model, Highlights of Spanish Astrophysics VI, Proceedings of the IX Scientific Meeting of the Spanish Astronomical Society held on September 13-17, 2010, in Madrid, Spain, 601–606. (http://adsabs.harvard.edu/abs/2011hsa6.conf..601S)

INTERNATIONAL CONFERENCES

Sánchez – Cano, B., Radicella, S.M., Herraiz, M., Witasse, O., Cartacci, M., Orosei, R., Rodríguez – Caderot, G., 2014. NeMars empirical model for the dayside martian ionosphere and its use to validate marsis instrument techniques: possible contribution to the Mars International Reference Ionosphere (MIRI). 40th COSPAR Scientific Assembly 2014, Moscow, Russia (Oral Communication).

Díaz-Michelena, M., Cerdán, M.F., Ramírez-Nicolás, M., **Sánchez-Cano, B.,** Sánchez-Bayton, M., Kilian., R., 2014. Terrestrial analogues models based on MOURA magnetometer data. Application to Gusev crater and Apollinaris volcano. European Geosciences Union (EGU) General Assembly 2014, Vienna, Austria (Poster).

Opitz, A., Witasse, O., Blelly, P.-L., Grandin, M., Sánchez-Diaz, E., Mazrouei, S., **Sánchez-Cano, B.**, Araujo-Sánchez, S., 2013. Vertical structure of the dayside ionosphere on Mars by comparison between Mars Express observations and models. America Geophysical Union (AGU) Fall Meeting 2013, San Francisco, United States of America (Oral Communication).
(http://adsabs.harvard.edu/abs/2013AGUFM.P12A..03O)

Sánchez-Cano, B., Ramírez-Nicolás, M., Sánchez-Bayton, M., Herraiz, M., Witasse, O., Radicella, S.M., Tréguier, E., Martin, P., Kereszturi, A., Vázquez, L., Rodríguez – Caderot, G., 2013. Geophysical martian studies developed at Universidad Complutense de Madrid: Ionosphere and Vulcanism. Planet Mars IV workshop, 20-25 Octubre, École de Physique des Houches, Les Houches, France (Poster).

Ramírez-Nicolás, M., **Sánchez-Cano, B**., Sánchez-Bayton, M., Vázquez, L., Usero, D., Herraiz, M., Montmessin, F., 2013. Geophysical martian studies developed at Universidad Complutense de Madrid: Electric and Magnetic Fields. Planet Mars IV workshop, 20-25 Octubre, École de Physique des Houches, Les Houches, France (Poster).

Sánchez - Cano, B., Witasse, O., Herraiz, M., Radicella, S.M., 2013. Effect of the topography on the ionosphere: results from the Mars Express MARSIS experiment. European Geosciences Union (EGU) General Assembly 2013, Vienna, Austria (Poster).
(http://adsabs.harvard.edu/abs/2013EGUGA..15.1445S)

Sánchez - Cano, B., Witasse, O., Herraiz, M., Radicella, S.M., Rodríguez-Caderot, G., 2012. Study of topographic effects on the main Martian ionospheric peak with the Mars Express MARSIS instrument. European Planetary Science Congress (EPSC), Madrid, Spain (Poster).
(http://adsabs.harvard.edu/abs/2012espc.conf..253S)

Morgan, D.D., Gurnett, D.A., Duru, F., Witasse, O., **Sanchez-Cano, B.,** Plaut, J.J., Gim, Y., Mouginot, J., 2012. Total Electron Content from Mars Express Topside Ionospheric Sounding. European Planetary Science Congress (EPSC), Madrid, Spain (Poster).
(http://adsabs.harvard.edu/abs/2012espc.conf..558M)

Ramírez-Nicolás, M., **Sánchez-Cano**, **B**., Usero, D., Vázquez, L., Herraiz, M., 2012. Charged particles behaviour with real data on Mars. European Planetary Science Congress (EPSC), Madrid, Spain (Oral Communication).
(http://adsabs.harvard.edu/abs/2012espc.conf..245R)

Sánchez – Cano, **B.,** Herraiz, M., Radicella, S.M., Witasse, O., Rodríguez – Caderot, G., 2012. NeMars: Martian ionospheric empirical model. Workshop on Mars – Connecting Planetary Scientists in Europe (MPSE), Budapest, Hungary (Oral Communication).
(http://www.konkoly.hu/MPSE/program.pdf)

Sánchez - Cano, **B.,** Herraiz, M., Radicella, S.M., Witasse, O., Rodríguez – Caderot, G., 2011. Different contributions for a Mars Ionosphere empirical model based on Mars Express MARSIS data. European Planetary Science Congress - Division for Planetary Sciences of the American Astronomical Society (EPSC-DPS), Nantes, France (Oral Communication).
(http://adsabs.harvard.edu/abs/2011epsc.conf..381S)

Sánchez - Cano, **B.,** Herraiz, M., Radicella, S.M., Witasse, O., Rodríguez – Caderot, G., 2011. A Mars M1 ionosphere layer empirical model based on MARSIS data. II Magnetometer Workshop, Sigüenza, Spain (Oral Communication).

Sánchez – Cano, B., Radicella, S.M., Herraiz, M., Rodríguez - Caderot, G., Witasse, O., 2011. A Mars M1 ionosphere layer empirical model based on MARSIS data. European Geosciences Union (EGU) General Assembly 2011, Vienna, Austria (Oral Communication).
(http://meetingorganizer.copernicus.org/EGU2011/EGU2011-1757-1.pdf)

Sánchez-Cano, B., Herraiz, M., Rodríguez Caderot, G., Radicella, S.M., 2010. Study of the ionosphere of Mars: application and limitations of the Chapman-layer model. IX Scientific Meeting of the Spanish Astronomical Society, Madrid, Spain (Oral Communication).
(http://adsabs.harvard.edu/abs/2011hsa6.conf..601S)

INVITED INTERNATIONAL SEMINARS

Sánchez – Cano, **B.**, 2012. A model of the Mars ionoshere. Seminar of applied Physics of Abdus Salam International Center for Theoretical Physics (ICTP), Trieste, Italy (Oral Communication). (http://users.ictp.it/~chelaf/ss298 html, http://users.ictp.it/~stefani/multimedia/Applied_Physics/sanchezcano.html)

INTENATIONAL SCIENTIFIC MEETINGS

Sánchez – Cano, B., 2014. NeMars model and TEC inter-comparison updates. Mars Upper Atmosphere Network (MUAN) meeting, Cologne, Germany (Oral Communication).

Sánchez – Cano, B., 2014. Total Electron Content. Mars Upper Atmosphere Network (MUAN) meeting, Cologne, Germany (Oral Communication).

Sánchez - Cano, **B.,** Radicella, S.M., Witasse, O., Herraiz, M., 2013. AIS data analysis, Mars Upper Atmosphere Network (MUAN) meeting, Boston, United States of America (Oral Communication).

Sánchez - Cano, **B.,** Radicella, S.M., Witasse, O., Herraiz, M., 2013. TEC inter-calibration [Subsurface mode versus AIS versus models], Mars Upper Atmosphere Network (MUAN) meeting, Boston, United States of America (Oral Communication).

Radicella, S.M., **Sanchez-Cano, B.,** 2012. MARS TEC inter-calibration:comments. Mars Upper Atmosphere Network (MUAN) meeting, Uppsala, Sweeden (Oral Communication).

Witasse, O., **Sanchez-Cano, B**., Morgan, D., Orosei, R., Cartacci, M., Kofman, W., Radicella, S.M., Herraiz, M., 2012. Total Electron Content Marsis inter-calibration. Mars Upper Atmosphere Network (MUAN) meeting, Uppsala, Sweden (Oral Communication).

Sánchez – Cano, B., Radicella, S.M., Witasse, O., Herraiz, M., 2012. MEX/MARSIS AIS data analysis and empirical model of the ionosphere & Consistency of topside sounding and radio-occultation data. Mars Upper Atmosphere Network (MUAN) meeting, Uppsala, Sweden (Oral Communication).

NATIONAL CONFERENCES

Sánchez - Cano, B., M. Herraiz, S.M. Radicella, O. Witasse, G. Rodríguez – Caderot, 2013. Modelo empírico NeMars de la ionosfera de Marte, III Encuentro sobre Ciencias Planetarias y Exploración del Sistema Solar, Madrid, Spain (Oral Communication). (http://3sistemasolar.files.wordpress.com/2012/12/programa_3e_ccpp_ess_folleto_dina4.pdf)

Sánchez - Cano, B., M. Herraiz, O. Witasse, S.M. Radicella, G. Rodríguez – Caderot, 2013. Variaciones en la altura de la ionosfera de Marte. ¿Relación con la topografía?, III Encuentro sobre Ciencias Planetarias y Exploración del Sistema Solar, Madrid, Spain (Poster).
(http://3sistemasolar.files.wordpress.com/2012/12/programa_3e_ccpp_ess_folleto_dina4.pdf)

M. Ramírez-Nicolás, **B. Sánchez-Cano,** M. Herraiz, 2013. Medida de B en Marte a partir de ionogramas, III Encuentro sobre Ciencias Planetarias y Exploración del Sistema Solar, Madrid, Spain (Poster).
(http://3sistemasolar.files.wordpress.com/2012/12/programa_3e_ccpp_ess_folleto_dina4.pdf)

Sánchez - Cano, B., Herraiz, M., Radicella, S.M., Witasse, O., Rodríguez – Caderot, G., 2011. Análisis de la ionosfera de Marte mediante sondeos obtenidos por MARSIS (Mars

Express), II Encuentro de exploración del sistema solar, Bilbao, Spain (Oral Communication). Abstract book: ISBN: 978-84-95809-91-9. (http://www.ajax.ehu.es/exploracion_sistema_solar/principal/Programa_II_Encuentros_exploracion_sist_solar.pdf)

NATIONAL SCIENTIFIC MEETINGS

Sánchez-Cano, B., Ramírez-Nicolás, M., Herraiz, M., Vázquez, L., Usero, D., 2012. Entorno magnético en la Universidad Complutense de Madrid, INTA, Madrid, Spain (Oral Communication).

PROJECTS AND RESEARCH GROUPS

Member of MUAN (Mars Upper Atmosphere Network) since 2012.

Member of Instituto de Geociencias (IGEO) (CSIC-UCM) since 2011.

Member of Instituto de Matemáticas Interdisciplinar (IMI) of Universidad Complutense de Madrid since 2010.

Member of UCM research group: "Estudios Ionosféricos y Técnicas de Posicionamiento Global por Satélite (GNSS)" since 2009.

Member of scientific team of METNET-PRECURSOR mission since 2009.
(Projects I+D+I: AYA2011-29967-C05-02, AYA2009-14212-C05-05/ESP and AYA2008-06420-C04-03)

CHAIRPERSON OF SCIENTIFIC SESSIONS

Planetary Magnetism session at European Planetary Science Congress (EPSC) 2012, Madrid, Spain.

REFEREE

Referee for the Science Citation Index Journal "ICARUS"(5-Year Impact Factor: 3.190)

Referee for the Swedish National Space Board (SNSB)

ICTP (The Abdus Salam International Centre for Theoretical Physics), Trieste, Italy.

- In total **195** days.
- Periods:

  - 19th April – 22nd April, 2013.
  - 20th January – 21st March, 2013.
  - 28th October – 7th November, 2012.
  - 6th May – 8th May, 2012.
  - 15th January – 11th March, 2012.
  - 19th June – 11th July, 2011.
  - 23rd March – 26th March, 2011.
  - 10th October – 10th November, 2010.
  - 30th June – 3rd July, 2010.

ESTEC (European Space Research and Technology Centre) of ESA (European Space Agency), Noordwijk, The Netherlands.

- In total **77** days.
- Periods:

  - 3rd April – 4th April, 2014.
  - 2nd March – 22nd March, 2014.
  - 1st September – 12th October, 2013.
  - 11th September – 16th September, 2011.
  - 3rd October – 9th October, 2010.

Observatorio del Ebro, Roquetes, Spain.

- In total **2** days.
- Periods:

  - 20th January – 21st January, 2011.

ATTENDANCE AT SCIENTIFIC COURSES

Technical conference about space meteorology III. 26th Novembre, 2013 at Escuela Nacional de Protección Civil, Rivas Vaciamadrid, Spain.

Workshop Planet Mars IV at École de Physique des Houches, Les Houches, France. 20-25 October 2013. Organized by European Space Agency.

Workshop: Dynamos, Electric Currents magnetic indexes at Abdus Salam International Centre for Theoretical Physics (ICTP), Trieste, Italy. 17th-21st February, 2013.

Technical conference about space clima II. 29th May, 2012 at Escuela Nacional de Protección Civil, Rivas Vaciamadrid, Spain.

Workshop: SPICE European Training Workshop 2012 at ESAC/ESA Madrid, Spain. 16th-19th April, 2012. Workshop taught by the NAIF team (NASA-JPL) at the facilities of the European Space Agency.

Summer school UCM-El Escorial: "Mars and society". 13st-15th July, 2011.

Workshop: International Advanced School on Space Weather Modelling and Applications. 18th-29st October, 2010 at Abdus Salam International Centre for Theoretical Physics, Trieste, Italy.

Summer school UCM-El Escorial: "Mars and its enigma". 12nd-16th July, 2010.

International Beacon Satellite Symposium. 7th -11th June, 2010 at Universidad Politécnica de Cataluña (UPC), Barcelona, Spain.

Workshop: "Modelos matemáticos y fenómenos no lineales" by Jorge Alberto González from Instituto Venezolano de Investigaciones Científicas. 12, 14, 19 y 21 of January of 2010.

Summer school UCM-El Escorial: "The Mars exploration". 13rd - 17th July, 2009.

ACADEMIC EXPERIENCE

"Laboratorio de Computación Científica (Scientific Computing Laboratory)", Universidad Complutense de Madrid. BS level. 30 hours, course 2013-2014.
(pp. 53 → http://fisicas.ucm.es/data/cont/docs/18-2014-02-06-Gu%C3%ADa%20Grado%20en%20F%C3%ADsica1314_v12.pdf)

"Geomagnetismo Campo Externo (Geomagnetism: Outer fields)", Universidad Complutense de Madrid. BS and MS level. 4 hours, course 2012-2013.

Collaboration in: "Campos Constituyentes del magnetismo de la Tierra (Constituent fields of Earth Magnetism)". Universidad Complutense de Madrid. MS level. 2 hours, course 2010-2011.

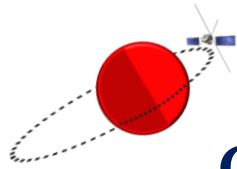

Glossary

Ionospheric layer formed in a radiative o dissociative recombination process, based on Chapman theory (equation 1.8 in this book)	**α - Chapman layer**
Active Ionospheric Sounding – Operational mode of the MARSIS radar on board Mars Express mission	**AIS**
Analyzer of Space Plasmas and Energetic Atoms – instrument of Mars Express mission	**ASPERA**
Astronomical Units (1 AU = 149597871 km)	**AU**
Ionospheric layer formed in an attachment recombination process, based on Chapman theory (equation 1.11 in this book)	**β - Chapman layer**
In an ionospheric profile, the part of the profile from the ground to the maximum electron density peak.	**Bottomside profile**
Electron density profile based on Chapman theory	**Chapman-like layer**
Chapman grazing incidence function (equation 1.13 in this book)	**Ch**
Centre National de la Recherche Scientifique	**CNRS**
Method to correct the phase distortion in the ionosphere (Picardi and Sorge, 2000)	**Contrast method**
Committee on Space Research	**COSPAR**
Mars Express planetary science archive interface control document	**EAICD**
Profile of the electron density distribution with altitude in the ionosphere	**Electron density profile**
Cyclotron frequency of the electrons around the MARSIS antennas which can be correlated with the magnetic field crossed by Mars Express (horizontal lines in the ionograms)	**Electron cyclotron echoes**
Electron Reflectometer instrument on board Mars Global Surveyor mission	**ER**
European Space Agency	**ESA**
European Space Research and Technology Centre	**ESTEC**
Extreme Ultraviolet solar radiation	**EUV**
Solar Index which is a measure of the solar radio flux per unit frequency at a wavelength of 10.7 cm, near the peak of the observed solar radio emission	**$F_{10.7}$ index**
Finnish Meteorological Institute	**FMI**
Global navigation satellite system currently being built by the European Union and European Space Agency	**GALILEO**
Geoscientific Instrumentation, Methods and Data Systems journal	**GI**
Global Navigation Satellite System	**GNSS**

Global Positioning System (from United States)	**GPS**
Method to retrieve TEC (Mouginot et al., 2008)	**"Grenoble" method**
Neutral scale height	**H**
Abdus Salam International Centre for Theoretical Physics	**ICTP**
Russian Space Research Institute	**IKI**
Interior Exploration using Seismic Investigations, Geodesy and Heat Transport mission (from NASA)	**InSight**
Instituto Nacional de Técnica Aeroespacial	**INTA**
Special Mars Express campaign where for one orbit, ionospheric and subsurface measurements were acquired alternately every few minutes	**"Interleaved" MARSIS orbits**
Photochemical model of the Mars' ionosphere (Peter et al., 2014)	**IonA model**
Dataset of the received power as a function of the time delay and frequency	**Ionogram**
Ionospheric trace inversion to get the vertical electron density profile	**Ionogram reduction**
Ionogram trace formed by the reflected frequencies in the ionosphere	**Ionospheric echo**
Institut de Recherche en Astrophysique et Planétologie	**IRAP**
International Reference Ionosphere	**IRI**
Lavochkin Association	**LA**
Solar Longitude	**Ls**
Tool to analyse MARSIS AIS data	**MAISDAT**
Mars Radio Science instrument on board Mars Express mission	**MaRS**
Mars Advanced Radar for Subsurface and Ionosphere Sounding instrument on board Mars Express mission	**MARSIS**
Matrix Laboratory (software)	**MATLAB**
Mars Atmosphere and Volatile Evolution mission (from NASA)	**MAVEN**
Spanish part of the MetNet mission	**Meiga**
Meteorological Network mission (from IKI, LA, FMI and INTA)	**MetNet**
Mars Express mission (from ESA)	**MEX**
Mars Global Surveyor mission (from NASA)	**MGS**
Mars International Reference Ionosphere	**MIRI**
Mars Orbiter Laser Altimeter instrument on board Mars Global Surveyor mission	**MOLA**
Triaxial magnetometer of the Meiga-MetNet Project	**MOURA**

Mars Reconnaissance Orbiter mission (from NASA)	**MRO**
Mars Upper Atmosphere Network	**MUAN**
National Aeronautics and Space Administration	**NASA**
Electron density	**Ne**
Empirical model of the Earth's ionosphere (Radicella and Letinger, 2001)	**NeQuick**
Empirical model of the Mars' ionosphere (Sánchez – Cano et al., 2013)	**NeMars**
Planetary Data System (data archive from NASA)	**PDS**
Doctor of Philosophy, in this context: Doctor Degree	**PhD**
Principal Investigator	**PI**
Electro static plasma oscillation (vertical lines in the MARSIS ionograms) uses to derive the local plasma frequency at the spacecraft altitude	**Plasma oscillation harmonics**
Planetary Science Archive (data archive from ESA)	**PSA**
Ground-penetrating radar (Figure 4.2 in the book)	**Radargram**
Technique to sound the ionosphere and derive vertical electron density profiles	**Radio-occultation**
Radio Frequency	**RF**
Method to retrieve TEC based on the so-called Contrast Method (Cartacci et al., 2013)	**"Rome" method**
Radio Potential Analyzer instrument on board Viking missions	**RPA**
Shallow Radar instrument on board Mars Reconnaissance Orbiter mission	**SHARAD**
Angle between the incident solar radiation and the zenith at a specific place	**Solar Zenith Angle (χ or SZA)**
Plot of the sounding frequency versus time (Figure 2.3 in the book)	**Spectrogram**
SubSurface mode – Operational mode of the MARSIS radar on board Mars Express mission	**SubS**
Total Electron Content	**TEC**
TEC unit (1TECu=10^{16} electrons/m^2)	**TECu**
In an ionospheric profile, the part of the profile from the spacecraft altitude to the maximum electron density peak.	**Topside profile**
Numerical /physical model (Witasse, 2000. Witasse et al., 2002, Morel et al., 2004, Bertaux et al., 2005, Leblanc et al., 2006)	**TRANSMARS**
Universidad Complutense de Madrid	**UCM**
International Union of Radio Science	**URSI**

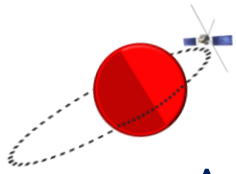

Acknowledgments

"Caminante, son tus huellas
el camino y nada más;
caminante, no hay camino,
se hace camino al andar".

(Antonio Machado)

Las huellas de mis pies me trajeron hasta aquí, siguiendo un camino marcado por mi propio caminar.

Nunca pretendí conocer dónde llegaré, tan sólo quiero caminar.

Y caminando, paso a paso, mi sendero se cruzó con el de grandes personas que compartieron mi carga y me ayudaron a andar, ¡Gracias!.

- ☼ -

Gracias a mis tres directores por guiar mis pasos y hacer que este trabajo haya sido realidad.

A **Miguel Herraiz Sarachaga** por brindarme la oportunidad, el empuje y el apoyo permanente de esta aventura marciana. Una vez me dijiste que una tesis doctoral era un maratón, gracias por estar siempre ahí para felicitarme en las pequeñas victorias, levantarme en las derrotas y sobretodo, gracias por ayudarme a llegar a la meta. Junto a ti mi camino se ha enriquecido de grandes experiencias de vida que han ayudado en mi formación y maduración.

A **Gracia Rodríguez Caderot** por estar siempre ahí con buenos consejos, apoyo y una "pluma" lista para cada paso andado. Gracias por ayudarme a quitar importancia a las cosas que no la tienen y por enseñarme a ver lo desconocido, que a veces afronto con miedo o desconfianza, como un reto digno de ser vivido.

Et merci beaucoup **Olivier Witasse** for being always next to me regardless of the distance. For your wise advises and your totally crazy but very good ideas. For being one of the drivers of this PhD by opening for me the doors of the Universe, and for doing the work super fluid. You know how proud would be Newton.

- ☼ -

No mi director oficial, pero sí un gran maestro. Gracias **Sandro M. Radicella** por tu ayuda incondicional, por compartir conmigo tu experiencia tanto profesional como moral. Gracias por confiar en mí -espero no haberte defraudado- y por mostrarme el "gusanillo" del modelado ionosférico. Realmente estos años han sido una gran experiencia de vida; no me arrepiento en absoluto de haber elegido este camino, puesto que me ha llevado a mi tercer hogar: Trieste, que ciertamente echo de menos. Por último, no me gustaría olvidar a **Marina**, cuyo cariño realmente siento muy cerca. Gracias de corazón.

- ☼ -

Gracias al big boss... **Luis Vázquez Martínez**. Sin ti, nada hubiera existido. Vi ringrazio moltissimo per la vostra fiducia!!. Gracias por enseñarme a ver que Newton fue un gran hombre y sobretodo un gran visionario, puesto que aún hoy en día, nadie ha derrocado su *Principia Mathematica*. Ahora sé que el Universo se puede tocar, que por presión osmótica todo se aprende y que la ilusión y el entusiasmo son los verdaderos motores del conocimiento. Gracias por estar siempre ahí, infatigable.

- ☼ -

Thank you very much to the **plasma scientific community**, who welcomed me to the **MUAN group** from the very beginning of this adventure. In special, I would like to sincerely thank **David Morgan,** from Iowa University, his kindly help with me and this work and **Mark Lester,** from Leicester University, his great vote of confidence.

In the same line, grazie mile **Roberto Orosei** and **Marco Cartacci,** from Istituto Nazionale di Astrofisica in Bologna and IAPS/INAF in Rome respectively. I sincerely thank you for all your support and consideration towards myself and my work.

Thank you so much **Luigi Ciraolo,** from ICTP, for all your selflessly advice, comments and suggestions.

And of course, heartfelt thanks to **Pierre-Louis Blelly**, from IRAP in Toulouse, for his support in the shade and his trust on me. He had the great initiative to develop the software MAISDAT with **Johannes Bauer**, which led to this PhD.

- ☼ -

Toda expedición parte con un gran grupo de gente. En mi caso, partí con una gran familia que me acogió desde el primer momento y que me enseñó a desenvolverme en el camino: el equipo **Meiga-Metnet**. Gracias a todas las personas en el **INTA** que han hecho posible con el desarrollo de sus instrumentos que este Proyecto haya salido adelante y que esta aventura hoy en día continúe. Me gustaría especialmente agradecer al equipo de **MOURA** todo su apoyo magnético con nuestro trabajo en la UCM, sobre todo a **Marina Díaz de Michelena** y a **Miguel Felipe Cerdán**.

Y cómo no, a todo el **entorno marciano de la UCM** creado por el "big boss". No me gustaría olvidar a nadie puesto que de todos he aprendido algo y con los que he vivido decenas e incluso ciento de aventuras inigualables. Gracias **Pilar Romero**, **Gonzalo Barderas**, **Paco Valero**, **Álvaro de Vicente-Retortillo**, **David Usero**, **Marta Folgueira**, **Pedro Pascual**, **María Luisa Martín**, **Carlos Aguirre**, **Salvador Jiménez** y **Mapi Velasco** (estos dos últimos no UCM…. pero como si lo fueran).

- ☼ -

No hay camino sin reposo, por eso gracias a todas y cada una de las personas de mi *alma mater* la **Universidad Complutense de Madrid** y en concreto del **Dpto. de FTTA I** que de una forma u otra han hecho de mi estadía un hogar. Mil aventuras contaré a mis

nietos sobre este periodo, y sobre cómo entablé amistad con otros caminantes con los que compartí largos periodos del camino y que sé, que seguiré haciéndolo en un futuro. Gracias **Lucía Prieto** por ser el alma del Departamento y siempre pensar en mí. Gracias **Salvador Crespillo** por tu paciencia y todo tu tiempo invertido en mí. Gracias **Mariano Sastre** por estar siempre ahí como un apoyo incondicional y sobretodo, regulador. Gracias **Diana Núñez** por todos los momentos inolvidables que hemos vivido. Gracias **Sergio Magdaleno** por todos tus consejos y tu ayuda. Gracias **Marta Rodríguez** por ser ese hombro de apoyo siempre disponible cuando se necesita. Gracias **Izarra Rodríguez** por vivir intensamente junto a mí y compartir tantos momentos especiales y únicos. Gracias **Marina Sánchez – Bayton** por tu cariño y amistad, por ser esa mirada crítica que tanto necesito y sólo tú sabes ver y por apoyarme en todo, pase lo que pase. Y sobre todo gracias **María Ramírez** por ser mi complemento y la armonía que cierra la trigonometría más esencial:

$$sen^2(x) + cos^2(x) = 1$$

- ☼ -

A veces el camino se bifurca y te permite conocer lugares y personas que jamás habrías imaginado. Hace más de cuatro años que por primera vez visité **Trieste**, una ciudad remota italiana fronteriza con Eslovenia con los atardeceres más hermosos del planeta. Mis pasos y el entorno de mis acompañantes de camino me guiaron hasta allí, permitiéndome conocer personas que considero mis amigos.

Thank you (dal cuore) **Sandra Paiero**. You know that I consider you like my Italian mother. Thank you for sharing your life with me, your home, your time, your family, your **Oona**, and the most important, your affection. Thanks for all your words of encouragement and for your trust on me, and of course, for showing me the wonderful carrot cake!!!.

Gracias al **ICTP** por acogerme siempre en sus instalaciones y en especial a **Stanka Tanaskovic** por tu gran simpatía y amabilidad y a **Stefano Pistocco** por hacerme infinitamente más agradable las estancias. Gracias a **Ermano Pietrosemoli** por esos grandes paseos en bici y por compartir parte de tu experiencia de vida conmigo, enseñándome la verdadera naturaleza de la vida. Grazie **Marzo Zennaro** e **Carlo Fonda** per tutta la simpatia. Thank you **Melesseu Nigussie** for sharing with me your knowledge and for the long walks along the sea path. Grazie **Claudia Paparini** por tu gran sonrisa y simpatía siempre disponible para hacerme reír. Gracias **Katty Alazo** por enseñarme como es la vida de verdad en Cuba, por compartir conmigo grandes momentos inolvidables y por ser una parte muy importante de la vida en Trieste. Sabes que tienes una parcela de mi corazón. Gracias **Bruno Nava**, sólo gracias. No hay palabras que expresen todo lo que tu apoyo, tu consejo, tu saber escuchar y tu tiempo ha significado para mí. Confío en que sepas que siempre podrás contar conmigo de forma incondicional. Y por último en este texto, pero los primeros en mi mente, gracias **Yenca Migoya** y **Johannes Grassberger** por vuestra amistad, por acogerme en vuestra vida como una más, por ayudarme a ser más amena la vida en Italia y por permitirme

conocer a vuestros tres soles **Serena**, **Isabella** y **Egon**. Siempre contaréis con mi amistad y gratitud allá donde la vida nos lleve.

- ☼ -

Another bifurcation in the road, led me visit the **European Space Agency**. I spent in **ESTEC** a wonderful time and I was immersed in a real space atmosphere, like in a movie. I met many people who gave me good advices and made me the stay there very enjoyable. In particular, I would like to thank **Antonio Muñoz** and **Andrew Walsh** their hospitality and to **Emmanuel Grotheer** his sympathy and goodness. And from **ESAC**, a sincere thanks to **Alejandro Cardesín** who always was available to help me and introduced me my third-supervisor who was a key element of this PhD.

- ☼ -

En un largo viaje como este la compañía es fundamental. No sé qué hubiera sido de mí sin la cercanía de mis **amigas**. Vosotras sabéis bien lo que este camino ha costado y por qué lares me ha llevado. Gracias **Natalia Gómez** por tu energía vitalizante, **Lidia García** por escucharme y apoyarme siempre que lo he necesitado, **Lidia San José** por alegrarme y levantarme el ánimo, **Bárbara Gómez** por tu eterna sonrisa y amistad, **Luz y Anita** por ayudarme con otro punto de vista, **Alicia Pascual** por ser tu misma y apoyarme incondicionalmente y **Emma López-Alonso**, por conectar tu cerebro al mío, ligar nuestras experiencias vitales, calmarme en las tempestades y animarme en los desafíos y sobre todo, por estar siempre ahí pase lo que pase. Gracias igual a toda la **Familia López – Alonso Conty** por vuestro sincero apoyo y por todos los momentos únicos vividos con vosotros.

- ☼ -

Mención especial merece mi **familia madrileña**. **Jessica**, **Mari**, **Jose**, **Juani**, **David**, **Lucía**, **Davicito**, **Bruster, Ella** y **Lukas**. GRACIAS por acogerme en vuestra vida y considerarme como una más de la familia. "Dios los crea, y ellos se juntan", nunca un refrán había tenido tanto sentido. Gracias por vuestro apoyo incondicional, por escuchadme siempre, por vuestros valiosísimos consejos, por alegraros sinceramente con mis éxitos y ayudarme de corazón en los malos momentos, por entender mi estilo de vida y sobre todo, por haberme robado el corazón. Estemos donde estemos, siempre me tendréis ahí.

- ☼ -

Y por último, mi agradecimiento más profundo a las personas más importantes de mi vida, que siempre han velado y sufrido por mí. Gracias a toda mi **FAMILIA**, sin la que no soy nada. Siempre incondicionales respetando mis excentricidades. Siempre mis circunstancias.

"Yo soy yo y mi circunstancia, si no la salvo a ella no me salvo yo".
(José Ortega y Gasset)

Directed by:

Dr. Miguel Herraiz Sarachaga
Dr. Olivier Witasse
Dr. Gracia Rodríguez Caderot

Supervised by:

Prof. Sandro M. Radicella

Credits: MEX VMC image

ISBN : 978-84-616-9995-7